Effect of sample height on stress-strain behavior and undrained shear strength of saturated red clay soil in Buno Bedelle using UU-tri-axial test: In case of Gechi-Yanfa road project.

Gemechis Dinsa Geleta

A Thesis Submitted to the Department of Civil Engineering,
School of Civil Engineering and Architecture

Office of Graduate Studies
Adama Science and Technology University

September 2023

Adama, Ethiopia

Effect of sample height on stress-strain behavior and undrained shear strength of saturated red clay soil in Buno Bedelle using UU tri-axial test:

In case of Gechi-Yanfa road project

Gemechis Dinsa Geleta

Advisor: Eleyas Assefa (Ph.D.)

A Thesis Submitted to the Department of Civil Engineering,
School of Civil Engineering and Architecture

Presented in Partial Fulfillment of the Requirement for the Degree of Master of Science in civil engineering.

(Specialization in Geotechnical Engineering)

Office of Graduate Studies
Adama Science and Technology University

September 2023

Adama, Ethiopia

DECLARATION

I hereby declare that this Master thesis entitled **"Effect of sample height on stress-strain behavior and undrained shear strength of saturated red clay soil in Buno Bedelle using UU tri-axial test: In case of Gechi-Yanfa road project"** is my original work. That is, it has not been submitted for the award of any academic degree, diploma, or certificate in any other university. All sources of materials that are used for this thesis have been duly acknowledged through appropriate citations.

Gemechis Dinsa	______________________	30/09/2023
Name of student	Signature	Date

RECOMMENDATION

I/we, the advisor(s) of this thesis, hereby certify that I/we have read the revised version of the thesis entitled "**Effect of sample height on stress-strain behavior and undrained shear strength of saturated red clay soil in Buno Bedelle using UU tri-axial test: In case of Gechi-Yanfa road project**" prepared under my/our guidance by Gemechis Dinsa submitted in partial fulfillment of the requirements for the degree of Masters of Science in Civil Engineering. Therefore, I/we recommend the submission of revised version of the thesis to the department following the applicable procedures.

Eleyas Assefa (Ph.D.)	Eleyas Assefa (signed)	30/09/2023
Major Advisor/Supervisor	Signature	Date
______________________	________________	_________
Co-advisors/ Co-supervisor	Signature	Date

APPROVAL PAGE

I/we, the advisors of the thesis entitled **"Effect of sample height on stress-strain behavior and undrained shear strength of saturated red clay soil in Buno Bedelle using UU tri-axial test: In case of Gechi-Yanfa road project**" and developed by Gemechis Dinsa, hereby certify that the recommendation and suggestions made by the board of examiners are appropriately incorporated into the final version of the thesis.

Eleyas Assefa (Ph.D.)	Eleyas Ay.	30/09/2023
Major Advisor/Supervisor	Signature	Date
________________	________________	__________
Co-advisor	Signature	Date

APPROVAL OF BOARD OF REVIEWERS

We, the undersigned, members of the Board of Examiners of the thesis by Gemechis Dinsa have read and evaluated the thesis entitled **"Effect of sample height on stress-strain behavior and undrained shear strength of saturated red clay soil found in Buno Bedelle using UU tri-axial test: In case of Gechi-Yanfa road project**" and examined the candidate during open defense. This is, therefore, to certify that the thesis is accepted for partial fulfillment of the requirement of the degree of Master of Science in Civil Engineering.

Fikreyesus Demeke (Ph.D.) _	__________________	______________
Chairperson	Signature	Date
Argaw Asha (Ph.D.) _______	__________________	________________
Internal Examiner	Signature	Date
Tezera Firew (Ph.D.) _______	__________________	_________________
External Examiner	Signature	Date

Final approval and acceptance of the thesis is contingent upon submission of its final copy to the Office of Postgraduate Studies (OPGS) through the Department Graduate Council (DGC) and School Graduate Committee (SGC).

_________________________________	___________________	_________________
Department Head	Signature	Date
_________________________________	___________________	_________________
School Dean	Signature	Date
_________________________________	___________________	_________________
Office of Postgraduate Studies, Dean	Signature	Date

ACKNOWLEDGEMENT

Chiefly, I would like to thanks to the Almighty God for the substantial welfare and courage to initiate and complete this thesis. I would also like to genuinely gratify my advisor, Dr. Eleyas Assefa, for helping me in all technical aspects, and productive reproach during my thesis work. Furthermore, I would like to extend my appreciation to the Ethiopian Institute of Architecture and Building Construction, ASTU and AASTU geotechnical laboratory staff members for letting me to perform valued experiments in their corresponding laboratories with astonishing direction and assistance. Finally, I would like to thank my beloved families for their nonstop honorable and economic support, friends and all those who have contributed to my success.

TABLE OF CONTENTS

LIST OF TABLES

LIST OF FIGURES

ABBREVIATIONS

AASHTO	American Association of State, Highway & Transport Official
AASTU	Addis Ababa Science and Technology University
ASTM	American Society for Testing Material
ASTU	Adama Science and Technology University
BP	Back Pressure
BS	British Standard
CBR	California Bearing Ratio
CD	Consolidated Drained
CP	Cell pressure
CU	Consolidated Undrained
ENMA	Ethiopian National Metrological Agency
FSI	Free Swell Index
FSR	Free Swell Ratio
GI	Group Index
LL	Liquid Limit
LS	Linear Shrinkage
MDD	Maximum Dry Density
NC	Normally Consolidated Clay
OMC	Optimum Moisture Content
OC	Over Consolidated Clay
PI	Plastic Index
PL	Plastic Limit
PP	Pore Pressure

SI	Shrinkage Index
SL	Shrinkage Limit
TP	Test Pit
T-O-T	Tetrahedron-Octahedron-Tetrahedron Bond
USCS	Unified Soil Classification System
UU	Unconsolidated-Undrained
XRD	X-ray Diffraction
ZAV	Zero Air Void

ACRONYMS

A	Activity of clay minerals
Φ	Angle of Internal Friction
K	Coefficient of Permeability
Cu	Coefficient of Uniformity
C	Clay
Cc	Compressibility Index
G	Gravel
e_0	Initial Void Ratio
NP	Non-plastic Materials
O	Organic Soil
S	Sand
M	Silt
C_r	Swelling index
Su	Undrained Shear Strength
e	Void Ratio
V_K	Volume of Soil in Kerosene
V_W	Volume of Soil in Water

ABSTRACT

The qualities of soil are highly heterogeneous and unpredictable natural materials that fluctuate with environment, loads, and drainage conditions. Clay is a fine-grained soil that is well-known as a very complex natural formation. Red clay soil is a type of clay soil commonly available in rainy areas of western and south-western regions of Ethiopia like Buno Bedelle zone as mentioned by ERA design manual, (2013). Therefore, it is very vital to study engineering properties of red clay soil in its saturated form because their characteristics rely not only on the sort of object but also on the circumstances in which it occurs. To use this type of soil for construction purposes, the detail knowledge of its engineering properties is very important. This research aims at investigating the characteristics of the soil found in and around Gechi Yanfa. To conduct this study soil samples from a test pit were collected to be classified as the red clay soil based on its basic behaviors like plasticity, low compressibility, gradation, permeability and XRD mineralogical analysis, stress-strain behavior, and undrained shear strength of the saturated clay soil at specified sample height (H/D) ratios. This research presents the results of some index and engineering properties including Atterberg limits, compaction, free swelling and finally the effect of sample size (H/D) ratios (1.5,2 & 2.5) on stress-strain behavior and undrained shear strength of disturbed SRCS. The result reveals that the H/D ratio of fully saturated red clay soil of 1.5,2 & 2.5 under chamber pressure (σ_3) of 60 kPa is Su=43.77 kPa at ϵ_a=2.67%, Su=42.46 kPa at ϵ_a=2.65% and Su=40.77 at ϵ_a=2.40% resp. and Su=43.76 kPa at ϵ_a=2.77% , Su=42.43 kPa at ϵ_a=2.70% and Su=40.76 at ϵ_a=2.56% under cell pressure 100 kPa whereas the increase in cell pressure from 60 to 100 kPa did not affect Su, ϵ_a & φu for the saturated red clay soil. Except for angle of internal friction (φu=0) in all cases, the values of undrained shear strength (Su) and axial strain (ϵ_a) were affected by the change of sample size (H/D) ratios and also the stress-strain curve changed from ductile to brittle failure as H/D ratios of the soil sample increases. The result shows that the value is reliable because the Su value is obtained from total stress, which is overestimated and hence H/D=2.5 gave us the smallest values of Su & ϵ_a become preferable to testing sample size for the saturated red clay soil.

Keywords: Red Clay Soil, Undrained Shear Strength, Undrained-Unconsolidated (U-U) Test, X-ray Diffraction (XRD)

CHAPTER ONE
INTRODUCTION

1.1. Background

The qualities of soil are highly heterogeneous and unpredictable natural materials that fluctuate as the environment, loads, and drainage conditions do. So, it seems sense that its characteristics rely not only on the sort of object but also on the circumstances in which it occurs. With high compressibility and low shear strength, clay is a fine-grained soil that is well-known as a very complex natural formation.

Red soil is a widely available material in Ethiopia as mentioned by Ethiopian Roads Authority design manual, ERA, (2013), is particularly in Buno Bedelle, the region I was most interested in studying. It is widely distributed in rainy areas in the western and south-western regions of Ethiopia; hence it is crucial for safety reasons to examine it in a saturated form. To use this type of soil as construction materials, its detailed engineering properties should be well studied and known. This research aims at investigating the engineering characteristics of red soil in and around Gechi Yanfa. For this to be achieved, different laboratory soil tests have been carried out and secondary data from private and governmental organizations was collected, processed, and analyzed during this research.

The underlying soil is put under stress by civil engineering constructions when they are in place, and the tension is dispersed throughout the soil mass. Because soil engineering properties vary, so does the response of the soil to applied stress.

Fine-grained soil behaves in a way that is highly influenced by loads, geological history, and soil structure. The term "structure of the soil" refers to the soil fabric, which describes the inter-particle forces as well as the geometrical arrangement of the soil mineral grains. The first one primarily influences soil volume change and water retention behavior, whereas the second mostly influences soil strength and deformation characteristics (Lukas, 2010).

Most issues in soil engineering have some connection to the soil's shear strength. It is the primary engineering characteristic that regulates a soil mass's stability under loads, which in turn controls a soil's bearing capacity, a slope's stability, the earth's pressure on retaining structures, and a variety of other issues relating to soil mechanics. As a result, for soil structure analysis and design, a precise assessment of shear strength characteristics is necessary.

Prior research recommended that sample size variation affects the stress-strain and undrained shear strength of clay soil and hence some codes and standards adopted certain testing sample size to evaluate soil shear related parameters and the behavior they exhibit. Accordingly,

Merga, (2016) discovered that the length of the stress-strain curve lengthened with decreasing specimen height in drained UCS tests on red clay sourced from Addis Ababa.

Although collecting, handling, and testing larger specimens is significantly more challenging, Seopal & *et al.*, (2023) used a range of specimen sizes from lower to bigger diameter (i.e., 30 to 110 mm dia.).

Omar & *et al.*, (2015) also employed four different specimen diameters (D) i.e., 38, 50, 70, 100 mm with height equal to twice the nominal diameter.

Mir, (2013) remarks that measuring the soil shear parameters (Su, Cu, and u) is essential for the short-term stability study of many different civil engineering projects. Therefore, in such cases, the undrained shear strength parameters (cu > 0, ϕ= 0) can be examined using the total stress approach by unconsolidated-undrained (UU) tri-axial compression tests.

In connection with this, different scholars recommended specimen sizes in tri-axial tests as summarized in Table 1.1 below.

Table 1-1: Recommended aspect ratios as per standards

S/No.	Standards	Designation	Name	Diameter (mm)	Aspect (H/D) ratio
1	ASTM	D 2166	ASTM 2002a	33	2-2.5
2	BSI 1377-7		BSI 1990	Between 33 &100	2
3	JIS A 1216		JIS1993	35 & L=80mm	L/D=80/35 =2.30
4	TS 1900-2		TSI 2006	50 (or preferably38mm if necessary	2
5	Das, (2002)		Das (2002)	427	2-3

As can be seen from the above table, British standards advise a ratio of 2 heights to diameter ratio while ASTM advises a ratio of 2 to 2.5.

However, it can be challenging to extrapolate specimen size in the lab to big size in actual field circumstances since the size of the specimen used to estimate shear strength parameters might have a marginal or major impact on the parameters chosen for analysis.

Therefore, this research is aimed to examine the effect of sample height on geotechnical properties of clay soil collected from the selected study area. Soil sample from Buno Bedelle zone, Gechi-Yanfa road project were collected and investigated for its various engineering and strength properties. The properties of the soil such as natural moisture content, grain size distribution, specific gravity, Atterberg limit, linear shrinkage, free swell, compaction, and UU were determined and as stress-strain behavior, undrained shear strength properties at different aspect ratios (H/D=1.5,2 & 2.5) under confinement pressure of 60 kPa and 100 kPa were investigated and compared. Finally, the sample size that gives more realistic behavior and shear stress parameter results within an acceptable range were proposed as conservative sampling size.

1.2. Statement of the Problem

Despite the availability and significance of residual soils, there have not been many concerted efforts to create a thorough document that describes their behavior. Red clay is a unique type of clay with several unique properties, including a high liquid limit, a high porosity ratio, a low to medium compressibility, and others. Using drained and undrained tri-axial and unconfined compressive strength tests as a control parameter, studies have been conducted on the examination of the effect of sample height in stress-strain behavior and shear strength of red clay soil. According to Merga, (2016) the length of the stress-strain curve, as determined by drained UCS experiments on red clay soil collected from Addis Ababa, increases with decreasing specimen height. Only drained stress and strain values were acquired in the investigation, which maintained the sample's diameter throughout the UCS test. It is impossible to accurately define the impact of stress-strain behavior and undrained shear strength for saturated and impermeable red clay soil using UCS as a control point. Tri-axial testing, which improves control of beginning stresses and loading conditions, causes soil to collapse along the weakest plane. The unconsolidated-undrained tri-axial compression test's main goal is to quickly determine a soil's approximate compressive strength in the restricted state and determine its undrained shear strength.

ASTM Standard D 2850 for sampling size states that specimens must have a minimum diameter of 30 mm and a height to diameter ratio of 2 to 2.5. Because soil can vary depending on its geological formations, topography, and environmental conditions and may not assumptions state for stress-strain computation. To reduce damage to foundations caused by overestimating or underestimating the shear strength of clay soil sample with minimum diameter of 30mm and H/D of between 2 and 2.5, one of the critical problems in geotechnical engineering analysis is investigating the effect of sampling height.

1.3. Objectives of the Study

1.3.1. General objective

The primary goal of this study is to investigate the influence of the sample height-to-diameter ratio on stress-strain behavior and undrained shear strength of saturated red clay soil in the construction of Gachi-Yanfa road project in Buno Bedelle zone.

1.3.2. Specific objectives

- To investigate the engineering properties of red clay soil collected from Buno Bedelle zone.
- To determine more applicable sampling size (H/D) ratio on stress-strain behavior of the saturated red clay soil.
- To determine the effect of H/D ratios on undrained shear strength parameters (Cu, Su & φu) of saturated red clay soil under rapid loading conditions in Gechi-Yanfa road project.

1.4. Research Question

- Is it possible to determine some of the engineering properties of red clay soil collected from Buno Bedelle?
- Does applying various lengths-to-diameter ratios in UU tri-axial tests affect the stress-strain behavior and undrained shear strength of the collected red clay soil?
- Is a UU triaxial test for the saturated red clay soil more effective than others test in determining undrained shear strength parameters?

1.5. Scope of the Study

This research was conducted by reviewing different literature, practical problems related to the area and performing a series of laboratory experiments on materials used for the study.

It concentrated on western and southwestern part of Ethiopia, Oromia National Regional State, Buno Bedelle Zone aiming to investigate the stress-strain deformation behavior and undrained shear strength parameters of saturated red clay soils collected from Gechi-Yanfa road project particularly at working station of 20+880, south-eastern part of Bedelle town, where sliding occurred just after construction activities took place.

The laboratory tests conducted were mineralogical characterization (XRD) tests, specific gravity test, grain size analysis, free swell index test, density-moisture relationship tests, Atterberg limit tests, linear shrinkage test, unconsolidated-undrained shear strength test and one-dimensional consolidation test. The standard method used for laboratory test was most commonly under control of ASTM standard, except British standard was used for linear shrinkage test and Indian standard was used for free swell index test. In UU-tri-axial test, various sample sizes used for identifying the effect of length to diameter ratio on stress-strain behavior and undrained shear strength of saturated red clay soil.

Finally, the result achieved from this study will be analyzed, presented, discussed, and concluded in a definite manner.

1.6. Significance of the Study

Construction on red clay soil in rainy areas is major problems due to its significant change of void ratio, the matric suction resulted from increase in the moisture content and finally reduces the shear strength and the stability of the slope because shear strength and slope stability are controlled by the pore-water pressure and underground water table. So, to mitigate the impact of non-uniform deformation and swelling of red clay soils on various construction projects, this study is more useful in understanding the effect of sampling size, proper tress-strain behavior and undrained shear strength of the red clay soil. Nowadays, an effort is also made to reduce the impact of slope instability because of shear failure on different construction sites understanding the geotechnical properties of weak soils and reduce the usage of high maintenance cost. And also, the study is going to be used as a source of information and reference for the future works in Ethiopia by introducing and exploring previous work done abroad on this related problem area.

1.7. Limitation of the Study

It was initially intended to collect both undisturbed and disturbed samples from the area of the sliding section where red clay is found and to conduct the availed types of triaxial tests too. Due to the absence of tri-axial test machine at closer place, the chance of bringing the undisturbed sample to laboratory is very cumbersome. It would have been worth to open additional test pits and collect samples from another additional sliding section where red clay is found. Therefore, only disturbed sample from a single test pit representing the problem area was taken.

1.8. Structure of the Thesis

This thesis consists of five Chapters. The first Chapter gives the basic introduction to the research general overview including statement of the problem, objectives, question, scope and significance of the research and structure of the thesis. Chapter Two reviewed previous related works and summarizes research gaps. Background of the study area, Material and research methodology are accessed in the Third chapter of the thesis. Chapter Four analysis test results and brief discussions of different laboratory results. Chapter Five closes the whole team of the thesis by making conclusion and recommendation. Finally, appendices of different tabular calculations regarding both index properties and stress-strain behaviors, and relevant tables and plots for each sample are attached.

CHAPTER TWO

LITERATURE REVIEW

2.1. Clay Definitions, Mineralogy and Properties

Clay refers to soil particles finer than 2 microns (0.002mm) which primarily composed of different materials of bedrock.

Decomposition of this type of soil can take place by Physical weathering which is the mechanical disintegration of rocks by heat exchange and others, biological weathering results from the activities of plants and animals within a rock whereas chemical alteration is weathering caused by the effects of oxidation, reduction, hydrolysis, carbonation, and organic acids in rocks (Andrade *et al*., 2011).

Clay soil is recognized by its property of plasticity when mixed with some amount of water which refers to the behavior of material that deforms in shape and keeps its deformation even after the removal of the pressure primarily caused the deformation and very fine material fragments or particles composed mostly of hydrous-layer silicates of aluminum but occasionally containing magnesium and iron. Nonetheless, despite the common use of a specific particle size as upper limit to differentiate clays from silts, the plasticity, and the capability to harden when dried or fired are the main characteristics of clays (Guggenheim, S, Martin, R.T., 1995).

2.2. Clay Minerals

According to the clay mineral concept, clay mineral particles are too small to be seen by the naked eye, so their arrangements are referred to as microstructure or micro fabric and our knowledge of particle structure comes largely from electron microscope study. They are essentially composed of particles of one or more members of small group that are commonly known as clay minerals. The engineering behavior of clay soils (shear strength, compressibility, consolidation, permeability, shrinkage, swelling, collapse, sensitivity etc.) will be better understood if the nature of the microstructure of the soil is appreciated (Herrmann & Bucksch, 2014).

Head I., (1994), proposed the concept of clay arrangement and stickiness of minerals to each other at the points of contact, with forces sufficiently strong to construct a honeycomb structure and this shape is a special structure in clay-containing soils. More common clay mineral groups include kaolinite, illite and smectite (montmorillonite). Kaolinite consists of silica and alumina plates, and are connected very strongly, because kaolin clay is very stable. Illite has layers made from two silica plates and one alumina plate. However, illite contains potassium ions between each layer making the structure of the clay stronger than smectite. Smectite has layers made from two silica plates and one alumina plate. Because there is a very weak bond between the layers, large quantities of water can easily enter the structure. See tables below.

2.3. Engineering Characteristics of clay Soil

2.3.1. Physical properties of clay soil

Mitchell & Soga, (2005) defines that physical properties of cohesionless none clay soils are determined mainly by particle size, shape, surface texture, and size distribution.

The mineral composition is of importance primarily as it influences hardness', cleavage and resistant to chemical attack that determines these characteristics. By and large however, the none clay particles may be treated as relatively inert materials whose interactions are predominantly physical in nature.

A soil mass, as explained by Nelson & Miller, (1975) is always subjected to changing environment, depending upon the chemical and physical properties of the soil, the necessary actions for construction purposes will be taken. Soil properties need to be studied to improve the workability of the soil, therefore studying soil properties inside out is very important. Soil properties can broadly be divided into two categories: physical properties and chemical properties.

Arora , (2003) concluded that sometimes the geotechnical engineer is interested to have some rough assessment of the engineering properties without conducting elaborate tests. This is possible if index properties are determined. The properties of soils which are not of primary interest to the geotechnical engineer but are indicative of the engineering properties are called index properties.

Prakash & Sridharan, (2004) states that tests required for determination of engineering properties of soils are generally elaborated and time consuming. The most widely used are the particle size distribution, soil consistency tests and moisture-density relationships are commonly used as index properties both in evaluating foundations and to control compaction, even though their determination is required in connection with other test results.

According to Das & Sobhan, (2014), determination of the moisture content is required as a guide to classification of soils and to evaluate the behavior of soils during construction. This is determined by using the oven drying method. It relates only to the water which is removable by oven drying at 105-110°C.

Herrmann & Bucksch, (2014), also suggested that soil description must convey sufficient information to enable the designers and constructors to appreciate the nature and properties of the soils to anticipate the likely behavior and potential problems.

2.3.2. Structure of clay and physio-chemical properties

Mitchell & Soga, (2005) states that clay minerals occur in particles of such small size that physio-chemical interactions with each other and with water-electrolyte phase of the soil may be great. Environmental temperature, precipitation, groundwater level, pH and salinity play roles in clay properties and in conversion of rock into clay.

Moisture content is a commonly used parameter to represent the structural nature of a clay soil since it is related to the open-ness of the micro-structure, provided the soil is fully saturated. If the soil is partially saturated then void ratio, porosity or specific volume are also used (Herrmann & Bucksch, 2014).

2.3.3. Characteristics of clay mineral

In nature, clay minerals are found with certain physical and chemical characteristics due to which these clay minerals play an important role in different fields from research to industries. The clay minerals are a class of rock-forming minerals having porous like sheet structure with different distances between the sheets.

The combination of the electrical conductivity of the matrix material and the pore fluid is the electrical conductivity of the porous material. The cation exchange capacity, a number of possible charged ions by the negatively charged surface of clay materials, depends on the number of sheets and the cations located in these structures (Seopal & Kumar, 2023).

Therefore, physical, and chemical properties of clay minerals depend significantly on their sheet structure, cation- and anion-exchange capacity, and absorption ability in different applications.

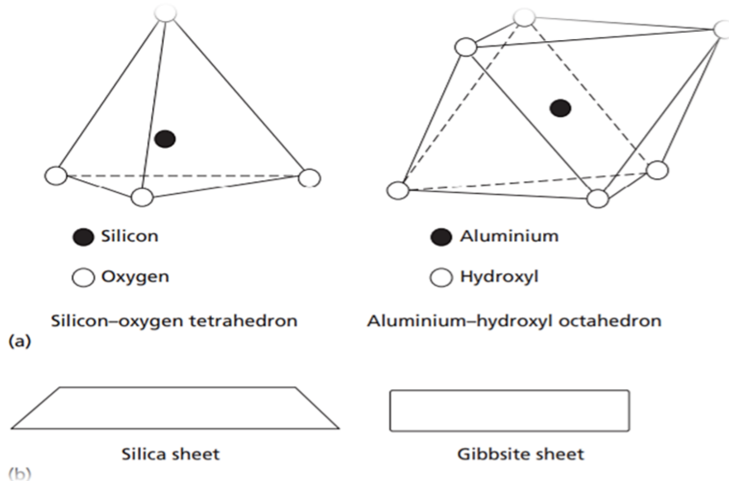

Figure 2-1: Clay minerals basic unit (Craig & Knappett, 2012)

2.4. Origin and Mineralogical Composition of Clay Soil

Clay minerals are a very distinctive type of particle that give characteristics to the soils in which they occur. The most well-known clay minerals are kaolinite, illite, and montmorillonite. These have a crystalline structure, the basic units of which are termed a silica tetrahedron and an alumina octahedron (Wiley, 2009).

2.4.1. Kaolite group

Kaolinite is composed of a single tetrahedron sheet and single aluminum octahedral sheet combined in a unit. The association of a silica tetrahedral sheet with aluminum octahedral sheet forms one layer of kaolinite. The thickness of kaolinite layer is about 7Ǻ. It is formed by stacking the layer one above the other with the relatively strong hydrogen bond. Therefore, the mineral is stable, and water cannot enter between the sheets to expand the unit cells (Lukas, 2010).

Most Ethiopian clay contain kaolinite and halloysite as the principal clay minerals, but montmorillonite is also frequently present in significant amounts. The red color of the Ethiopian soil indicates the presence of iron (Berhanu *et al*., 2014).

According to ERA, (2013) red soils can be formed from many kinds of rocks if the weathering conditions, climate, and drainage are suitable. It is commonly found in Buno Bedelle on the eastern and south-east parts of the town. Its depth ranges from a few centimeters to about 20 meters. In the areas covered by the study, in Gechi-Yanfa road project at working stations of 20+880 & 22+360 however, the thickness of the soil is found to be 3 meters.

As index properties tests results determined in the laboratory by classic consulting engineer's plc for design purpose shows, the soil is not potentially expansive and further, the results show that with in the investigated depth the index properties of the soil have no significant variation.

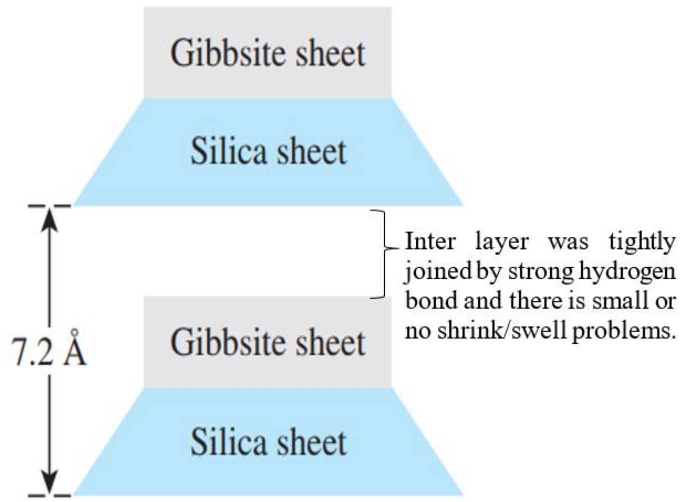

Figure 2-2: General structural arrangements of kaolinite clay mineral (Das & Sobhan, 2014)

2.4.2. Illite group

Illite is made up of octahedral sheet bonding with two silica sheets: These layers are bonded by potassium ions and their particles range from 50Å to 500Å in thickness and have specific surface area of about 80m^2/g. The structure of illite was formed of two silica tetrahedral sheets with a central sandwich of aluminum or magnesium octahedral sheet arranged with a 2:1 lattice type.

When they compared to montmorillonite minerals, illite minerals have low plasticity and swell potential due to their larger particle diameter of 0.5-10μm and lower specific surface area of 65-180 m^2/g (Chen, 1975).

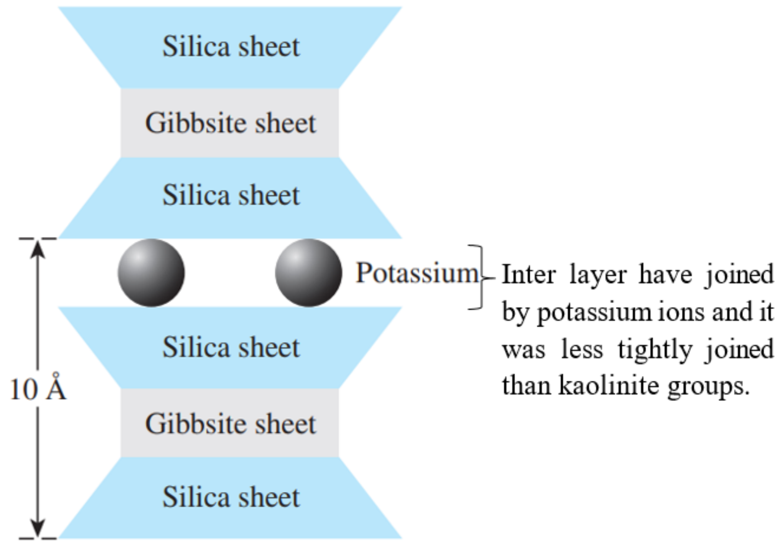

Figure 2-3: General structural arrangements of illite clay minerals (Das & Sobhan, 2014)

2.4.3. Montmorillonite or smectite group

Montmorillonite has a similar structure to illite. The structure has one octahedral sheet sandwiched between two silica sheets and bonded with weak Vander walls forces. A large amount of water is attracted into the space between the layers and causing the layers to expand significantly. Montmorillonite particles have the lateral dimension of 1000Å to 5000Å and thickness of 10 Å to 50 Å, and its specific area is about 800m^2/g.

Chemically, it was a hydrated sodium calcium aluminum magnesium silicate hydroxide, with a chemical formula $(\mathrm{Na, Ca})_3(\mathrm{Al, Mg})_2(\mathrm{Si_4O_{10}})(\mathrm{OH})_2.\mathrm{Nh_2O}$.

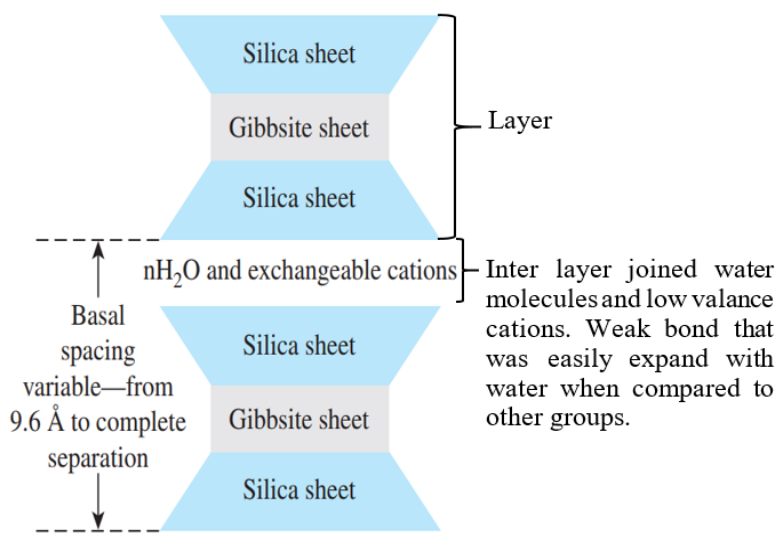

Figure 2-4: General structural arrangements of smectite clay mineral (Das & Sobhan, 2014)

2.5. Methods of Identifying Clay Soils

Investigation of red clay soils on earth crust was generally done through two important methods. The first method is visual identification and recognize the material as red clay soil and the second method is sampling, characterizing, testing, and measuring of material properties to be used as the basis for design.

2.5.1. Field identification

The most significant properties of clay are its cohesion and plasticity. If when pressed together in the hands at a suitable moisture content the particles stick together in a relatively firm mass, the soil shows cohesion. If it can be deformed without rupture (i.e., without losing its cohesion), it shows plasticity. Clay dries more slowly than silt and sticks to the fingers; it cannot be brushed off dry (KH Head, 1994).

Soils that can exhibit high swelling potential can be identified by field observations, mainly during reconnaissance and preliminary investigation stages (Nelson & Miller, 1975).

2.5.2. Laboratory identification

Mineralogical identification: Clay mineralogy is a fundamental governing factor that control property of clay soil (Mitchell & Soga, 2005). Clay minerals can be identified using a variety of techniques of which are: X-ray diffraction (XRD), Differential thermal, analysis (DTA), Chemical analysis and Electron microscope resolution (EMR). Chen, (1975) argued that these techniques should be used in combination with each other to get better and consistent outcomes.

Inferential Testing Methods: is tried to link some of the index properties of fine-grained soils with the soil clay mineralogical composition to estimate their swell potential in two ways.

Indirect methods: this makes use of soil index properties such as liquid limit, shrinkage limit, percent clay size composition of soils. Moreover, certain indices are used (plasticity index, and shrinkage index) to estimate the swell potential of soil (Asuri & Keshavamurthy, 2016).

Liquid limit: is determined by the conventional Casagrande method or by the fall cone method. It is regarded as the water holding capacity of the soil, which in turn has been taken as a measure of soil swell potential as shown in table 2-1

Table 2-1: Red clay soil classification based on LL (Asuri & Keshavamurthy, 2016)

Swell potential	Liquid limit (%)		
	Chen (1975)	Snethan *et al*. (1977)	IS:1498(1970)
Low	<30	<50	20-35
Medium (marginal)	30-40	50-60	35-50
High	40-60	>60	50-70
Very high	>60	-	70-90

Plasticity Index: It is the difference between the liquid limit and plastic limit of fine-grained soils. Higher the plasticity index, more plastic the soil is and have higher soil swell potential.

Table 2-2: Clay soil classification based on PI (Asuri & Keshavamurthy, 2016)

Swell potential	Plasticity Index (%)		
	Holtz and Gibbs (1956)	Chen (1975)	IS:1498(1970)
Low	<18	0-15	<12
Medium	15-28	10-35	12-23
High	25-41	20-55	23-32
Very high	>35	>35	>32

Shrinkage limit: It represents the lower bound water content for any volume reduction of a soil mass and regarded as a measure of volume stability of the in situ soils (Asuri & Keshavamurthy, 2016). The table given below presents the schemes available to recognize swelling potential of fine-grained soils based on shrinkage limit.

Table 2-3: Clay soil classification based on SL (Emmanuel et al., 2021)

Swell Potential Holtz and Gibbs (1956)	Shrinkage Limit (%)	Volume change Altemeyer (1956)	Shrinkage Limit (%)
Low	>15	Non-critical	>12
Medium	10-16	Marginal	10-12
High	7-12	Critical	<10
Very high	<11		

Shrinkage Index: is the numerical difference between shrinkage limit and plastic limit for remolded soils (IS 2809, 1972). The classification of the swell potential of fine-grained soils based on their shrinkage index is given in the table below.

Table 2-4: Clay soil classification based on SI(IS:1498, 2007)

Swell Potential	Shrinkage Index (%)
Low	<15
Medium	15-30
High	30-60
Very high	>60

Free swell index: Free swell index is also one of the most commonly used simple test method to estimate the swelling potential of clay (Rao, 2006). In this method, two oven-dried samples weighing 10g each and passing through 0.425 mm sieve were taken. One sample is put in a 100ml graduated glass cylinder containing kerosene which is nonpolar liquid, and the other sample is put in a similar cylinder containing distilled water. Then free swell index is expressed as:

$$\text{Free swell index}(\%) = \left(\frac{V_W - V_k}{V_k}\right) * 100 \quad (1)$$

Where: V_w and V_k are final soil volume soaked in water and kerosene, respectively.

Table 2-5: Relationship between FSI and degree of expansiveness (Rao, 2006)

Degree of expansiveness	Free swell index (%)
Low	<20
Moderate	20-35
High	35-50
Very High	>50

Free swell ratio: To determine the swell property Prakash & Sridharan, (2004), proposed the free swell ratio method of characterizing the soil swelling. The free swell ratio is defined as the ratio of sediments volume of 10 cm^3 oven dried soil passing through 0.425 mm sieve in distilled water to that of kerosene.

$$\text{Free swell ratio} = \frac{V_w}{V_k} \quad (2)$$

Where: V_w and V_k are final soil volume soaked in water and kerosene, respectively.

Table 2-6: Classification of soil based on FSR (Prakash & Sridharan, 2004)

FSR	Clay type	Dominant mineral type
<1.0	Non-swelling	Kaolinite

1.0-1.5	Mixture of swelling & non-swelling	Kaolinite and montmorillonite
1.5-2.0	Swelling	Montmorillonite
2.0-4.0	Swelling	Montmorillonite
>4.0	Swelling	Montmorillonite

Cation exchange capacity (CEC): quantity of exchangeable cations required to balance the negative charge on the surface of the clay particles and expressed in milli equivalents per 100 grams of dry clay and related to clay mineralogy. Clays having high CEC values have a high surface activity and have a greater water holding capacity (Nelson & Miller, 1975). See the fig below.

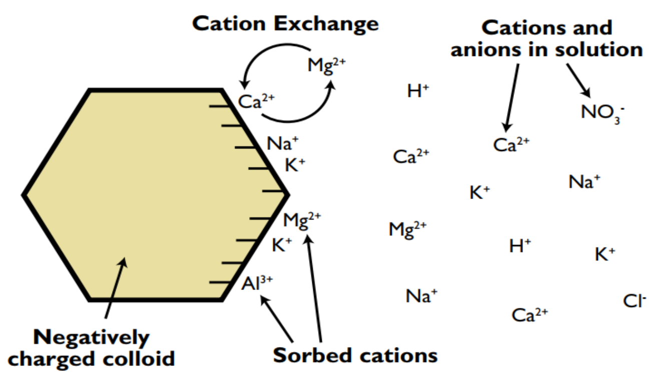

Figure 2-5: Simplified representation of cation exchange capacity (McCauley *et al*., 2005)

Table 2-7: Typical CEC values of basic clay minerals (Nelson & Miller, 1975)

Clay mineral	CEC $\left(\frac{\text{meq}}{100\text{gm}}\right)$
Kaolinite	3-15
Illite	10-40
Montmorillonite	80-150

Activity of clays: As per Venkatramaiah, (2006) revealed, indirect method of obtaining information on the type and effect of clay mineral in a soil is to relate plasticity index to the amount of clay size particles. It is known that for a given amount of clay mineral, the plasticity resulting in a soil will vary for the different types of clays. Activity (A) can be determined from the results of the standard laboratory tests such as the hydrometer test, liquid limit, and plastic limit test and defined as follows.

$$\text{Activity(A)} = \frac{\text{Plasticity index}}{\text{\% Clay fraction}} \tag{3}$$

Clays containing kaolinite will have relatively low activity and those containing montmorillonite will have high activity. Based on this classification:

Montmorillonite clay (expansive clay) is defined as active. Illite clay as normal and, Kaolinite clay is as inactive.

Table 2-8: Degree of colloidal activity (Venkatramaiah, 2006)

Degree of activity	Activity
Inactive clay	<0.75
Normal clay	0.75-1.25
Active clay	>1.25

Direct methods: The most satisfactory and convenient method of determining the swelling potential and swelling pressure of clay is by direct measurement. It can be achieved by the use of the conventional one dimensional consolidation (Chen, 1975). These methods offer the most useful data, and tests are simple to perform and do not require complicated equipment.

2.6. Soil Classification System

Soils differ according to their origins, compositions, locations, geological histories, and a variety of other characteristics. Even if two soils were recovered from close boring holes on the same building site, they may be substantially different in their geotechnical properties. However, it is more convenient and comfortable for engineers when soil is classified with comparable engineering properties. Without doing laboratory or field-testing, engineers may comprehend the approximate engineering properties of such categorized soils. Soil classification is a procedure that assists engineers during the early design stage of geotechnical engineering problems.

There are many soil classification systems that are currently used in many countries. Those methods mostly use consistency limits and soil gradation information for the classification of soils. There are two classification systems that are widely used in geotechnical engineering aspects: -

A. Unified soil classification system (USCS) and,
B. American Association of State Highway and Transportation Officials (AASHTO) classification system.

2.6.1. Unified soil classification system

This system was firstly developed by Arthur Casagrande for wartime airfield construction in 1940 and the system was modified and adopted for regular use by army corps of engineers and then by the bureau of reclamation in 1952 as the unified soil classification system which currently incorporated on ASTM standard manual. According to this method, soils are divided into two sub major categories.

1) Coarse grained soil that is gravelly and sandy in nature with less than 50% of soil sample passing through the sieve size of 0.075 mm, i.e., $F_{200}<50\%$. Naming of categorization starts with prefix G for gravelly soils and S for sandy soils.

2) Fine-grained soils when 50% or more of soil sample passing through the sieve size 0.075 mm, i.e., $F_{200} > 50\%$. Naming of group symbol starts with M for inorganic silts, C for inorganic clays, O for organic silt and clays, and Pt for peats and muck for highly organic soils.

Soil can also be gravel and sand based on amount of soil retained on sieve with opening size of 4.75 mm. Soil is gravel if more than 50% is retained on sieve No.4 and sandy soil if more than 50% of them pass sieve No.4. Similarly, fine-grained soils could be silt and clay based on their plasticity chart shown on figure 2-6.

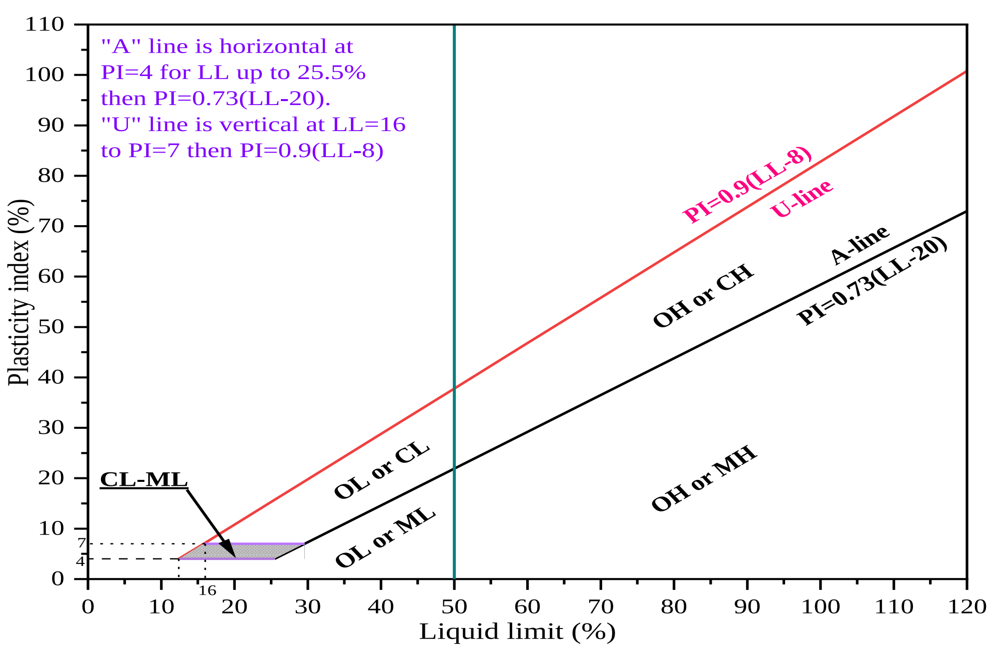

Figure 2-6: Plasticity chart for fine-grained soils classification by USCS (ASTM D 2487, 2000)

Table 2-9: Soil classification based on particle size range by USCS.

Soil type		Particle Size (mm)
Clay		$\leq$0.002
Silt		0.002-0.075
Sand	Fine	0.075-0.425
	Medium	0.425-2.0
	Coarse	2.0-4.75
Gravel		4.75-75

There are also some additional qualitative suffixes added on group symbol based on amount of Coefficient of uniformity (C_u) and coefficient of curvature (C_C) obtained from gradation curve for coarse grained soils and suffixes added on group symbol of fine-grained soil based on amount of plastic index and liquid limit amount as summarized in table 2-10.

Table 2-10 : Unified soil classification system chart (ASTM D 2487, 2000)

Criteria for Assigning Group Symbols and Group Names Using Laboratory Tests [A]				Soil Classification: Group Symbol	Soil Classification: Group Name [B]
COARSE GRAINED SOILS More than 50% retained on No. 200 sieve	Gravels More than 50% of coarse fraction retained on No. 4 sieve	Clean Gravels Less than 5% fines [E]	$C_U \geq 4$ and $1 \leq C_C \leq 3$ [C]	GW	Well-graded gravel [D]
			$C_U < 4$ and/or $1 > C_C > 3$ [C]	GP	Poorly graded gravel [D]
		Gravel with Fines More than 12% fines [E]	Fines classify as ML or MH	GM	Silty gravel [D,F,G]
			Fines classify as CL or CH	Urule; 1>GC	Clayey gravel [D,F,G]
	Sands 50% or more of coarse Fraction passes No. 4 sieve	Clean sands Less than 5% fines [I]	$CU > 6$ and $1 \leq CC \leq 3$ [C]	SW	Well-graded sand [H]
			$C_U < 6$ and/or $1 > C_C > 3$ [C]	SP	Poorly graded sand [H]
		Sands with Fines More than 12% fines [I]	Fines classify as CL or CH	SM	Silty sand [F,G,H]
			Fines classify as CL or CH	SC	Clayey sand [F,G,H]
FINE-GRAINE SOILS 50% or more passes the No. 200 sieve	Silts and Clays Liquid limit less than 50	Inorganic	$PI > 7$ and plots on or above "A" line [J]	CL	Lean clay [K,L,M]
			$PI < 4$ or plots below "A" line [J]	ML	Silt [K,L,M]
		Organic	$\frac{LL(\text{oven dried})}{LL(\text{dried})} < 0.75$	OL	Organic clay [K,L,M,N]
				OL	Organic silt [K,L,M,O]
	Silt and Clays Liquid limit 50 or more	Inorganic	PI plots on or above "A" line	CH	Fat clay [K,L,M]
			PI plots below "A" line	MH	Elastic silt [K,L,M]
		Organic	$\frac{LL(\text{oven dried})}{LL(\text{dried})} < 0.75$	OH	Organic clay [K,L,M,P]
					Organic silt [K,L,M,Q]
HIGHLY ORGANIC SOILS	Primarily organic matter , dark in color , and organic odor			PT	Peat

[A] Based on the material passing the 3-in. (75 mm) sieve. [B] If field sample contained cobbles or boulders, or both, add "with cobbles or boulders, or both" to group name. [C] $C_U = D_{60}/D_{10}$ & $CC = (D_{30})^2 / D_{10} \times D_{60}$. [D]

If soil contains ≥ 15% sand, add "with sand" to group name. [E] Gravels with 5 to 12% fines require dual symbols: GW-GM: well-graded gravel with silt, GW-GC: well graded gravel with clay, GP-GM: poorly graded gravel with silt, GP-GC: poorly graded gravel with clay. [F]

If fines classify as CL-ML, use dual symbol GC-GM, or SC-SM. [G] If fines are organic, add "with organic fines" to group name. [H]

If soil contains ≥ 15% gravel, add "with gravel" to group name. [I] Sand with 5 to 12% fines require dual symbols: SW-SM: well-graded sand with silt, SW-SC: well graded sand with clay, SP-SM: poorly graded sand with silt, SP-SC: poorly graded sand with clay. [J]

If Atterberg limits plot in hatched area, soil is a CL-ML, silty clay. [K] If soil contains 15 to 29% plus No.200, add "with sand" or "with gravel," whichever is predominant. [L] If soil contains ≥ 30% plus No.200, predominantly sand, add "sand" to group name. [M]

If soil contains ≥ 30% plus No.200, predominantly gravel, and add "gravelly" to group name. [N] PI ≥ 4 and plots on or above "A" line. [O] PI < 4 and plots below "A" line. [P] PI plots on or above "A" line. [Q] PI plots below "A" line.

2.6.2. AASHTO classification system

The AASHTO system was developed specifically for highway construction and is still widely used for that purpose. With practice and experience, a reasonably accurate field classification can be determined. However, it is necessary to run sieve analyses and plasticity determinations to precisely classify a soil with this method.

According to this system, granular soils are soils in which 35% or less are finer than the No. 200 sieve. Silty clay soils are soils in which more than 35% are finer than the No. 200 sieve (Muni Budhu, 2010). The classification method uses liquid limit, plastic limit and information obtained from grain size distribution curve to classify soils into seven major groups, A-1 through A-7.

The first three groups, A-1 through A-3, are granular (coarse grained) soils, while the last four groups, A-4 through A-7, are silty clay (fine-grained) soils. Figure 2-7 and table 2-12 were used for the soil classification system.

The procedure of classification uses an elimination method of column, from the upper left corner toward downward and right. If the condition on the row is not satisfied, the entire column is eliminated, and it is never referred. After the last row check for PI, one or possibly more than one column may survive this elimination process. If more than one column survived, the first column from the left is selected as a group or subgroup.

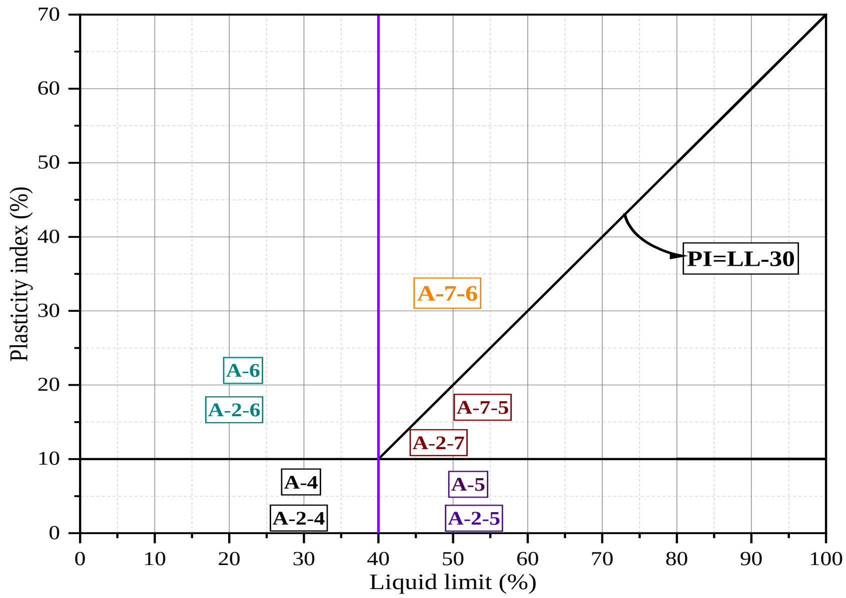

Figure 2-7: Liquid limit and plasticity index ranges for fine-grained materials (AASHTO:M 145-91, 2008)

Table 2-11: classification of soils and soil-aggregate mixtures (AASHTO:M 145-91, 2008)

General Classification	**Granular Materials (35 Percent or Less Passing 75μm)**							**Silt-Clay Materials (More Than 35 Percent Passing 75μm)**			
Group Classification	A-1		A-3	A-2				A-4	A-5	A-6	A-7
	A-1-a	A-1-b		A-2-4	A-2-5	A-2-6	A-2-7				A-7-5 A-7-6
Sieve analysis, percent passing											
2.00mm(No.10)	50 max	-	-	-	-	-	-	-	-	-	-
0.425mm(No.40)	30 max	50 max	51 min	-	-	-	-	-	-	-	-
75μm(No.200)	15 max	25 max	10 max	35 max	35 max	35 max	35 max	36 min	36 min	36 min	36 min
Characteristics of fraction passing 0.425mm (No.40)											
Liquid limit		-	-	40 max	41 min	40 max	41 min	40 max	41 min	40 max	41 min
Plastic index		6 max	NP	10 max	10 max	11 min	11 min	10 max	10 max	11 min	11 min[a]
Usual type of significant constituent materials	Stone fragments, gravel and sand		Fine sand	Silty or clayey gravel and sand				Silty soils		Clayey soils	
General rating as subgrade	Excellent to Good							Fair to Poor			

[a] Plasticity index of A-7-5 subgroup is equal to or less than LL minus 30 and, Plasticity index of A-7-6 subgroup is greater than LL minus 30. Placing of A-3 before A-2 is necessary in the

"left to right elimination process" and does not indicate superiority of A–3 over A–2. Group index (GI) value is appended additionally in parentheses to the main group to provide a measure of quality of a soil as highway subgrade material and calculated through the following formula.

$$\mathrm{GI} = (\mathrm{F} - 35)[0.2 + 0.005(\mathrm{LL} - 40)] + 0.01(\mathrm{F} - 15)(\mathrm{PI} - 10) \qquad (4)$$

Where: F is percentage passing 75 μm (No. 200) sieve, expressed as a whole number, LL is liquid limit, and PI is plasticity index.

When the calculated group index is negative, the group index shall be reported as zero and should be reported to the nearest whole number. And, when calculated GI is more than 20, it is assumed to be taken as 20. Soil having less GI has good strength and quality, but soil having higher group index has less quality and is not appropriate to use as construction material.

2.7. Mechanical Behavior of Soil

Natural soil is made up of tri-particulate, discontinuous, and heterogeneous materials, hence it is necessary to adopt the most reliable testing method when determining the mechanical properties of a discontinuous material (Mir, 2021).

2.7.1. Hydro-mechanical behavior /Permeability

The mass of soil is composed of solid particles of various sizes connected by interconnected hoover regions. Due to the ongoing vacuum spaces in soil, water can flow from a place of high energy to a point of low energy. Soil is said to be permeable if it allows liquids to pass via its network of connected vacant spaces. There are many variables that determine a soil's permeability: the size of the soil grains, the properties of the pore fluid, the void ratio, the structure and form of the pores, and the saturation level. Testing soil permeability can be done in a lab or out in the field. Laboratory methods for determining permeability include the falling or variable head test, the constant head test, and the direct or indirect measurement during the odometer test.

2.7.2. Stress – strain behavior

Most shear tests are conducted with strain control. The stress-strain characteristic can be easily acquired in these experiments since the shape of the stress-strain curve beyond the peak point can only be seen in a strain-controlled test. A strain-controlled test is easier to carry out than a stress-controlled test.

In a test where the shearing strain is regulated, the strain is raised over the course of the test at a predetermined rate. The specimen's vertical deformation is commonly calculated using the piston's travel when pressing on the specimen's top. The deformation indicator is typically a linear variable differential transformer (LVDT) or another measurement device that complies with ASTM D2850-15's accuracy and range standards.

Despite a few exceptions, Güneyli *et al*., (2016) found that the stress-strain curves of the specimens seen both during and after the UCS testing showed that the specimens generally tended to attain their peak strengths at a lesser axial strain as the L/D ratio grows and its rises, the stress-strain curve's peak and decrease after it becomes sharper and more pronounced, indicating brittle failure behavior. Red clay soil exhibits similar behaviors in both its undisturbed and remolded states.

2.7.3. Failure criteria

Failure, according to KH Head, (1994), often refers to the situation in which the specimen can no longer withstand an increase in stress and has reached its maximal resistance to deformation in terms of axial stress. He also recommended that consideration be given to the specimen's bulging or "barreling" when it is compressed, as well as to the impact of the rubber membrane employed in a triaxial test. An important aspect of the description of the soil’s qualities is the mode of failure.

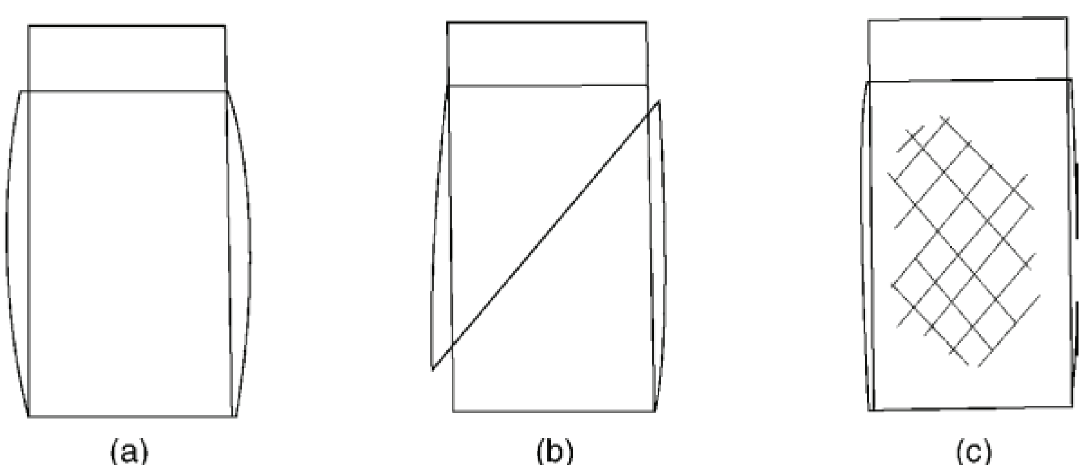

Figure 2-8: Modes of failure in compression test specimens: (a) plastic failure (barreling); (b) brittle failure (shear plane); (c) intermediate type (Head, 1994)

Consequently, three primary failure categories are identified as shown above. When a plastic object fails, it will swell laterally and take on a "barrel shape." The specimen shears along one or more clearly defined surfaces in a brittle failure that falls somewhere between types 1 and 2.

2.7.4. Shear strength of soil

According to Herrmann *et al.*, (2014), soil failure happens when the maximum amount of shear stress the soil can support is mobilized. The ultimate (failure) load necessary to cause collapse of a soil mass will be determined by the shear strength of the soil. The factor of safety, the ratio of the applied load to the maximum load possible must have an acceptable value for the designer to be confident in the stability of the earth structure.

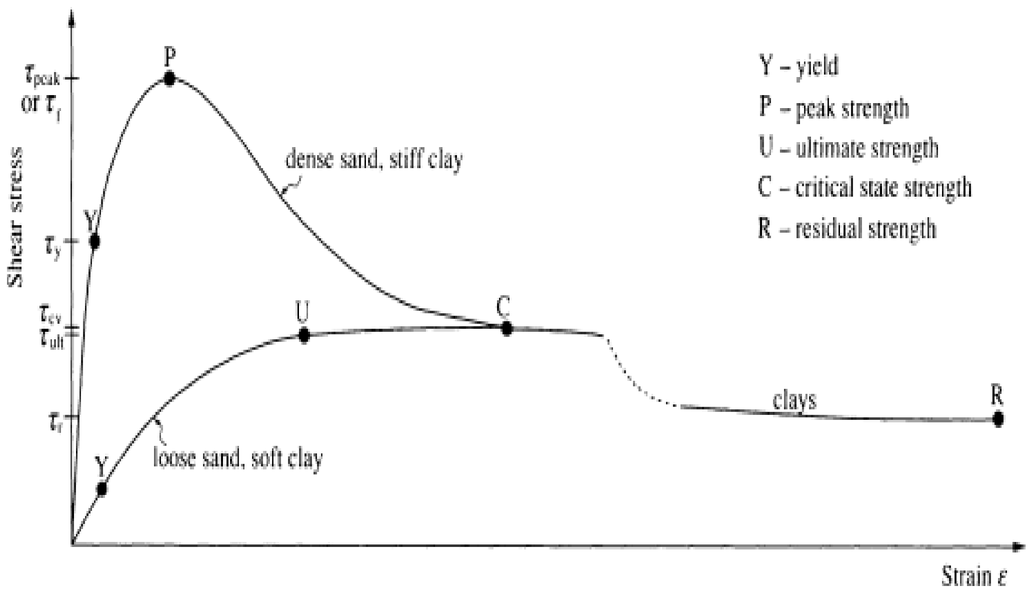

Figure 2-9: Definition of failure (Herrmann *et al.*, 2014)

Wiley, (2009) found that two crucial factors set soil strength apart from that of other engineering materials (steel, concrete, wood, etc.): (1) It all comes down to strength alone. The three main design issues that engineers deal with are slope stability, earth pressures on retaining walls, and foundation load capability. (2) Shear strength varies depending on the soil. Deep subsurface soil is more resilient than soil that is near the surface. An embankment's lowest layers are more resilient than its top ones.

Wesley, (2010) referred that undrained shear strength in conditions when there is no change in water content, whether in field measurements or laboratory tests, the strength remains constant regardless of changes in the total pressures acting on the soil if the soil is entirely saturated and undrained since no volume change is possible. The soil behaves as though its friction angle is zero in terms of total stress. It is crucial to understand that this φ= 0 instance results from two crucial and significant elements: (1) The soil is completely saturated. (2) The environment is undrained. The behavior in the φ= 0 scenario is independent of the kind of soil; if the first two requirements hold, clays and sands exhibit the same behavior.

Factors affecting Mechanical behavior of Cohesive Soils (Clay soil)

a) Effect of clay content and mineralogy**: -**the undrained shear strength of a clay is influenced by its mineralogy and clay content in addition to its moisture content, which decreases as moisture content rises.

Clay content: - The final friction angle of cohesive soil is dependent on the amount of clay present. The angle lowers as the amount of clay rises.

Structure of clay: Due to its structural strength, even condensed clay usually displays a slight peak. The structural strength predominates in over-consolidated clays. Due to the presence of macro-fabric, such as inclined joints in fissured clays or encountered, particularly with the presence of stones, varied strengths can be produced for clays, even those with the same moisture content.

b) Size of specimen: -The test is typically then conducted on 100 mm diameter specimens (i.e., directly out of the U 100) to prevent further disruption and to reflect the in-situ mass fabric more accurately.

c) Confining Pressure: -The cell pressure is applied to the specimen in three or more steps to saturate the specimen. The pressures to apply depend on the total overburden pressure σ_{v0} at the depth at which the sample was taken (Mir, 2021).

d) The multi-stage (UU) test**: -** No matter the cell pressure, the soil should only have one failure strength when tested at a constant moisture content. Results are thus frequently presented with three different Mohr circles that have a smaller cohesion intercept Cu and φu value greater than zero up to 10 degrees which is not in actual. Using these small φu values in a shallow foundation or immediate slope analysis leads to a dangerous over-estimate of stability.

e) Partially saturated clays: - when the triaxial test is conducted on a partially saturated sample, the application of the cell pressure (σ_3) results in pore water pressure that is less than the value of σ_3 ($B < 1$). A check on the degree of saturation (moisture content and bulk density values) should be made to confirm the state of the specimen and its relevance to in-situ conditions.

f) Fissured clays: - Most over consolidated clays have fissures, which result in weak points. These fissures' strength is known as their fissure strength, and it is significantly lower (by as much as 10%) than the strength of the clay between them when it is unbroken.

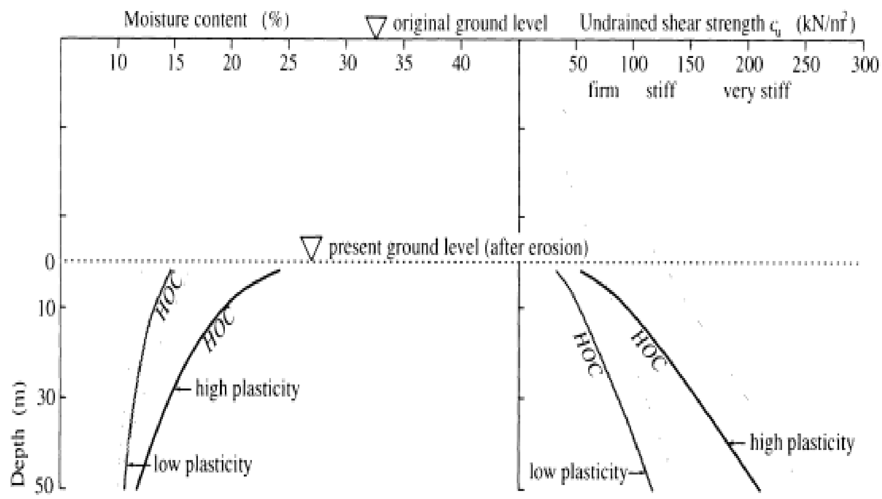

Figure 2-10: Strength variation with depth heavily- OC clays (Herrmann & Bucksch, 2014)

g) Variation with depth**: -** As with a typically consolidated clay, the effective stress rises with depth and the void ratio falls. The fluctuation of moisture content for low and high plasticity clays has been depicted in:

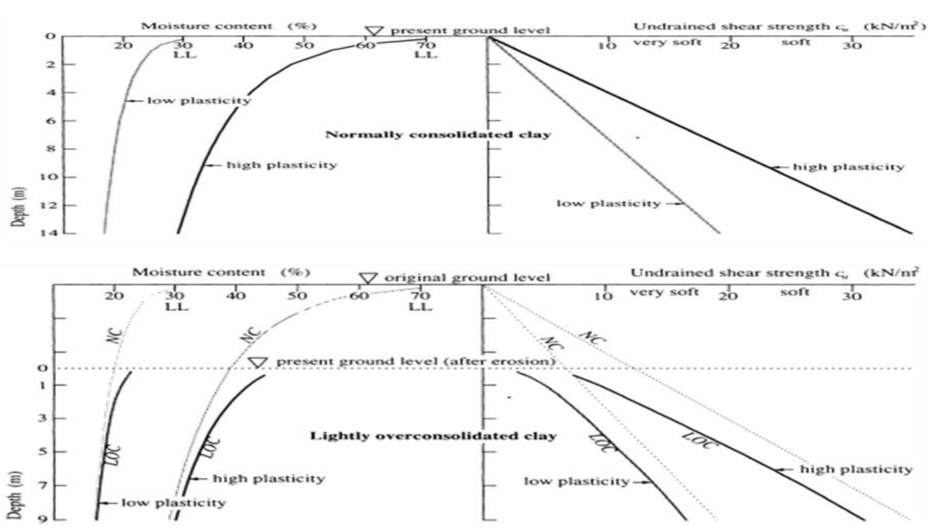

Figure 2-11: Strength variation with depth-NC and lightly OC clays (Herrmann & Bucksch, 2014)

Shear strength of clay - frictional characteristics: - It cannot be stressed enough that the shear strength of clay is determined by the effective stresses and the frictional characteristics both of which reside in the mineral grain structure.

j) Drainage Condition: - Cohesive soils have low permeability and hence the shear strength will vary depending on whether the soil is drained or not.

k) Rate of strain: The rate of strain has a minimal impact on the angle of shearing resistance in the case of typically cemented clays. When the rate of strain is reduced, some of the shear strength inevitably decreases in the case of over-consolidated clays.

l) Plasticity Index: - The value of shear strength decreases with an increase in Plasticity Index.

m) Stress history: - The values of strength parameters depend on the stress history. The stress history dictates the behavior during shear in that the mineral grain structure of normally consolidated clays contracts in a drained test resulting in reducing volumes.

n) Disturbance: - shear strength of disturbed sample is less than that of the undisturbed samples.

2.8. Shear Strength Tests

When the shearing stress reaches its limit value due to failure of a loaded soil mass, soil deformation occurs. Shear strength of soil is crucial and useful for design work to produce safe and economic geotechnical structure. Soil shear strength is derived from two main components: (1) cohesion, c: - is a component independent of the normal stresses applied. (2) Internal friction angle (φ): - it is developed from the frictional resistance to translocation between the individual soil particles at their contact points (Al-Khafaji *et al*.., 1992).

Three tests were adopted: Direct shear Test, an unconfined compression test and fast undrained triaxial test as follows (Herrmann *et al.*, 2014).

Table 2-12: Classification of Clay soils based on undrained shear strength (KH Head, 1994)

Consistency Description	Undrained shear strength (kPa)
Very soft	<20
Soft	20-40
Firm	40-75
Stiff	75-150
very stiff	150-300

Hard	>300

2.8.1. Direct shear test (DST)

To measure the shear strength parameters (c & φ) of soils under drained, undrained, or consolidated-undrained conditions on preset failure surfaces, the direct shear test (DST) is employed. In contrast to the tri-axial test, the DST is an easy and quick test. Due to the shallow depth of the soil sample (e.g., 20 mm only), fast drainage of pore water in the soil sample during this test is typically simple. Most coarse-grained soils can use it. But tests can also be performed on fine-grained soils (Mir, 2021).

(a) Shear box test**: -** The 'immediate' or short-term shear strength of soils is measured using the shear box test, which is the simplest, most traditional, and easiest method in terms of total stresses. In this test relative movement of two halves of a square block of soil takes place along a horizontal surface. The shear box test is, in essence, an "angle of friction" test in which a continuous load is provided perpendicular to the plane of the relative movement while a horizontal shearing force causes one part of soil to slide along another (Head I., 1994).

(b) Vane shear test (VST): **-** In this type of shear test, relative rotational movement takes place between a cylindrical volume of soil and the surrounding material. An alternate test that can be used to gauge the undrained shear strength of excessively sensitive or soft clays is the vane shear test. Furthermore, it can be used to characterize saturated clays with soft to medium consistency, very sensitive or very soft clays, fissured soils, or soils that are particularly vulnerable to sampling disturbance without causing the sample to be disrupted (Mir, 2021).

2.8.2. Unconfined compressive strength test

In this test, the soil is solely subjected to an increase in axial load; no additional confining forces are applied to the soil. However, some restrictions, such as (1) the specimen needs to be completely saturated; otherwise, any air gaps will be compressed and expelled, increasing strength, and perhaps causing excessive movement to be recorded. When testing compacted clays, keep this in mind, especially if their moisture content is at or below the ideal level. (2) Premature failure may occur because of the specimen's inherent vulnerabilities. (3) Premature failure is more likely if the specimen contains little clay since it will have weak cohesiveness. (4) There is no control over the drainage conditions. (Herrmann *et al.*, 2014).

Its test results are the same regardless of the confining (cell) pressure when soil is saturated. For situations in which these conditions apply, measurement of total stresses might be all that is necessary (Wiley, 2009**)**.

2.8.3. Tri-axial test

Tri-axial tests are undoubtedly the most popular and common test method used today for measuring shear strength. They are preferred for theoretical reasons and because of their versatility. All types of strength tests can be carried out in the tri-axial cell (Wesley, 2010).

First, an equal amount of stress is applied to each surface of a cylindrical soil specimen under a confining pressure of σ_c. Then, until the specimen fails, the axial stress is raised, ϵ_a. As there is no shearing stress on the sides of the cylindrical specimen, the primary and minor principal stresses are, resp, axial stress (ϵ_a) and confining stress (σ_c) (Herrmann et al., 2014).

Unconsolidated-undrained (UU) tri-axial compression tests, also known as "Short-Term Stability Analysis," can be used to determine the undrained shear strength parameters (Cu > 0, φ= 0) for large engineering structures like embankments or dams built on or in cohesive soils when the construction time is too long and pore water pressure may dissipate very slowly under the gradual application of loading with time (Mir, 2021).

The three categories of triaxial test based on loading and drainage conditions are:

A) Consolidated drained test (CD)

The shear stresses (via the axial stress) must be applied slowly so that excess pore pressure which may develop in the middle of the specimen can dissipate to ensure fully drained conditions throughout. The rate of strain and hence time to failure will be determined by the permeability of the clay. This test involves allowing the specimen to drain as the axial load is applied (Herrmann *et al.*, 2014).

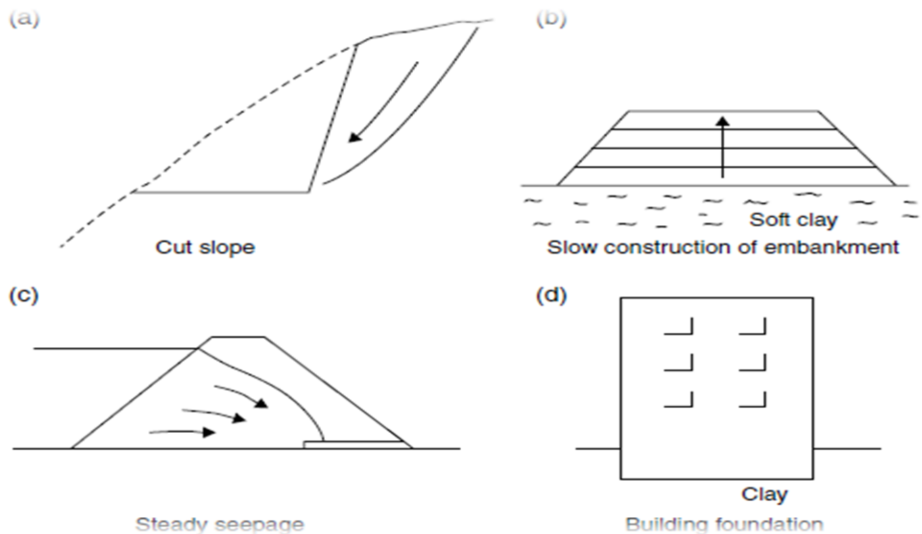

Figure 2-12: Long term stability analysis determined based on CD-test result.

B) Consolidated undrained test (CU)

Where during the undrained shearing stage the pore water pressure is measured at the base of the specimen sufficient time must be allowed to ensure that the pore pressure produced in the middle of the specimen is the same as at the base (equalization) where it is measured.

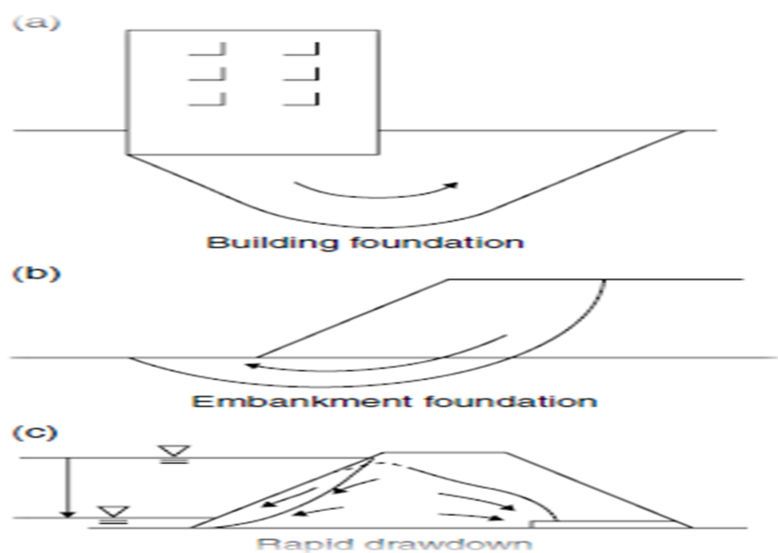

Figure 2-13: Long term stability analysis determined based on CU-test result (Lade, 2016).

If practical tests are conducted properly, both CD and CU provide the same strength because CU testing takes less time than CD testing, it is the most common tri-axial testing method. As a result, tube sampling was used to collect undisturbed samples from the field for CU testing.

C) Tri-axial unconsolidated undrained test (UU)

One of the most frequently used tests in practice to ascertain a clay's undrained shear strength at its in-situ natural moisture content is the UU test. Its primary use is in the design of shallow and piling foundations, in determining the initial stability of embankments on soft clays, and in determining whether clay fill is appropriate for the construction of earthworks. (1) A rate of strain of 2% of specimen length per minute is typically used in fast undrained compression tests (UU), when pore pressures are not monitored (Herrmann *et al.*, 2014).

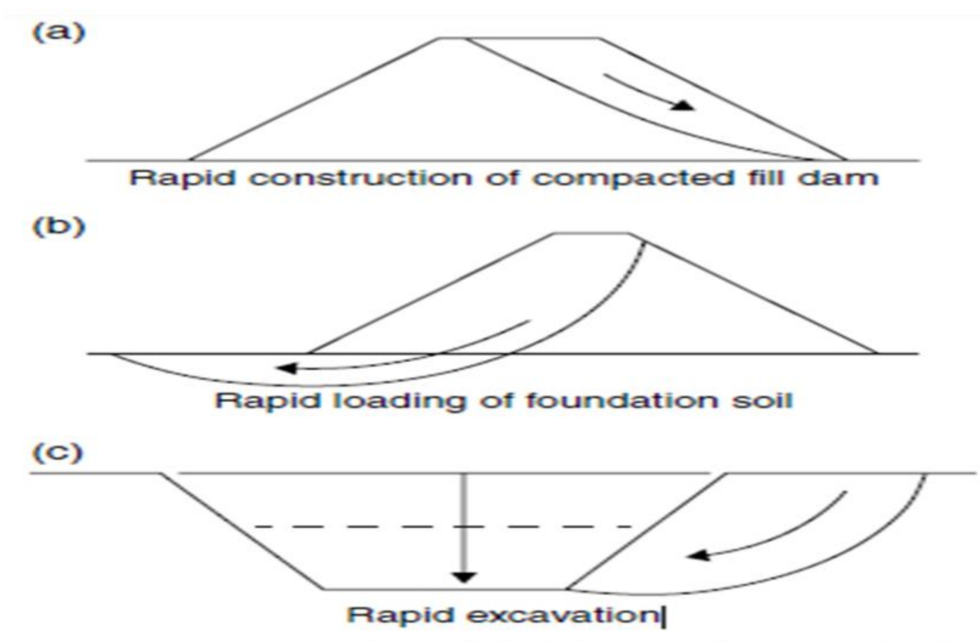

Figure 2-14: Short term stability analysis determined based on UU-test result (Lade, 2016).

According to Barness, (1995) the unconsolidated undrained (UU) test offers a good indicator of in-situ shear strength and is appropriate for analysis methods where the rate of loading is quick enough to prevent pore pressure dissipation, for bearing capacity, trench stability, etc**.**

According to Dr.Kr. Arora & et al., (2003), the failure envelope cannot be drawn in terms of effective stresses in a UU test. He also concluded that tests carried out at various confining pressures give constant effective stress because an increase in confining pressure causes an increase in pore water pressure for saturated soil under undrained conditions**.**

(OU, 2006) suggested that the outcome of the UU-tri-axial test is impacted and hence the larger undrained shear strength of the soil is produced by the test's vertical loading and higher strain rate, while the stress state and the sampling disturbance result in lower values of Su. As a result, the two factors balance one another out to produce a result that accurately represents the in-situ soil.

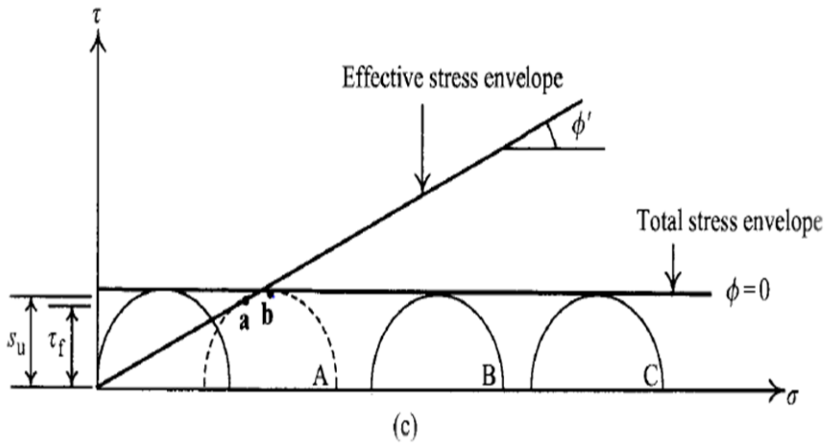

Figure 2-15: Principle of total and effective stress result in UU-tri-axial test (OU, 2006)

However, the self-compensation effect of the tri-axial UU test renders the obtained undrained shear strength capable of representing the inside undrained shear strength and the effect is not always reliable; the extra amount does not necessarily equal the lowered amount (Ou, 2006).

According to (Wiley, 2009) there are two situations in which the strength in terms of effective stress and the undrained strength will be the same.

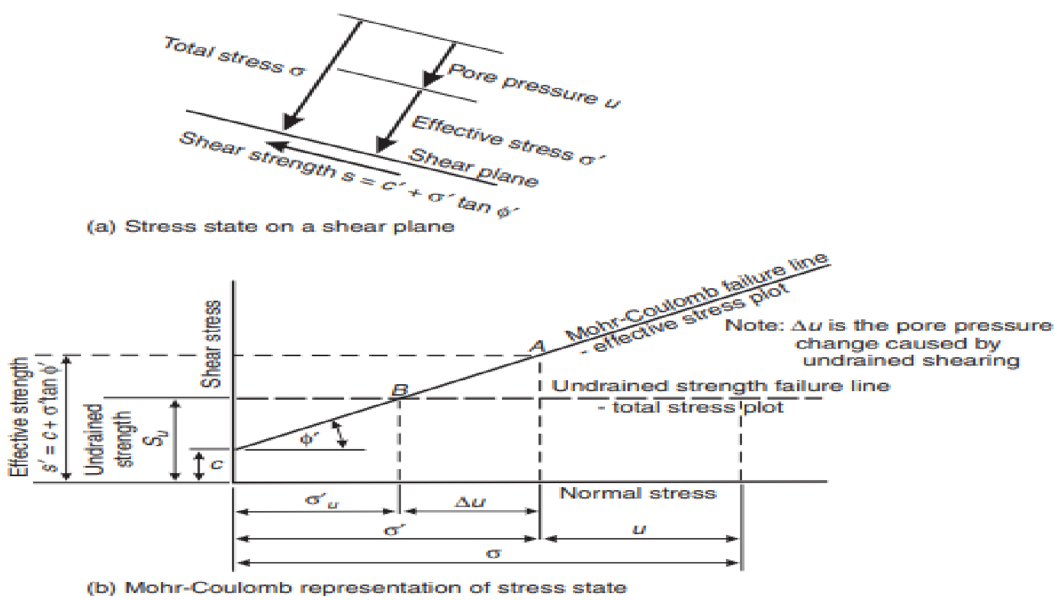

Figure 2-16: Principle of total and effective stress result in UU-tri-axial test (Wiley, 2009)

In an undrained situation the soil behaves as though it has no frictional component of shear strength. This reflects the test conditions under which the strength is measured; it still has a frictional component of shear strength dependent on its φ' value (Wiley, 2009).

2.9. Testing Program on UU-Tri-axial Test

2.9.1. Preparation of UU-Tri-axial Test Specimen

Specimens can also be created in the lab using a variety of techniques in addition to intact specimens from the field. This is crucial, particularly for clean sand deposits that cannot be sampled without causing disruption unless they are frozen in place, cored, and molded into the proper specimens while still frozen, and then analyzed after thawing inside the tri-axial equipment (Lade, 2016).

(a) Compaction of clayey soil: **-** Clayey soils are compacted in the field to improve their strength, dry density, and compressibility while reducing their compressibility, permeability, and volume change from swelling and shrinking. On the dry side of the ideal water content, there is minimal difference in strength, but on the west side, and at the same water content, they produce increasing strength in the order of kneading, vibratory, and static compaction (Lade, 2016).

The ASTM D698 (2014) Standard Test Methods for Laboratory Compaction Characteristics of Soil Using Standard Effort [12 400 ftlb/ft3 (600 kNm/m3)] or ASTM D1557 (2014) Standard Test Methods for Laboratory Compaction Characteristics of Soil Using Modified Effort [56 000 ftlb/ft3 (2700 kNm/m3] or other preferred procedures may be used to determine the dry density

(b) Soil preparation**: -** Unless specific conditions call for the inclusion of larger particles, air-dried, crushed soils used for compaction are then sieved through a No. 4 U.S. sieve. The needed number of specimens are then weighed off together with a buffer for determining the water content and specimen cutting waste. The wet dirt is again properly mixed by hand before specimen compression (Lade, 2016).

(c) Static compaction: - Simulating the soil structure created in the field by smooth steel drums or rubber tyre rollers, specimens that have been statically compressed mimic that soil structure. A steel tube with the appropriate specimen's diameter and length can serve as the cylindrical mold. To contain the dirt, mold with an extension collar would be needed. The specimen of compacted dirt is then pushed out of the cylindrical. When using multiple layers, the soil interface needs to be scarified before the next dirt layer is added. While the specimen is still in the compression mold, the ends are carefully cut to create square and smooth ends (Lade, 2016).

d) Vibratory compaction. Structure and attributes from vibratory compaction are like those from static compaction and kneading compaction.

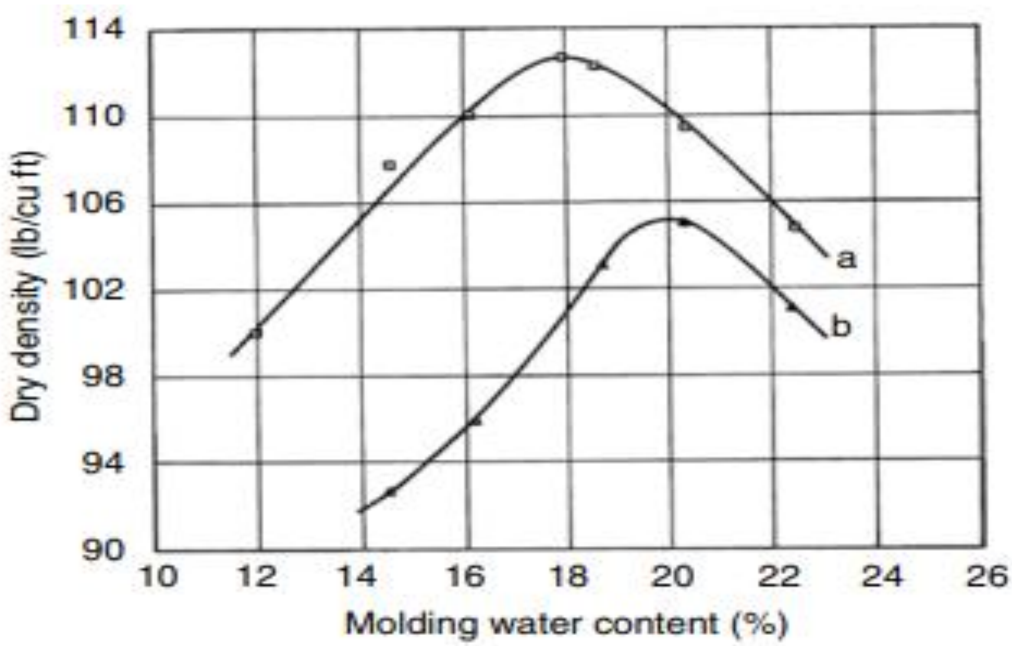

Figure 2-17: Influence of molding water content on particle orientation for compacted samples of Boston Blue clay (Lade, 2016)

(d) Kneading compaction: - Kneading compaction mimics the compaction produced by a sheep foot roller, which imparts significant shear pressures to the soil and creates a scattered structure. The compactive effort may be calculated as the compactive force per tamp multiplied by the number of tamps per layer multiplied by the number of layers in the specimen divided by the volume of the specimen. Thus, the compactive effort is measured in force per volume (lbf/ft3 or kN/m3) (Lade, 2016).

(e) Effects of specimen aging: - Clayey specimens may get stronger over time due to thixotropic action after compaction (Mitchell 1960).These specimens can be put in a water or oil bath to keep them at the same temperature and shield them from the environment (Lade, 2016).

(f) Compacted specimens: - To determine the specimen's weight, height, and diameter for specimens compacted in an external split mold, the specimen should be carefully taken out of the split mold. To the closest 0.01 g, calculate the weight. However, rounding measurements to the closest 0.1 g is sufficient for specimens weighing more than 1000 g. (Lade, 2016).

(g) Specimen installation: - The soil sample is now ready to be installed in the triaxial apparatus, regardless of the technique used to prepare it for triaxial testing outside the triaxial cell, such as trimming intact samples, compacting clayey soil, or another technique that enables the specimen to be free standing without collapsing (Lade, 2016)

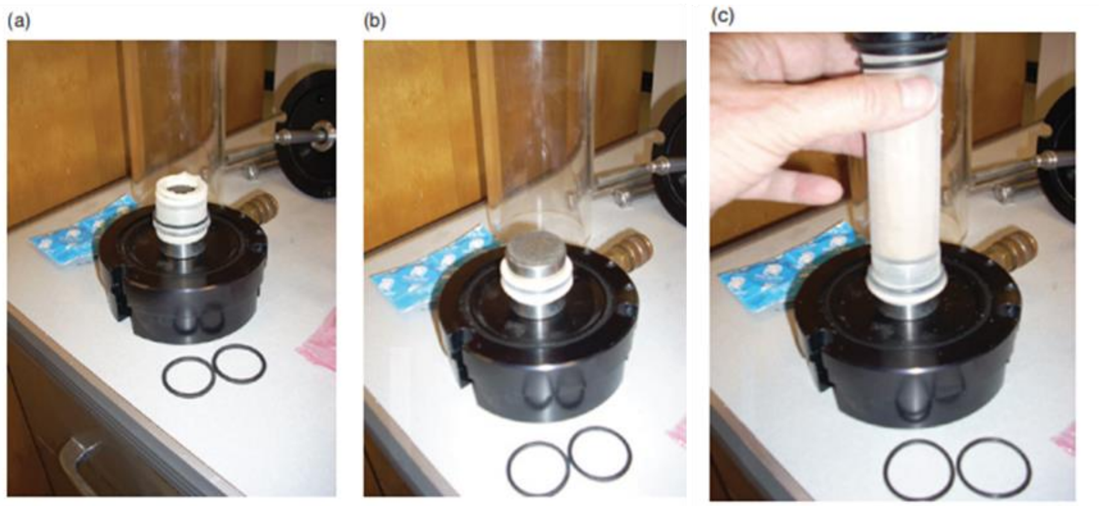

Figure 2-18: (a) and (b) prophylactics placed around base and sealed with O-rings and (c) rolled up around the specimen and sealed with O-rings around the cap (Lade, 2016)

(H) Unsaturated clayey soil specimen: - The membrane is positioned around the unsaturated clayey soil specimen as previously mentioned, and the specimen is set on the high air entry filter stone (Lade, 2016).

2.9.2. Saturation stage for “UU” tri-axial test

The various initial parameters of the soil sample before the saturation stage are recorded as:

1. Length = Lo (cm)
2. Diameter, Do (cm)
3. Cross-sectional area, $\text{Ao} = \frac{\pi}{4} * \text{Do}^2\ (\text{cm}^2)$ (5)
4. Volume, , $\text{Vo} = \text{Ao} * \text{Lo}\ (\text{cm}^3)$ (6)
5. Wet mass, Ms (g)
6. Water content, w_o (%)
7. Total soil particle density, $\rho\text{b} = \frac{Ms}{\text{Vo}} \left(\frac{\text{g}}{\text{cm}^3}\right)$ (7)

7. Dry density, $\rho d = \frac{\rho s}{1+wo/100}\left(\frac{g}{cc}\right)$ (8)

8. Voids ratio, eo $= \frac{\rho s}{\rho d} - 1 = Gs * \frac{\rho w}{\rho d} - 1$ (9)

9. Degree of saturation, So $= Gs * \frac{Gs*wo}{eo}(\%)$ (10)

Before shearing the soil sample in the "UU" test, make sure that the soil sample is fully saturated. But if not to saturate the soil sample, apply the first increment of cell pressure of about 35 kPa and watch/measure the pore water pressure being developed under the applied cell pressure until it remains constant (Mir, 2021).

Table 2-13: Cell pressures for saturation stage (Mir, 2021)

Sr No.	Depth, z (m)	Cell pressure increment for saturation stage (kPa)		
		Step-1	Step-2	Step-3
1	Less than 5	2.0σ'	1.5σ'	3σ'
2	5-10	1.5σ'	2σ'	2.5σ'
3	10-40	1.0σ'	1.5σ'	2σ'
4	Greater than 40	800	1200	1600

By applying alternate back pressure and cell pressure steps, saturation is maintained. Small differential pressures (5 or 10 kPa) or a minimal differential pressure equal to the initial effective stress can also be used to apply pressure. It takes longer to complete but is desirable because it tends to lessen the scatter of observed strengths (Mir, 2021).

Close the drainage valve and raise pore pressure to roughly 90-95 kPa (check pressure transducer or select using software as necessary) by applying back pressure (ub) against a constant cell pressure of 100 kPa (as an example). Make sure to maintain the appropriate cell pressure (100 kPa) and pore pressure (also referred to as back pressure, which will compel water to flow into the soil specimen in order to reach saturation) values (Mir, 2021).

Now let the water run into the soil sample by opening the drainage valve. Keep track of the pore water pressure's reaction, which will be rising. When the pore water level is steady, close the drainage valve and wait approximately an hour to see how the pore water reacts.

Record the original value of the pore water pressure as u1) i once it has stabilized.

• Increase the cell pressure by the subsequent predetermined increment (c)2, then measure how the pore water pressure changes. Drainage valve should be maintained closed, though.

• After the pore water pressure has been stable for roughly an hour, note the final value of the pore water pressure (u1) f) and calculate the net difference between u1) i and u1) f as the net increase in pore water pressure in comparison to the (c)2 cell pressure increment.

• Calculate the B-factor to determine the saturation level: $B = \frac{(\Delta u)f-(\Delta u)i}{(\Delta\sigma c)2i}$ (11)

• The saturation is complete if the B-value is close to one (> 0.98), and soil samples must be saturated for reliable measurements of pore water pressure and volume change. In an undrained triaxial test, the circumstance of no volume change may be simulated if the specimen is completely saturated. In a drained triaxial test, the volume change of the specimen can be calculated using the amount of water that enters or exits the saturated soil (Mir, 2021).

(Lade, 2016) explained that the major categories of field settings, replication of saturated soil conditions in the lab is essential due to the following reasons.

1. Natural soil deposits that have not been altered beneath the groundwater table. This includes dirt found in areas of the ocean with high pore pressure.

2. Naturally occurring or compacted soils that have saturated or may do so due to (a) percolation or (b) compression brought on by overburden pressure. It is necessary to test these two types of soil samples under completely saturated conditions.

(i) Insufficient complete saturation: Soil samples are frequently not completely saturated shortly before testing. The potential causes of insufficient saturation include the following:

1. Specimens from natural deposits may develop cracks because of sampling and unloading.

2. Specimens from heterogeneous deposits, such as varved clay, could undergo pore water redistribution and partial air replacement.

3. At the surface of samples of coarse-grained soils, menisci cannot form. Air entry, disturbance, and occasionally specimen collapse result from this.

4. As pore water pressure decreases because of sampling, dissolved gases are released, which causes partial saturation. This effect is more pronounced in (a) organic-rich soils where methane is created on-site and (b) soils found on the ocean floor where the pore water pressure change (from large, positive to negative) is more pronounced.

5. Air may be introduced when moving and pruning an unaltered specimen.

6. Air may get trapped between the specimen and membrane during configuration of the specimen setup.

7. Even when performed under water, granular soil deposition specimens are typically not completely saturated.

8. At the optimal water content, only 80–95% of samples produced by compaction are saturated. It should be noted that an originally saturated specimen may become unsaturated throughout the test if the soil tends to expand during shear, causing a fall in pore pressure. This unintended release of dissolved gases may subsequently lead to cavitation of the pore water, which occurs at 1 atm (or more precisely, at 17 mm Hg) for clean, de-aired water at room temperature.

(j) Consequences of partial saturation include Even a small amount of air will have a major impact on the pore pressures that develop during an undrained test. The lack of full saturation affects the pore pressure as well as the stress-strain relationship, the effective stress path, and the undrained strength. Figure 2.24 shows the effect of partial saturation on the compressive strengths of compacted kaolinite.

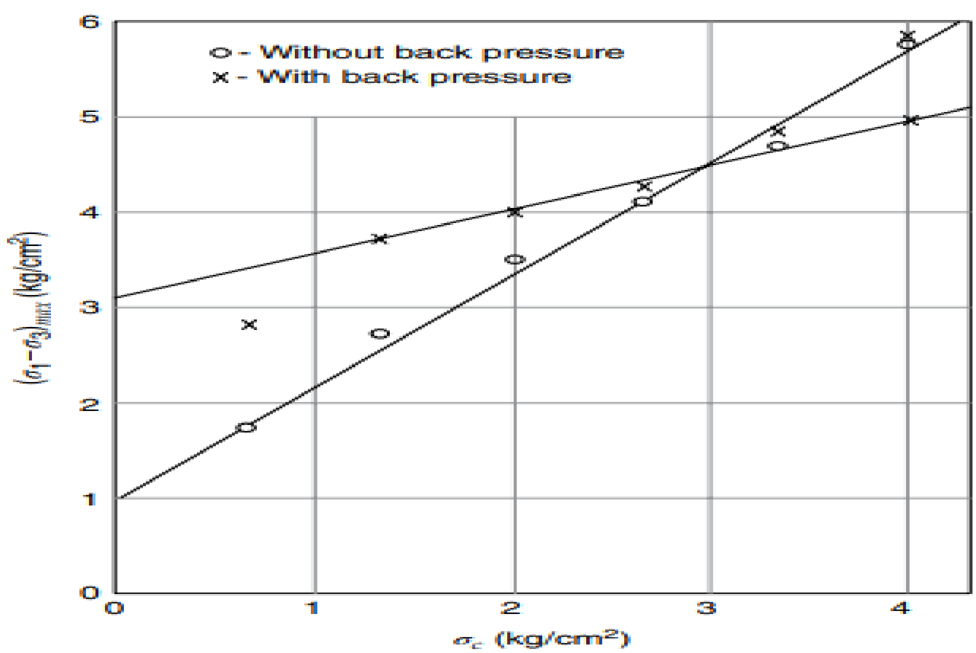

Figure 2-19: Effect of lack of full saturation on the compressive strength of compacted kaolinite. Reproduced from Allam and Sridharan 1980 by permission of ASTM International (Lade, 2016)

Thus, the compressive strength envelopes in Fig. 2.24 cross one another. The tri-axial specimens must be fully saturated because soils that contract under shear have lower undrained strengths when tested in the saturated condition than when evaluated at partial saturation. Testing such material at full saturation is prudent even though the soil may not reach complete saturation in the field. However, soils that expand under shear have higher undrained shear strengths when tested in the saturated condition, therefore if the soil in the field is consistently saturated, using the lower undrained shear strength from a half-soaked specimen might be too conservative (Lade, 2016).

(l) Application of back pressure: - Fundamental rules relating to gas-liquid systems can be used to describe the fundamental physical processes occurring during the process of saturating a soil specimen under pressure:

(m) Passive development of back pressure: -this is applied by raising the cell pressure and keeping the specimen in an undrained state where neither gases nor water is permitted to pass through the specimen boundaries. Air content of the sample at the initial pore pressure, u_0 is:

$$Vo = Va + Vad = Vs.(1 - So).eo + H.Vs.So.eo \tag{12}$$

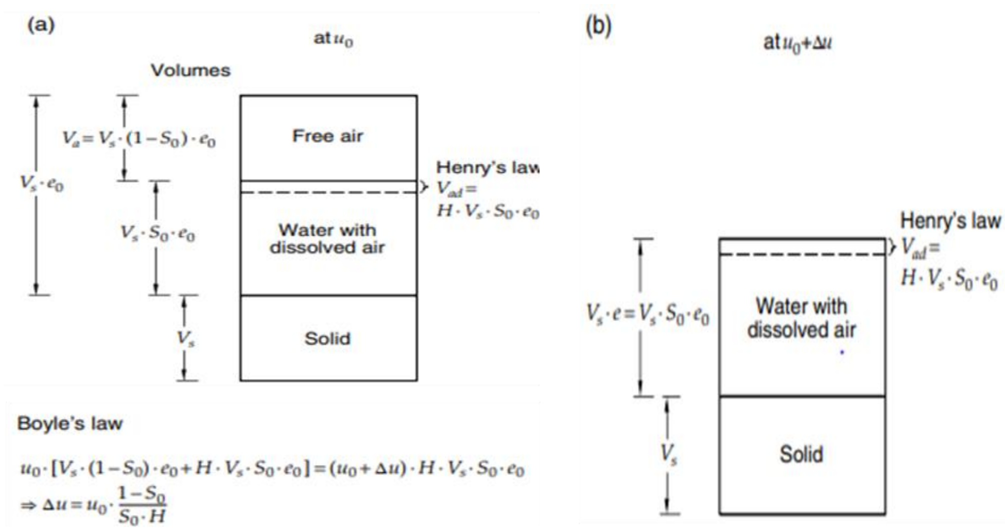

Figure 2-20: Determination of Δu, required to produce saturation of a soil specimen by passive back pressure. (a) Initial conditions of soil and (b) complete saturation of soil (Lade, 2016).

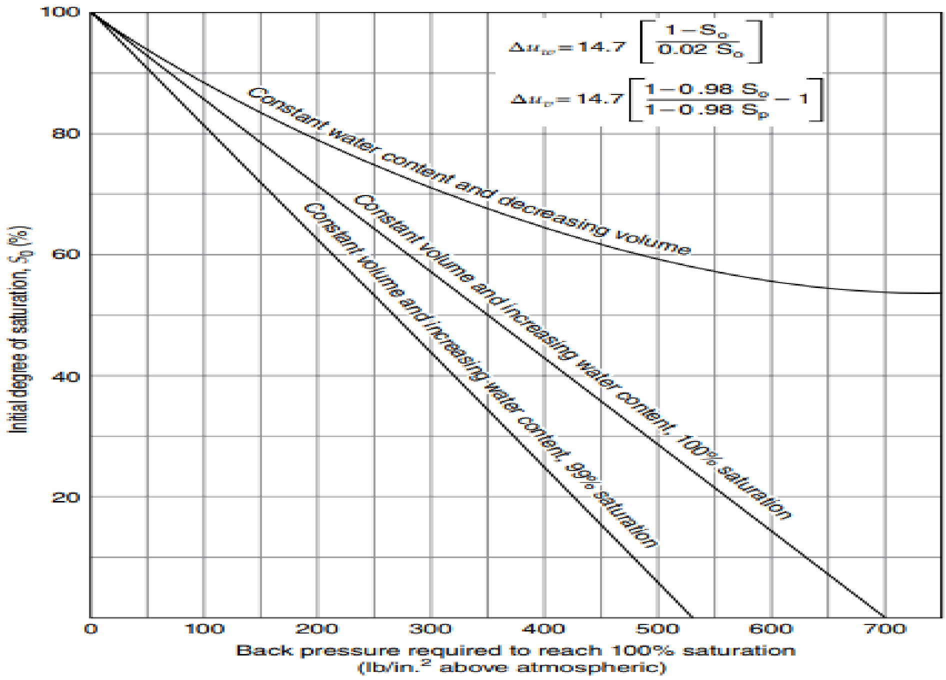

Figure 2-21: Magnitudes, Δu, increment above atmospheric pressure, required to saturate soil specimens, Reproduced from Lowe and Johnson 1960 by permission of ASCE. (Lade, 2016)

The first term in this expression accounts for the free air, and the second term represents the volume occupied by the dissolved air if it were extracted from the water and compressed at the current pore pressure.

$$uo.\,[Vs\,(1 - So).\,eo + H.\,Vs.\,So.\,eo\ ] = (uo + \Delta u).\,H.\,Vs.\,So.\,eo \qquad (13)$$

Which can be reduced to yield the increment in pore pressure:

$$\Delta u = uo.\frac{1 - So}{So.\,H} \qquad (14)$$

In which u_0 is the initial absolute pore pressure and S_0 is the initial degree of saturation. The total pore pressure or back pressure required in the specimen to cause full saturation is then:

$$Uback = uo + \Delta u = uo.\frac{1 - So.\,(1 - H)}{\mathrm{So.\,H}} \qquad (15)$$

Where the absolute pressure is u_{back}. The upper curve in Fig. 2.26 represents the increases in pore pressure, Δu, needed to completely saturate soil samples with different initial levels of saturation at atmospheric pressure. The UU test, in which the soil responds similarly, is the equivalent kind of laboratory test.

(n) Back pressure techniques: -To keep the effective confining pressure constant when a back pressure is applied, an equal amount of pressure is added to the cell pressure. Even if the back pressure and cell pressure are applied simultaneously. As a result, raising the cell and back pressures will initially result in a rise in the effective confining pressure of:

$$\Delta\sigma3' = \Delta\sigma3.(1 - B) \tag{16}$$

Because of this, applying the full amount of back pressure necessary to achieve complete saturation may cause the soil to be excessively compressed.

(o) Time for saturation by dissolving air: -Dissolving air in the pore water is a diffusion process that takes time. However, the time to reach full saturation can be substantially decreased by increasing the back pressure above the value required, td is given by:

$$td = \left\{\frac{1}{\mathrm{k}}\left[.\frac{1 - So}{1 + \frac{(1-H)}{\mathrm{H}}.R.(1 - So)} - (1 - Sf)\right]\right\}^{1/x} \tag{17}$$

Where R is the back pressure ratio—the difference between the applied and the necessary back pressure for full saturation, K and x are coefficients that can be derived from:

K = 0.0094- 0.01. So for So < 0.8

K = 0.0014 for So > 0.8 and x=0.085+0.0133. So, for 0≤ S ≤ 1. These expressions were created using experimental data that revealed some scatter, especially at low saturation levels. Even so, the calculation from equation K = 0.0094–0.01. So is accurate.

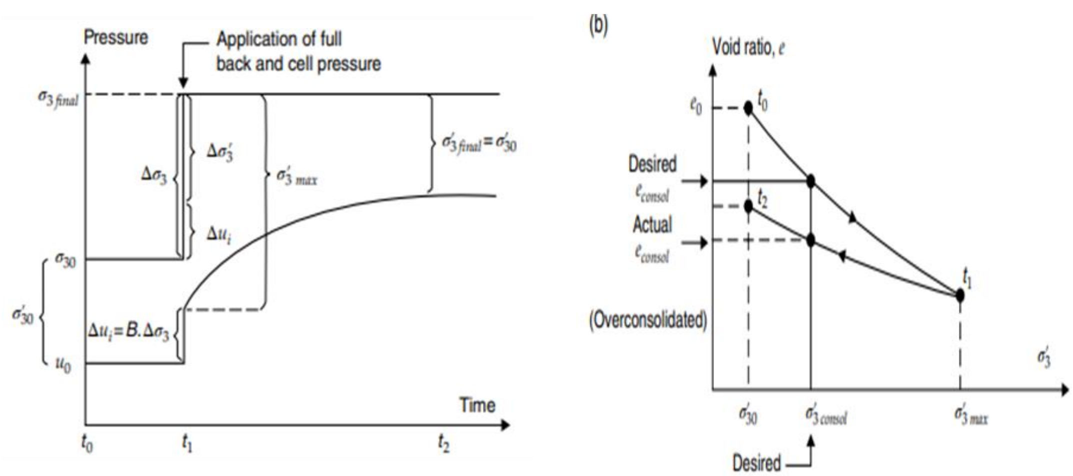

Figure 20-22: Application of full increments of U_{back} and σc for OC soil. (a) order application of cell and back pressure with time and (b) effects on σ’ void ratio relation (Lade, 2016)

The predicted time delays first rise and then fall with increasing value of so because K and x change with the initial degree of saturation. These relationships suggest that a wet specimen may require more time to saturate than a dry specimen for a given applied relative back pressure. Very high back pressures may occasionally be needed to fully saturate soil samples and shorten the time it takes for saturation to occur.

2.9.3. Shearing stage for "UU" tri-axial test

Mir, (2021) Once the saturation stage of tri-axial testing is complete, make sure that all drainage valves are closed, and it is ensured that effective cell pressure (σc' = σc-ub) remains constant. Now increase the cell pressure (effective confining pressure) to the desired value under which the soil sample is to be sheared in the "UU" test. The various initial parameters required for an undrained shear test are:

• Constant cell pressure, σc (kPa)
• Back pressure, ub (kPa), if used during saturation stage
• Eff. stress, σ′c (= σc - ub) (kPa)
Post saturation length, Lsat ≅ Lo(mm)
• If presumed that there is no volume change in soil specimen during saturation stage
• Post saturation X-sec Asat ≅ Ao (cm2)
• Strain rate, εr (mm/min), depends on data derived from consolidation stage.

The maximum strain rate to be applied is: $\epsilon r = \frac{\epsilon f * L}{100tf}\left(\frac{mm}{minute}\right)$ (18)

Where: εf = failure strain (tentatively assumed for undrained test), L = initial is length or height of soil specimen taken during shearing test (e.g., post-saturation in the UU test), and tf = time to failure unconsolidated-undrained tests on saturated soil for unconsolidated-undrained tests on saturated soil the volumetric strain is zero. According to (Bashir Ahmed, 2021)

According to (Lade, 2016) for unconsolidated-undrained tests on saturated soil, the volumetric strain is zero and using the small strain expressions for membrane corrections the following equation holds true.

$$\Delta\sigma acorr = -4Em * \frac{to}{Do} * \epsilon a = 0 \quad (19)$$

1. Bring the load cell piston in touch with the top loading cap on the soil sample very carefully.

2. Set the zero readings of load cell/proving ring and LVDT/dial gauge and record their initial readings, respectively.

3. Select the designated strain rate; usually 1%/min or 1.27 mm/min or 0.021 mm/s and start the load application.

4. Record the load readings corresponding to 50 divisions of displacement reading until the soil sample fails or at least 20% axial strain is achieved.

5. Once the soil sample fails (e.g., load decreases after peak point), record at least 6 to 8 points after failure to access the residual or ultimate shear strength of the soil sample.

6. Stop the test and release the cell pressure (e.g., after tri-axial shear failure of soil specimen) and dislodge the tri-axial cell cover from the tri-axial cell base carefully.

7. Remove the specimen from the tri-axial cell and place it on a white sheet of paper to sketch the mode of shear failure plane.

8. Weigh the soil specimen again and put the specimen into the oven for 24 hours for determination of final water content.

Note: In the "UU" test, it is presumed that the water content of the soil sample remains constant during the shearing stage by increasing the deviator stress.

- Designated confining stress or cell pressure = σc = σr (kg/cm2 or kN/m2)
- Change in length after tri-axial shear test, ΔL (cm) for each time increment
- Calculate axial strain, εa = (ΔL/L) ∗ 100 (%) for each time increment (Note that "L" is length of soil specimen after the Saturation Stage in the case of the "UU" test and length of soil specimen after Consolidation Stage in the case of the "CU" test).
- Corrected cross-sectional area for each value of strain is computed as: $\mathrm{Ac} = \frac{\mathrm{A}o}{1-\left(\frac{\epsilon \mathrm{a}}{100}\right)}$ (20)
- Calculate the load for each time increment, P (from load cell-data logger) (kg or kN)
- Corrected load, Pc (kN) = P ∗ F (where F is a conversion factor if required so)
- Calculate the deviator stress, σd = Δσ = P/Ac (kg/cm2 or kN/m2) each time increment

• Corrected deviator stress, $\sigma dcor = \sigma d - \frac{4Em * \frac{tm}{1000} * \frac{\epsilon a}{100}}{\left(\frac{Dc}{100}\right)}$ (21)

after applying membrane correction where: Em (kPa) is the modulus of rubber membrane, tm (mm) is the thickness of the rubber membrane, εa (%) is the axial strain. Dc (mm) is the corrected post-saturation diameter of the sample (= √4Acπ), and Ac is the corrected post-saturation average cross-sectional area of the sample.

• Calculate the axial stress, $\sigma a = \sigma 1 = \sigma d - \sigma c$ (kg/cm2 or kN/m2 for each time increment

An Unconsolidated Undrained (UU) triaxial test is a 'total stress' test since it is an approximate technique used to determine a soil's mechanical properties and give same deviatoric stress results for saturated soil under different confining pressure magnitude at failure.

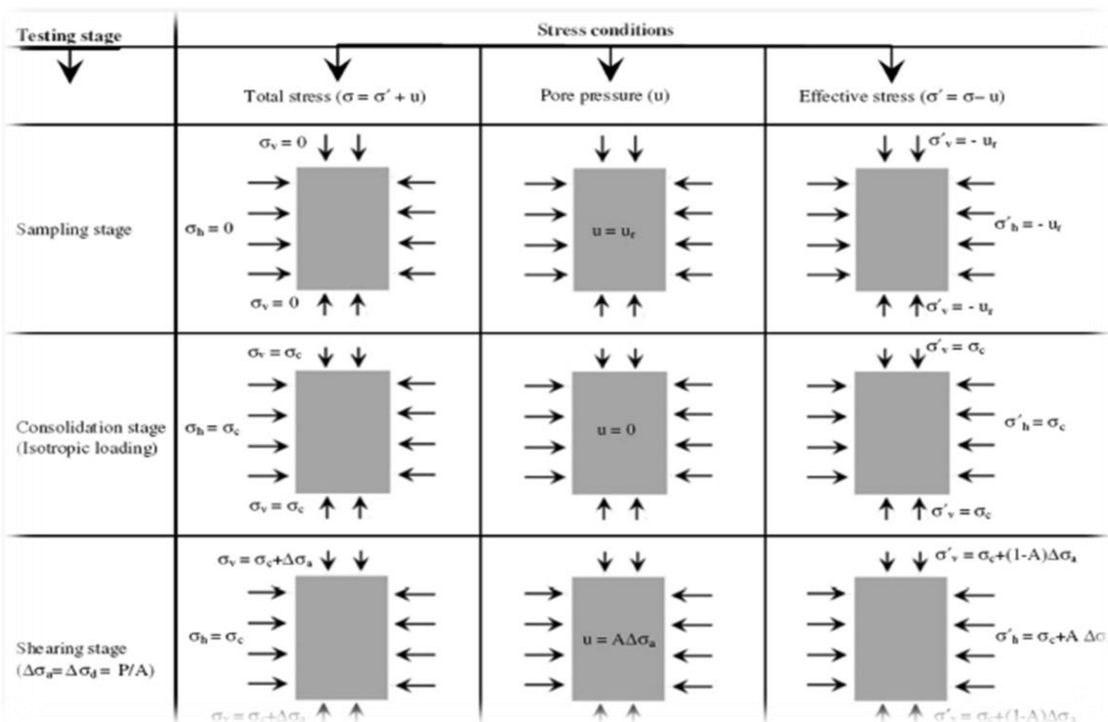

Figure 2-23: Stress state during tri-axial compression of a soil sample (Mir, 2022)

2.10. Previous Works Related to the Study.

2.10.1. Effects of specimen size on stress-strain and undrained shear strength of soil

ASTM 2850-15, (2015) specification for specimens said that they were to be cylindrical and have a minimum diameter of 3.3 cm (1.3 in.). The ratio of diameter to height must be between 2 and 2.5.

Chew et al., (2011) concluded that the combined effect of sampler size and testing sample size is also clearly visible when comparing the results of undrained shear strength tests using conventional (38 mm) and 200 mm diameter samples. The latter results are 20–70% lower than the former, indicating that the conventional small sample size result is not conservative.

According to Venkat Raman et al., (2015), increasing or reducing the length-diameter ratio of the specimen indicates a decline in strength. He also recommended that (L/D ratio) 2 is effective in determining the unconfined compression test for soils.

Table 2-14: Length-to-diameter ratios of 2.7,3.4 & 4.4 specimen diameters (Venkat Raman et al., 2015)

Diameter (cm)	L/D	Soil 1 (kN/sqm)	Soil 2 (kN/sqm)	Soil 3 (kN/sqm)	Soil 4 (kN/sqm)
2.7	1.5	12.753	13.734	14.715	16.677
2.7	1.75	30.411	4.905	8.829	29.43
2.7	2	5.886	18.639	5.886	22.563
2.7	2.25	11.772	10.791	4.886	13.734
2.7	2.5	17.656	17.658	7.848	26.487
Diameter (cm)	L/D	Soil 1 (kN/sqm)	Soil 2 (kN/sqm)	Soil 3 (kN/sqm)	Soil 4 (kN/sqm)
3.4	1.5	3.924	4.905	6.867	11.772
3.4	1.75	7.848	2.943	4.905	16.677
3.4	2	6.867	12.753	4.905	25.506
3.4	2.25	2.943	12.753	3.924	20.601
3.4	2.5	4.905	3.924	3.924	18.639
Diameter (cm)	L/D	Soil 1 (kN/sqm)	Soil 2 (kN/sqm)	Soil 3 (kN/sqm)	Soil 4 (kN/sqm)
4.4	1.5	3.943	8.829	4.905	4.905
4.4	1.75	2.943	9.81	2.943	4.903
4.4	2	0.981	17.658	1.962	2.943
4.4	2.25	5.886	9.81	6.867	1.962
4.4	2.5	1.962	10.791	3.924	1.962

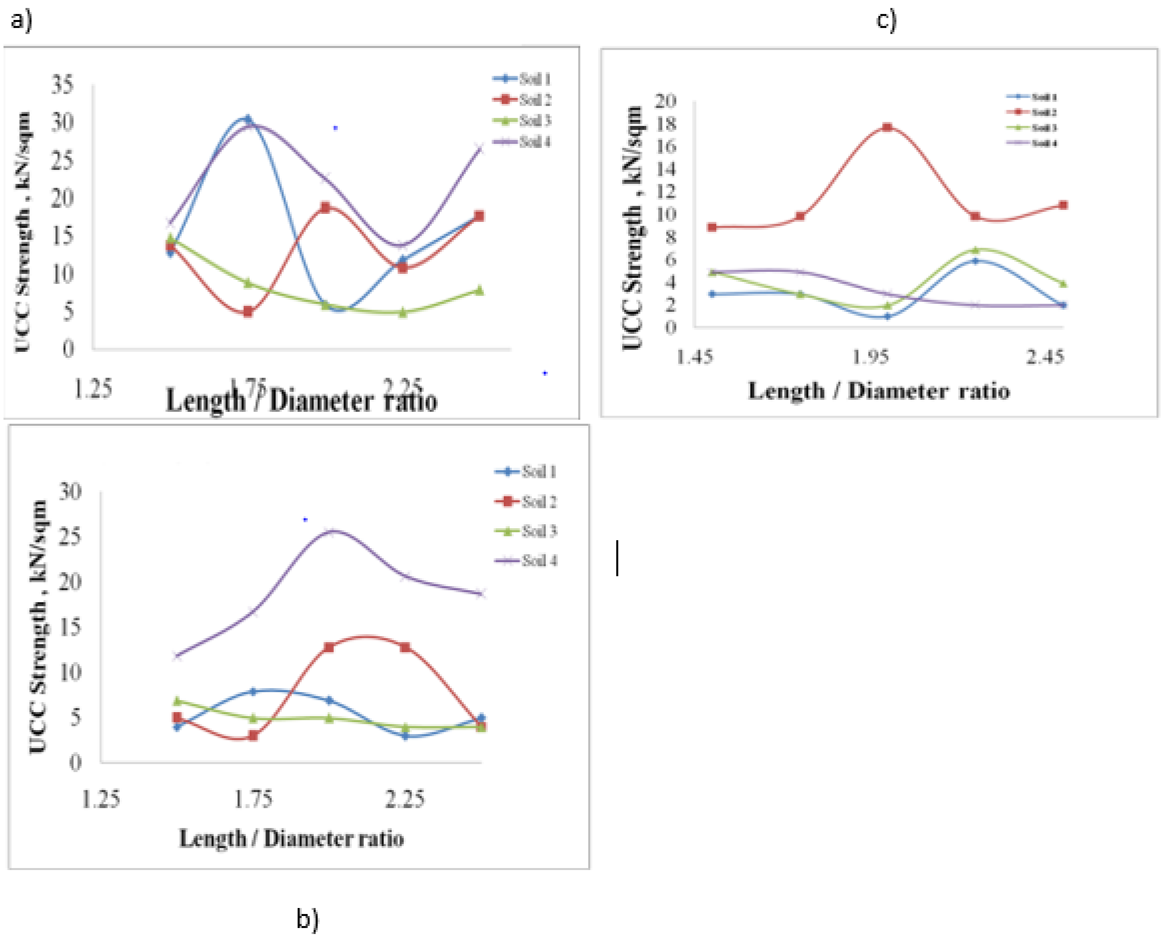

Figure 2-24: showing Length-to-diameter ratios of 2.7,3.4 & 4.4 specimen diameters (Venkat Raman et al., 2015)

The difference in length to diameter (2.7 cm) ratio and unconfined compressive strength conducted on all four soil samples is depicted in Figure 2.24 (a) above. In comparison to the soil 1, the graph demonstrates a 20% increase in compressive strength. There is a 30–40% reduction in compressive strength when comparing soil 2 to soil 3. When compared to soils 1, 2, and 3, the compressive strength of soil 4 increases as the length to diameter ratio increases.

The variation in the length to diameter (3.4) ratio and the unconfined compressive strength for each of the four soil samples is shown in Figure 2.24 (b). In the graph, the increase in compressive strength between the soil 4 and the other soils is seen to be 40%. The compressive strength of soil 3 is 10% lower than soil 2 when compared to it. When compared to soils 4, 2, and 3, the compressive strength of soil 1 decreases as length to diameter increases.

For each of the four soil samples that were taken, the length to diameter (4.4) ratio and the unconfined compressive strength are displayed in Figure 2.24 (c). The increase in compressive strength between the soil 4 and the other soils is seen to be 40%. When compared to soils 4, 2, and 3, the compressive strength of soil 1 decreases as length by diameter increases.

Unconfined compression experiments were conducted by H. Goonyella and T. Rusen (2015) while taking the influence of length-to-diameter ratio into consideration. They prepared 11 various length-to-diameter (L/D) ratios of cylindrical soil samples, ranging from 0.5 to 3 and concluded that strength and deformation behavior changed from ductile (for L/D = 0.50) to brittle (for L/D = 1.25) and a combination of ductile and brittle failure (L/D = 2.70). Moreover, although there are rare exceptions, peak stresses often occur within narrower axial strain ranges as L/D ratio increases. The failure pattern generally changes from ductile to brittle with increasing L/D ratio. Especially in the range of 1.25 < L/D < 2.5, brittle deformation predominates, as characterized by a distinct failure plane. At larger L/D ratios, the failure mechanism is mostly complex and chaotic.

(Amšiejus *et al*., 2009) among the writers to test various H/D ratios on clay, he concluded that it is insignificant effect of the H/D ratio on the shearing strength. When examining the rupture mechanism, one only sees a line failure in conventional samples and not in samples with smooth ends and H/D=1. Additionally, because of the impact of end constraint, the strength characteristics are marginally higher for the conventional samples. For samples with low H/D, both the stress-strain curve and the strains after failure are smoother and greater.

(McCauley *et al*., 2005) investigated the characteristics of Moraine clay and concluded that the cohesiveness value is larger in the sample with H/D=1 than with H/D=2, despite their almost identical friction angle.

(Güneyli & Rüşen, 2016) conducted unconfined compression tests on various clay sample types with H/D values of 0.5 to 3.0. For the samples with lower H/D, this study indicates a greater unconsolidated undrained shear strength. In undisturbed samples of normally consolidated and in some over-consolidated clays high strength failure may occur at 2 – 5 % axial strain.

(Amšiejus *et al*., 2009)) concluded that smooth ends combined with H/D=1 guarantee uniform stress and strain conditions, but do not eliminate it. Correspondingly, different papers were published as the non-uniformity of stress-strain behaviors of soils occurred depending on sampling height- to-diameter ratio during determination of soil strength using triaxial compression test.

Therefore, (Zarei *et al*., 2023) concluded that the specimen with H/D ratios and the friction between the triaxial sample ends and the platens are the main causes of the non-uniform stress-strain distribution in the soil sample. He also suggested that it is better to test large specimens of fine-grained soils at a low strain rate in the laboratory to have results more useful for engineering applications. Therefore, removing friction and shorter soil samples can be used, which cuts down on testing time, preserves samples, and prevents the measured strength increase brought on by friction between the sample ends and the platens. Compared to the standard height/diameter (H/D) ratio 2, the sample height could be smaller.

CHAPTER THREE

MATERIALS AND METHOD

3.1. Description of Study Area

The study was conducted in western part of Ethiopia, Bedele (also called Buno Bedele) town and separate Aanaa in south-western Ethiopia of the Oromia Region. Buno Bedelle zone at Gechi-yanfa road project which is located at about 466 km from Addis Ababa along the main road run from Bedelle-Agaro-Jimma to Addis. The geographical location of the project area is approximately in between 8°38'37"N to 8°39'25"N latitude and 36°36'33"E to 36°35'30"E longitude. The area has a temperature range from 15.39ºC (59.7ºF) and it is -6.84% lower than Ethiopia's averages with total average annual precipitation of 92.37 mm and altitude depth of 2006.99m above mean sea level. The area is found in the western part of the country and experiences the temperate climate of the Tropical wet and dry or savanna climate (Classification: Aw).

The Precambrian crystalline rocks are primarily felsic intrusive rocks with minor high-grade metamorphic rocks. The Ashangi Groups' trap series, which are composed of alkali olivine basalt and tuffs from the Paleocene through the Oligocene to the Miocene, cover most of the area. Rhyolites are an uncommon occurrence.

The soil throughout the route corridor is mostly silt, silty clay, sand, and clay that ranges in color from reddish, dark brown to light brown, with a small amount of gravel. The following part will deal with the specifics of the route corridor's soil extension. Although native subgrade is expected to have CBR over 3%, from visual inspection of the alignment subgrade, the liquid limit and plasticity index are high, and most of the alignment subgrade is evaluated as unsuitable roadbed materials.

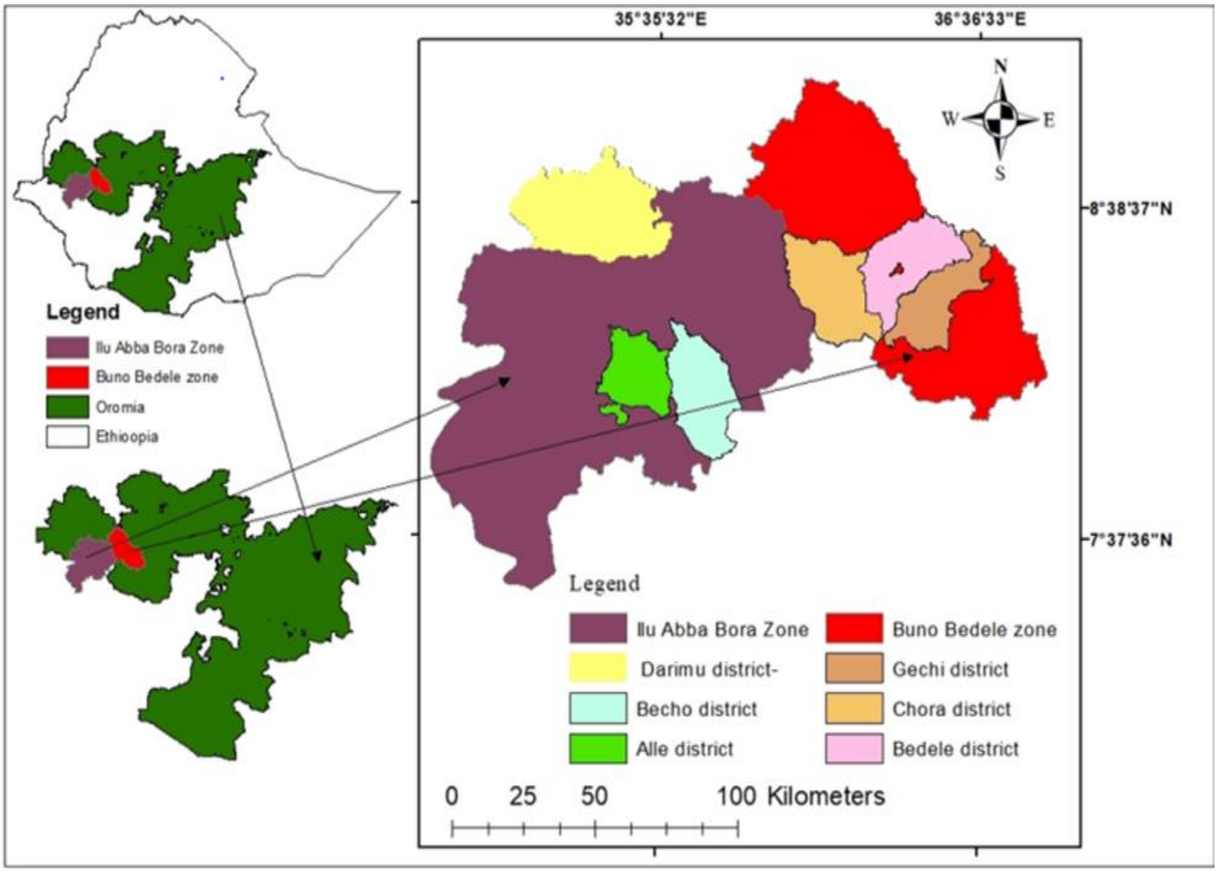

Figure 3-1: Map of study area

3.2. Weather and Climate of Study Area

It ranges from the high cold area known as "wurch" to the highly hot climatic condition area known as "Berha," having different physical measurement characteristics such as altitude, mean annual precipitation, and temperature as shown below. According to Berhanu *et al*., (2014), climate in Ethiopia is geographically quite diverse, which most commonly follows varied topography and categorized in to five different sub zones based on altitude, rainfall, and temperature variation.

Table 3-1: Climate zones of Ethiopia and their physical characteristics (Berhanu et al., 2014)

Zones	Altitude (m)	Mean annual rainfall (mm)	Mean annual temperature (°C)
Wurich (cold to moist)	>3200	900-2200	Below 11.5
Dega (cool to humid)	2300-3200	900-1200	11.5-17.5
Weynadega (cool sub-humid)	1500-2300	800-1200	17.5-20
Kola (warm semi arid)	500-1500	200-800	20-27.5
Berha (hot arid)	< 500	Below 200	Above 27.5

For this situation, the research region is situated at an altitude of 1950 m, or between 1500 m and 2300 m, and is designated as being in the Weynadega (cool sub-humid) climatic zone. According to ENMA statistics, the research area's mean monthly temperature is roughly 17.8 °C, falling within the designated climate zone's range (17.5 mm–20 mm). Additionally, August recorded the most monthly mean rainfall, at 218 mm, while December had the lowest monthly mean rainfall, at 4 mm.

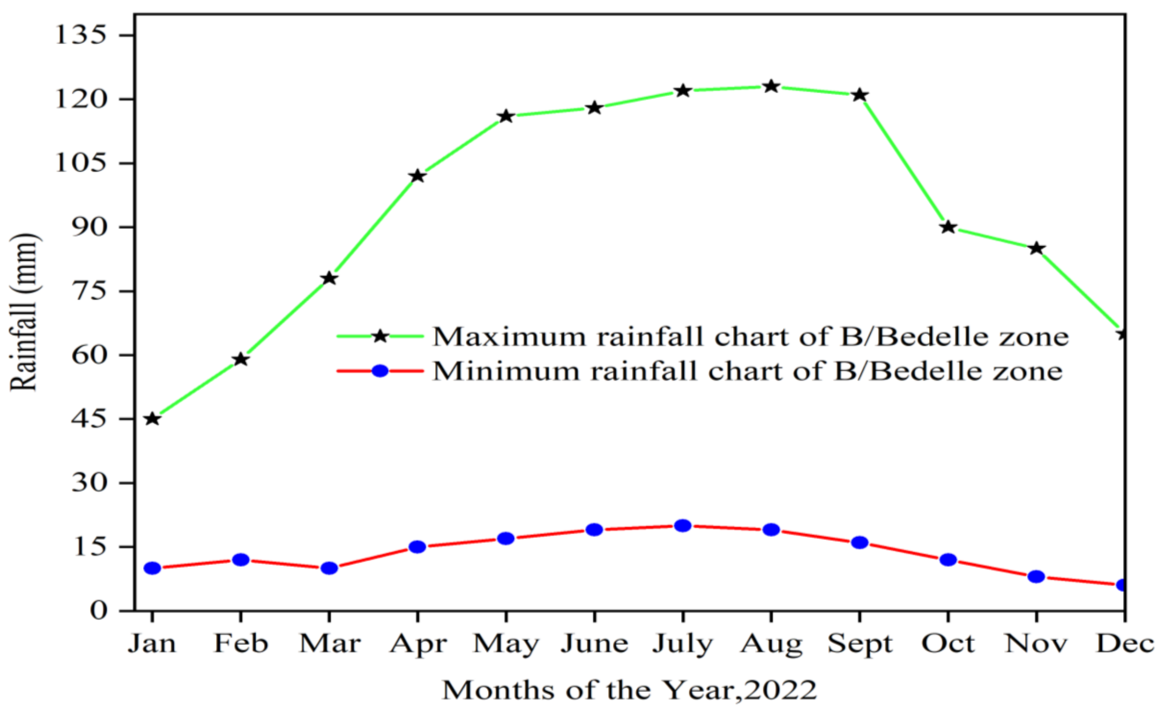

Figure 3-2: Monthly mean minimum and maximum rainfall of Bune Bedelle town (Source ENMA)

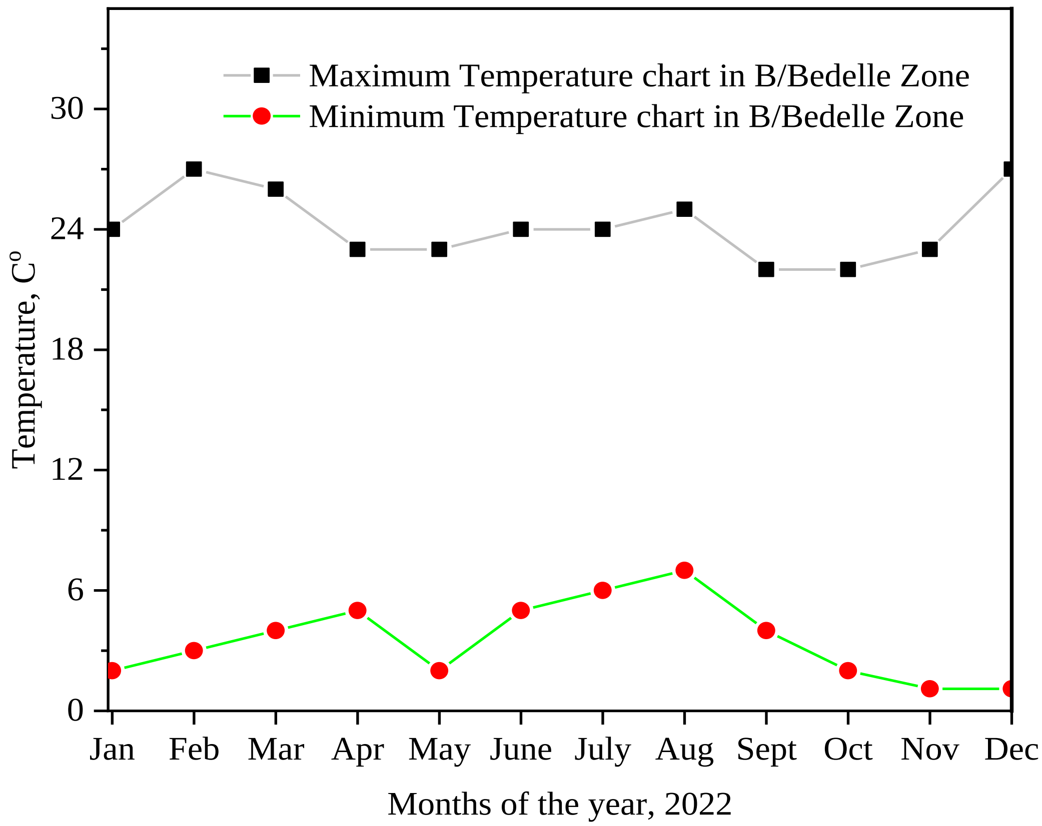

Figure 3-3: Monthly mean minimum and maximum Temperature of Bune Bedelle town (Source ENMA)

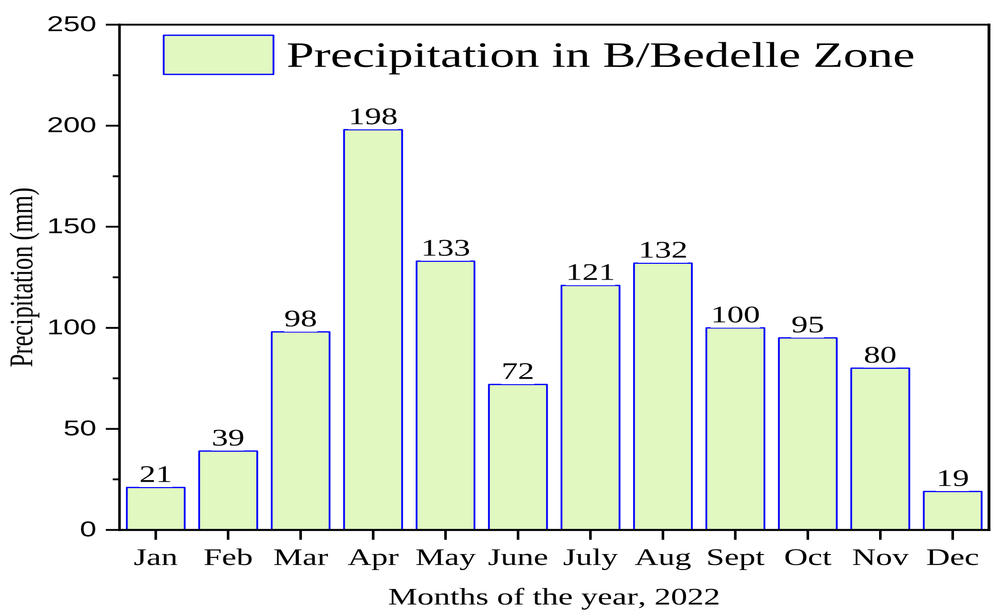

Figure 3-4: Monthly mean precipitation of Bune Bedelle town (Source: ENMA)

3.3. Materials

Red clay soil was chosen as the investigational material for this research project.

3.3.1. Red clay soil

The disturbed red clay soil used in this investigation was collected from working station 20+880 on the Gechi-Yanfa Road Project segment in Buno Bedelle. This area is selected due to its problematic area (unstable slope) just after construction activities took place. Then soil samples were packed into plastic bags having specified identity of borehole and transported to geotechnical laboratory for further investigation. And soil samples for natural moisture content determination from each of the test pits was collected and covered with plastic bags to maintain its moisture. The disturbed clay soil sample was air dried and then pulverized.

Figure 3-5: Geographical location of the test pits (20+880)

Table 3-2: Geographical locations of sampling sites

Sampling site	Latitude (Northing)	Longitude (Easting)
TP @CRW (20+880)	8°15'6.04"	36°34'19.21"

Figure 3-6: Red clay preparation process & sample used for the study.

As per (ERA, 2013) studied properties of 40% of soils in this area is characterized and classified as in organic clay (CH) having red color and existing road construction constructed on this soil is instable slope failure or shear failure especially during rainy season. Based up on this site characterization, borehole was selected to take samples from a test pit from around the slide or the appearance of shear failure sampling sites geographical locations shown on table 3-5. Laboratory tests such as Atterberg limits, linear shrinkage, differential free swell test, particle size distribution analysis, standard compaction, specific gravity, and consolidation and the main, undrained-unconsolidated triaxial tests were performed on saturated disturbed soil samples to determine the properties of soil in the study area and to define stress-strain behavior and undrained shear stress of the soil based on proper sampling size.

According to BS 1377: Part 2: 1990, samples were prepared for the proctor compaction procedure. The soil sample collected was air dried and sieved with sieve size of 4.75 mm as required for laboratory test. Then disturbed soil having known weight was remolded at minimum of 95% of maximum dry density with optimum moisture content by using appropriate molds under control of certain standard. Accordingly, three different sample sizes with heights of 75mm, 100mm, and 125mm and a constant 50mm diameter of total six samples were prepared. The modified protector compaction method was applied in this investigation. Maximum dry density (MDD) of (1373 kg/m3), and the optimal moisture content (OMC) of 27.34% of all samples are approximately kept constant. To achieve the same density for each remolded red clay soil samples, 181.57, 242.14, and 302.65-gram pair masses were, respectively, maintained constant.

3.4. Sample Preparation for Characterization Test

The bigger soil mass particles were crushed to a maximum particle size of 4.75 mm and removed from the dried soil sample that was taken from the test pit to prepare it for laboratory testing. Open-air drying was used for the sample.

Figure 3-7: standard compaction test (a) sample preparation (b) sample quartering (c) compacting (d) compacted sample trimming

3.5. General Flow Chart of the Study

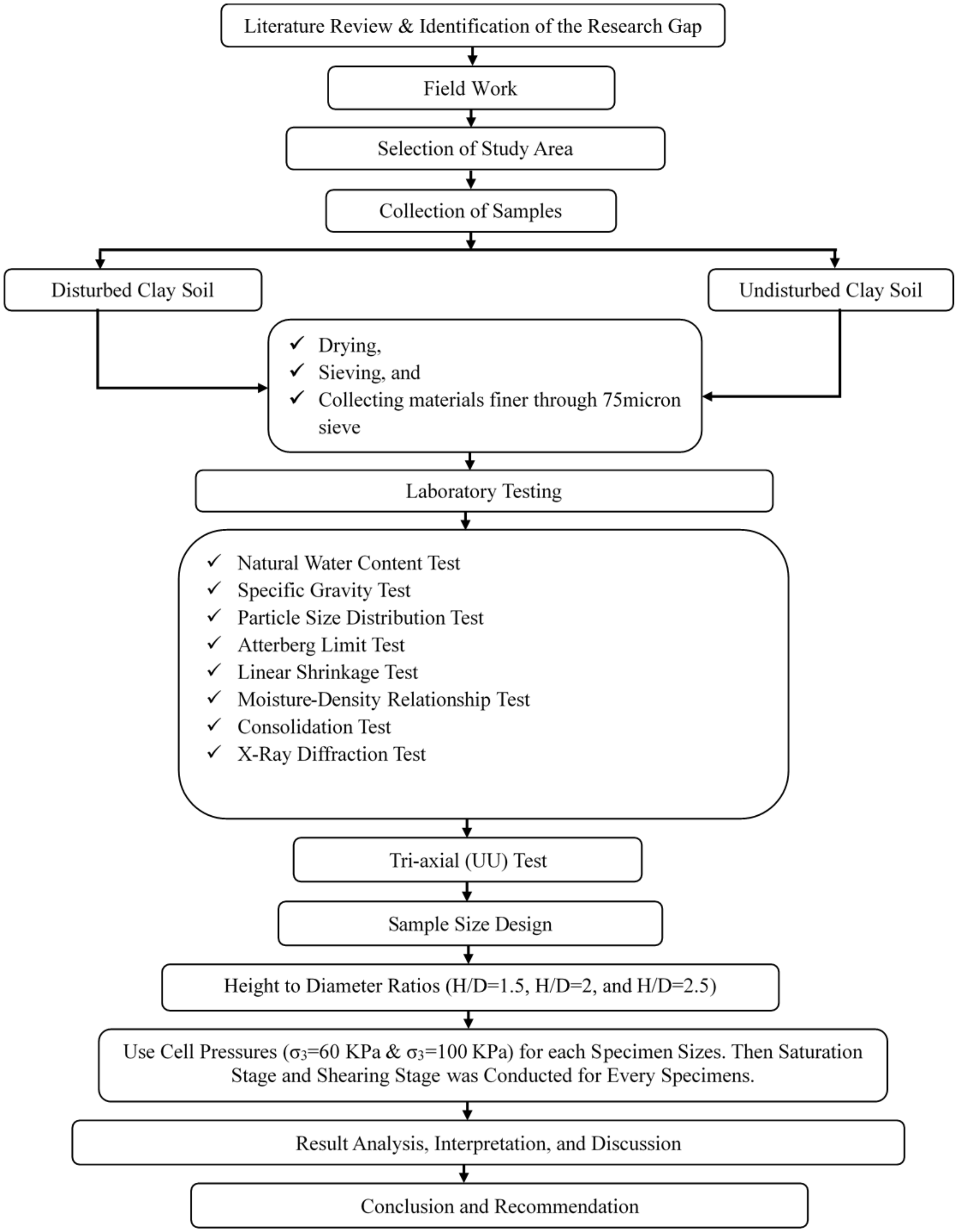

Figure 3-8: Summarized methodology chart of the study

3.6. Standard Laboratory Testing Procedures

The laboratory specifications used for this study were from ASTM and AASHTO standards that are presented in Table 3.3

Following preparation of the material required for the study, different laboratory experiments were performed to explore the effect of specimen size (H/D) ratios on geotechnical properties of red clay soil using undrained-unconsolidated-tri-axial test. Laboratory tests conducted for this study were listed with their standard test operation method in table 3-3.

Table 3-3: Laboratory tests conducted on materials.

No.	Name of Tests	ASTM	AASHTO	Others	Conditions
1	Moisture Content	D4643-00			Undisturbed
2	Specific gravity tests	D854-02			Air dried
3	Grain size analysis test	D 6913			Air dried
4	Free swell index tests			IS 2720-40	
5	Linear shrinkage tests				
6	Atterberg limit test	D 4318		BS 1377-2	Air dried
7	Standard compaction tests	D 698			Air dried
8	California bearing ratio	D 1883			Air dried
9	UU-tri-axial tests	D 2850-03a		BS 1377-7	Saturated

3.6.1. Clay soil moisture content

The natural moisture content will give an idea of the state of soil in the field, and also it shows the depth of groundwater table. The natural water content, also called the natural moisture content is the ratio of the weight of water to the weight of the solids in each mass of soil. This ratio is usually expressed as percentage. Tools used for this test were oven dry machine, digital balance having accuracy of 0.01g, moisture cans, gloves, and spatula. This test was conducted under control of ASTM D 2216 standard test methods for laboratory determination of water content of the soil.

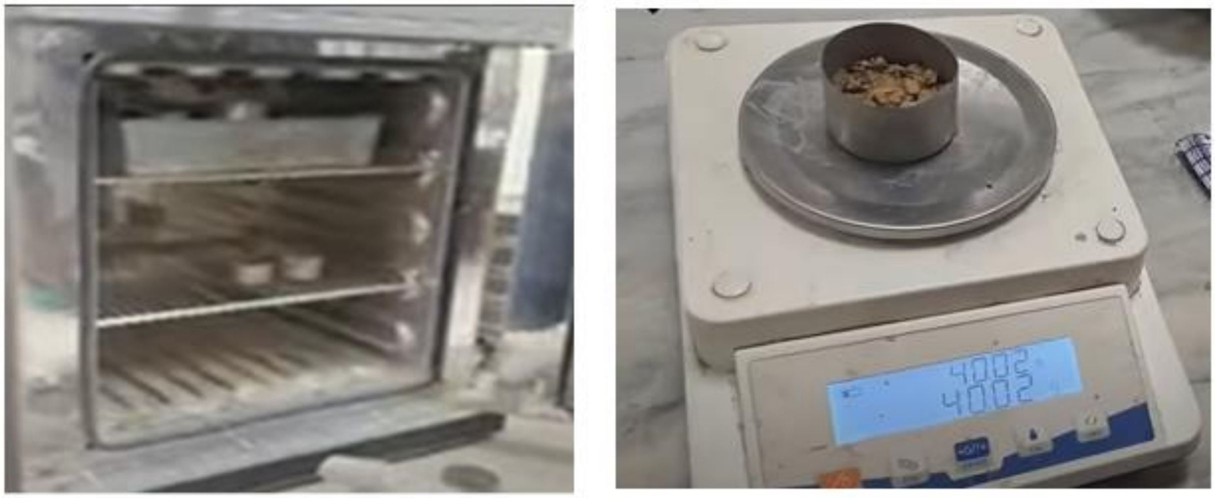

a) b)

Figure 3-9: Photograph view of (a) oven dry apparatus (b) specimen weighing.

3.6.2. Specific gravity test

The specific gravity of a material is the ratio of the mass of a unit volume of soil solids at a specific temperature to the mass of an equal volume of gas free distilled water at the same temperature. This test method is applied to the soil fraction that passes through sieve size of 4.75 mm and in case it was used to determine phase relationship of solids such as the degree of saturation, void ratio, and other soil properties. However, the test is used to determine the specific gravity of soil by using the density of water and usually reported at 20 °C temperature i.e., if testing temperature is different from room temperature (20 °C), result obtained is going to be corrected for temperature effect. To determine specific gravity of a single material, at least two trial tests were needed to take the average of the two result and report it as specific gravity. For the case of this study, about 10gm of dry soil sample finer than sieve No.4 was used to determine specific gravity of each material and calculated by the following formulas.

$$G_T = \frac{M_s}{M_s + (M_a - M_b)} * \rho_{w(T)} \qquad (22)$$

Where G_T is specific gravity of soil at testing temperature T(°C), M_s is mass of dry soil in gram, M_b is mass of pycnometer containing soil and water, M_a is mass of pycnometer filled with water at temperature T(°C) which is calculated from:

$$M_a = \frac{\rho_{w(T)}}{\rho_{w(T')}} * \left(M'_a - M_p\right) + M_p \qquad (23)$$

Where $\rho_{w(T)}$ is density of water at temperature $T(°C)$, $\rho_{w(T')}$ is density of water at temperature T'(°C), M'_a is weight of pycnometer filled with water in grams, M_p is weight of empty pycnometer in grams.

Finally, specific gravity calculated at temperature $T(°C)$ was corrected and reported for temperature effect by multiplying it with some factor k as shown in equation 15.

$$G_{20} = k * G_T \tag{24}$$

3.6.3. Grain size analysis test

Grain size analysis is a typical laboratory test conducted in the soil mechanics field, which used to determine the particle size distribution of soils. The analysis is conducted via two techniques which are through sieve analysis which can determine the particle size ranging from 0.075 mm to 100 mm, whereas distribution of particles smaller than 0.075 mm can be determined using the hydrometer analysis method.

i) Sieve analysis: is a method that is used to determine the grain size distribution of soils that are greater than 0.075 mm in diameter. It is usually performed for sand and gravel but cannot be used as the method for determining the grain size distribution of finer soil. The sieves used in this method are made of woven wires with square openings. Data obtained from sieve analysis may also be useful in developing relationships concerning the porosity and packing in the soil mass. Information obtained from the particle size analysis, uniformity coefficient (Cu), coefficient of curvature (Cc), and effective size (D_{10}), are also used to classify the soil and determine whether the soil is suitable for construction purposes. And also, this test result gives clue about soil water movement if permeability test is not available. The standard test method used for this test was ASTM D 6913.

ii) Hydrometer analysis: The hydrometer analysis of soil is based on Stokes law to determine size of soil particles from the speed at which they settle out of suspension in water. For this study around 50g of dry soil passing 75 µm sieve was considered and mixed with distilled water and dispersing agent like sodium hexa-metaphosphate, (NaPO3)6 to form a gentle slurry mix. Then the prepared slurry was backfilled to a cylinder having 1000ml mark capacity and 152H hydrometer was immersed into the cylinder to record a reading as per ASTM D 7928 standard method. Then from recorded data percent finer and respective particle diameter was determined which shows the grain size distribution for soils finer than No.200 sieve. However, when this result was combined with a sieve analysis, it can offer a complete gradation profile called particle size distribution curve of soils and addresses some interesting information such as C_u and C_C which are obtained by the following equations.

$$C_u = \frac{D_{60}}{D_{10}} \quad \text{and} \quad C_C = \frac{(D_{30})^2}{D_{10} * D_{60}} \tag{25}$$

Where: D_{10}, D_{30}, and D_{60} are the particle size that corresponds to the percent finer of 10%, 30%, and 60%, respectively.

3.6.4. Atterberg limit

The soil's plastic limit (PL), liquid limit (LL), and plasticity index (PI) were all determined using this accepted laboratory test protocol. The plastic limit is the moisture content at which the soil pastes crumble when rolled to a diameter of 3 mm. The soil sample for the plastic limit test should pass through a 475 m sieve. Atterberg limit tests are an investigation conducted on fine-grained soils to determine the amount of water required to attain different behavioral states. This test is done to determine the liquid limit, plastic limit, and the plasticity index of the soil which has a significant role in soil classification system. The mass of dry sample passing through sieve No.40 (425 µm) was used to perform the tests as per ASTM D 4318 standard process.

Liquid limit (LL): is arbitrarily defined as the water content, in percent, at which a paste of soil in a standard cup and cut by a groove of standard dimensions will flow together at the base of the groove for 13 mm when subjected to 25 shocks from the cup being dropped 10 mm in a standard liquid limit apparatus operated at a rate of two shocks per second. To conduct the test first, the soil sample was exactly mixed with water by repeatedly stirring, kneading, and chopping with the spatula and placed it in the Casagrande cup. The cup containing the sample was lifted and dropped at a rate of 2 drops/sec until the two sides of the sample come in contact at the bottom of the groove, along with about 13 mm. The number of blows required to close the grove to this distance was recorded, and its moisture content was determined. The relationship between the water content and the number blow is plotted on xy plane and the water content correspond to 25 blows is called liquid limit of the materials.

Plastic limit (PL): is the water content at which soil change its state from a plastic to a semi-solid state. This test involves repeatedly rolling sample paste on a smooth glass plate into a 3 mm thread until it reaches a point where it crumbles. Then, water content of rolled thread was determined and recorded as a plastic limit.

Plasticity index (PI): is the difference between the liquid limit and the plastic limit of soil and described as the range of moisture at which a material behaves in a plastic state, which used in classifying fine-grained soils. The Atterberg limits of cohesive soil depend on several factors, such as amount and type of clay minerals and type of adsorbed cation. Nevertheless, like any classification system, the Atterberg limits when used properly, provide a reliable index to the clay properties. Depending on the test procedures stated above, liquid limit and plastic limit tests were conducted.

3.6.5. Linear shrinkage test

Linear shrinkage is the percentage decrease in length of a wet soil sample filled into the standard mold when it gets fully dried, starting with a moisture content of the sample from liquid limit. The test was conducted based on BS 1377-2 standard method. To perform the test, an oven dried sample of about 150g passing through a sieve size of 425 µm is needed. Then a sample having known mass was mixed with water to attain its liquid limit. Finally, mud prepared was filled and compacted into standard mold which have greased its inner faces and put it inside an oven dry machine to remove available moisture in the soil sample and determine the compressed length of dry sample. Then linear shrinkage was calculated by the following equation, shown for every sample separately.

$$\text{Linear shrinkage(LS)} = \frac{(L_O - L_D)}{L_O} * 100\% \tag{26}$$

Where: L_O is original length of wet sample and, L_D is oven dried length of dry sample.

3.6.6. Moisture-Density Relationship

Laboratory standard compaction tests were carried out on plain soil to determine optimum moisture content and maximum dry density of material Specimen. In this research, standard proctor compaction test was employed by 600KN-m/m^3 standard effort in the mold having 4 inches (101.6 mm) diameter & internal effective height of 4.6 inches (117 mm) under which the material was compacted into three layers by applying 25 blows in each layer(ASTM D 698, 2000). Moisture was started from 10% (250ml) for the initial sample, and the wet density was measured in each step until it becomes maximum and then decreasing after increasing water content. After measuring wet mass for the soil sample for different water content, a portion of the sample from top, middle, and bottom was considered to in an oven dry to fix average moisture content available in the soil. Then the dry density of each sample at different moisture content was calculated using equation:

$$\rho_{dry}(g/cm^3) = \frac{\rho_{wet},\ g/cm^3}{1+w} \tag{27}$$

Where: ρ_{dry} is dry density of sample, ρ_{wet} is wet (bulk) density of sample and w is average moisture content in decimal number.

Dry density obtained was limited to be under the linear portion called ZAV line which illustrates that the soil mass was below saturated condition and all void volume between particles were filled with water and calculated by equation.

$$\gamma_{dry}(ZAV) = \frac{G_s\gamma_w}{1 + wG_s} \tag{28}$$

Where: $\gamma_{dry}(ZAV)$ is dry unit weight of saturated soil, γ_w is unit weight of water and w & G_s are respective average water content and specific gravity of samples.

3.6.7. Consolidation test

The consolidation test was conducted according to the procedure given by ASTM D 2435 standard method. The samples for the consolidation test were prepared by mixing the soil with the respective optimum moisture content that was obtained from standard compaction test and then compacted to attain MDD in standard odometer specimen ring having 60 mm diameter and 20 mm height. The samples were fixed in the consolidation cell with height of 20 mm and immersed in water to make it under fully saturation. Then a consolidation test was conducted by applying incremental loads starting with 800 kPa and ending with 1600 kPa. At each loading stage, the deformation at 0.1, 0.25, 0.5, 1, 2, 4, 8, 15, 30, 60, 120, 240, 480, and 1440 minutes was recorded on an observation sheet for further analysis using Casagrande's logarithm of time fitting method. When the loading of 1600kpa reached, unloading stages were start conducting by reducing constant load. This test was conducted for natural red clay soil to investigate effect on coefficient of consolidation, compressibility index, coefficient of the volume of compressibility, and initial void ratio of the sample.

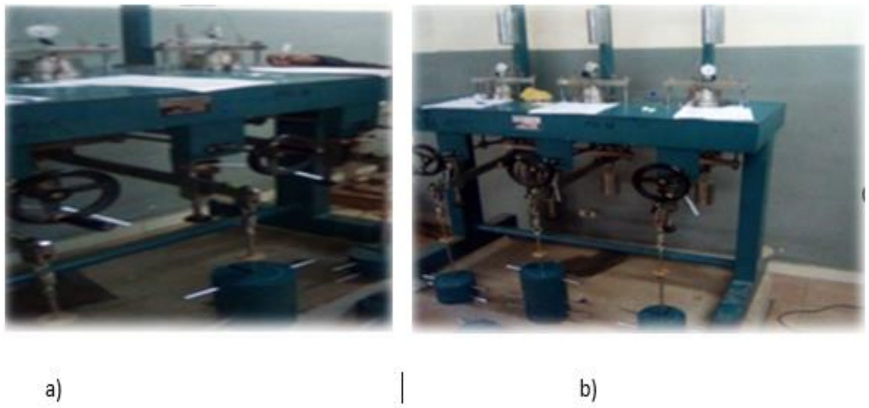

Figure 3-10: Photographic view of (a) consolidation apparatus (b) specimen mounted in consolidation cell.

3.6.8. X-ray diffraction

XRD is a technique used to identify the different mineral components present in the sample materials. The percentage of the fine powder from the weakest red clay soil that passed through the screen with a size of 75 m was used for X-ray diffraction testing. CuK radiation (= 1.5406) and an X-ray diffractometer were used to record an X-ray diffraction pattern. The diffraction angle, 2, varied from 10° to 80° in steps of 2=0.02°. The peaks of the XRD data patterns were analyzed using the "X-Pert High Score" software program to identify the various phases of each material, and the interplanar spacing (d) was computed using the Bragg's equation shown below.

$$d=n\lambda/2\sin\theta \tag{29}$$

Where: n is Bragg’s constant equal to 1, λ is wavelength =1.5406Å, θ is Bragg’s angle in radian and d is inter planar spacing in Å.

Red clay soil samples were taken from road construction sites in Gechi Yanfa below a depth of 3 meters, preventing the presence of organic materials and obtaining representative samples. The XRD test curves (see figure below) show that the absolute peak magnitude of the 2-theta value is 27.56°, which corresponds to the chemical formula $Al_2O_3\,(SiO_2)_2(H_2O)_2$. This is a sign that the chosen soil sample contains a high concentration of quartz as well as interspersed illite and Kaolinite clay minerals.

3.7. UU-Tri-axial Testing Procedure

Tri-axial test is the most widely used test method for determining the strength and stress-strain properties of soil. It is assumed that soil specimen deforms uniformly during the test. Cohesive soils mobilize shear resistance through their cohesion, and therefore cohesion resistance is considered as the most important mechanical property to analyze cohesive soils' response to loading. The mechanical behavior of soil is complex and is often evaluated by obtaining the stress-strain behaviors and volumetric response using single element laboratory testing.

3.7.1. Red clay soil specimen preparation for UU-Tri-axial Test

(A) Sample Preparation

Samples were collected from Gechi-Yanfa road Project from one test pit of working station at 20+880 in Buno Bedelle zone. Once sampled, the nominal moistures content of the sample was first determined by drying the sample at 110 C^0 for 24 hours. Larger particles of soil mass were pulverized to the maximum particle size of 4.75 mm and prepared for the laboratory tests. The dry soil was mixed thoroughly at the OMC values, by adding the required amount of water to avoid the effects of moisture content (w), void ratio (e), and natural density (w). So therefore, soils were remolded and compacted based on OMC and MDD results. To perform an unconsolidated undrained tri-axial shear test at various length-to-diameter ratios, ASTM 2850-15, (2015) recommends that cylindrical soil sample having a length to diameter ratio of 2 to 2.5.

However, as the aim of this thesis is to investigate the effect of specimen size of red clay soil at full saturation, checking another specimen size with 50 mm in diameter and aspect ratios of 1.5, 2 & 2.5 is the intent of the work. Thus, preparations of the samples were conducted by using a thin-walled stainless steel sampling tube with an inner diameter of 50 mm, with varying lengths. The soil sample was then prepared using sample tubes of 50 mm diameter and extracted from the sampler tubes using sample extruder. The samples extracted were then trimmed to the required length for the H/D ratio as shown below. Table 3-4 shows three selected heights to diameter ratios used in the laboratory tests.

Table 3-4: Prepared sample into selected different heights to diameter ratios

S. No.	Height (mm)	Diameter (mm)	Height to diameter ratio
1	75	50	1.5

2	100	50	2
3	125	50	2.5

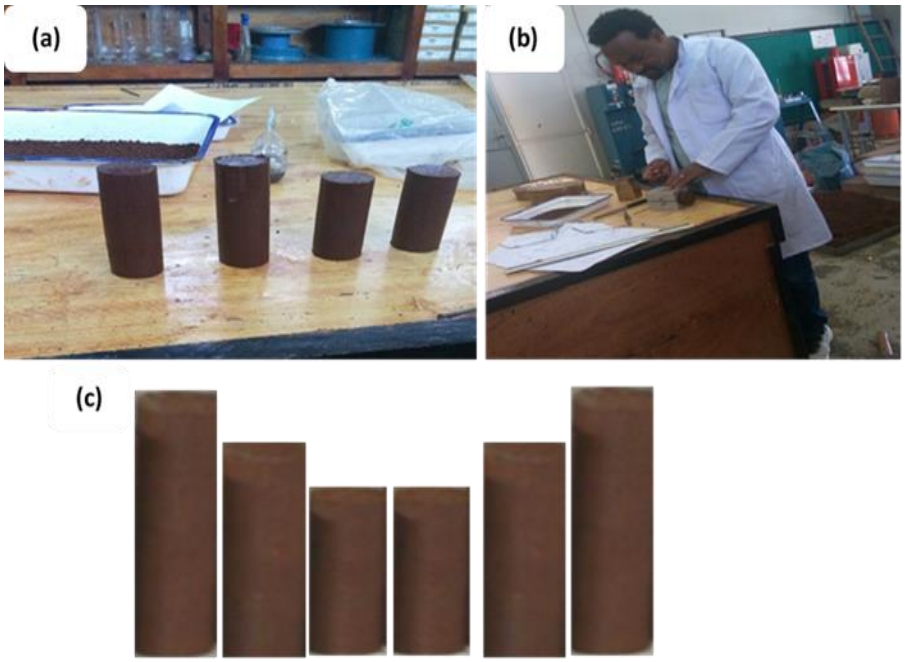

Figure 3.11: Image (a) Remolded sample (b) trimming of remolded sample into different aspect ratios (c) Specimen after trimming.

Unconsolidated undrained Tri-axial tests were conducted on the soil sample with different H/D ratios of 1.5, 2 and 2.5. The test program was designed to study the effect of aspect ratio (H/D) on the stress-strain behavior and undrained shear strengths of the clay soil. The shear test was conducted under strain-controlled conditions or at a constant loading rate of 1mm/min.

To conduct UU tri-axial test, the specimens need to pass through two important stages with constant initial conditions and specified confining pressures.

Accordingly, the test has passed through two stages: -Saturation stage and shearing stage.

3.7.2. Specimen saturation stage for UU-Tri-axial Test

In this stage soil sample was wetted until it is fully saturated. This could be conducted by filling up the cell cylinder with de-stilled water and/or allowing water to flow into the specimen through the back pressure line. As a result, to determine the effect of pore-pressure coefficient (B), in this study the UU tri-axial shear test was conducted by varying the cell pressure between 60KPa and 100KPa.Skempton's parameter B, which is assessed before shearing, was used to develop criteria for the verification of full saturation in tests and three different types of over consolidated cohesive soil: low, medium, and high plasticity clays were known with these initial values 0.8, 0.7, and 0.4, of B respectively. Equation (15) was used to determine the B value for each specimen (BS 1377- Cl-8, 1990).

Tibebu, (2008) stated that back pressure is employed to saturate soil sample before any triaxial test is commenced and done by increasing pore water pressure and confining pressure at the same time. The magnitude of a cell pressure increment is 50 KPa until the back pressure reaches 300 KPa. Increase in the cell pressure was done until the pore pressure parameter B is equal to or greater than 0.95 for each increment maintaining the difference between cell pressure and back pressures as 10 kPa.

According to Head, (2011) for over consolidated clays the lowest cell pressure should not normally be less than vertical effective stress ($\sigma v'$), and hence need to be in the range of 0.5 $\sigma v'$ to 2 $\sigma v'$. Accordingly, cell pressures of 60 kPa, and 100 kPa were selected based on effective overburden pressure of the in-situ soil from the soil specimen was taken. Procedures were shown in fig 3-12 below.

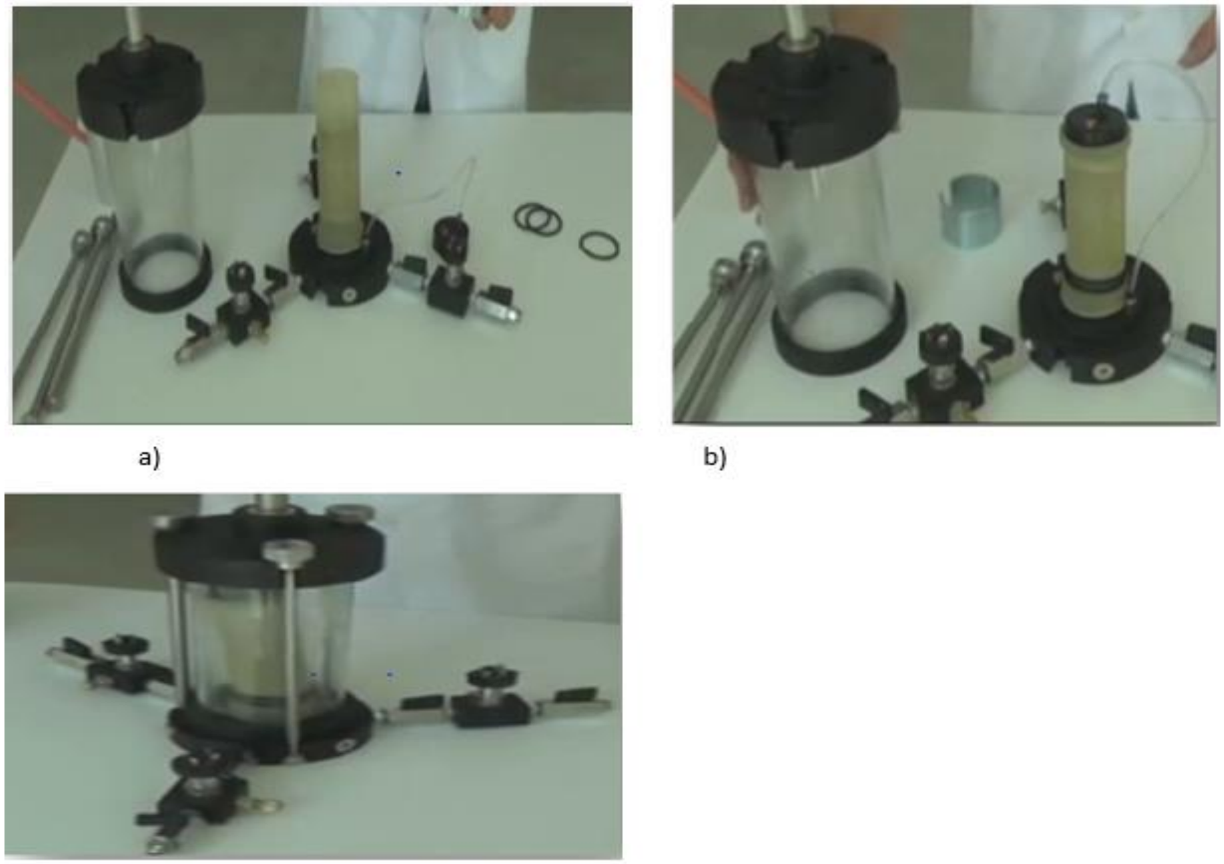

a) b) c)

Figure 3.12: UU-triaxial procedure photos (a) some testing apparatus (b) specimen with back pressure line supply (c) installed specimen in tri-axial apparatus.

Measurement of pore water pressure is only necessary for sample saturation purpose but not for effective shear stress determination. Following saturation stage, soil is not to be strengthened or there is no compression; cell pressure (σ_3) is isotopically applied; Water to flow out of the specimen is not allowed (unconsolidated) and due to the closure of drainage valves.

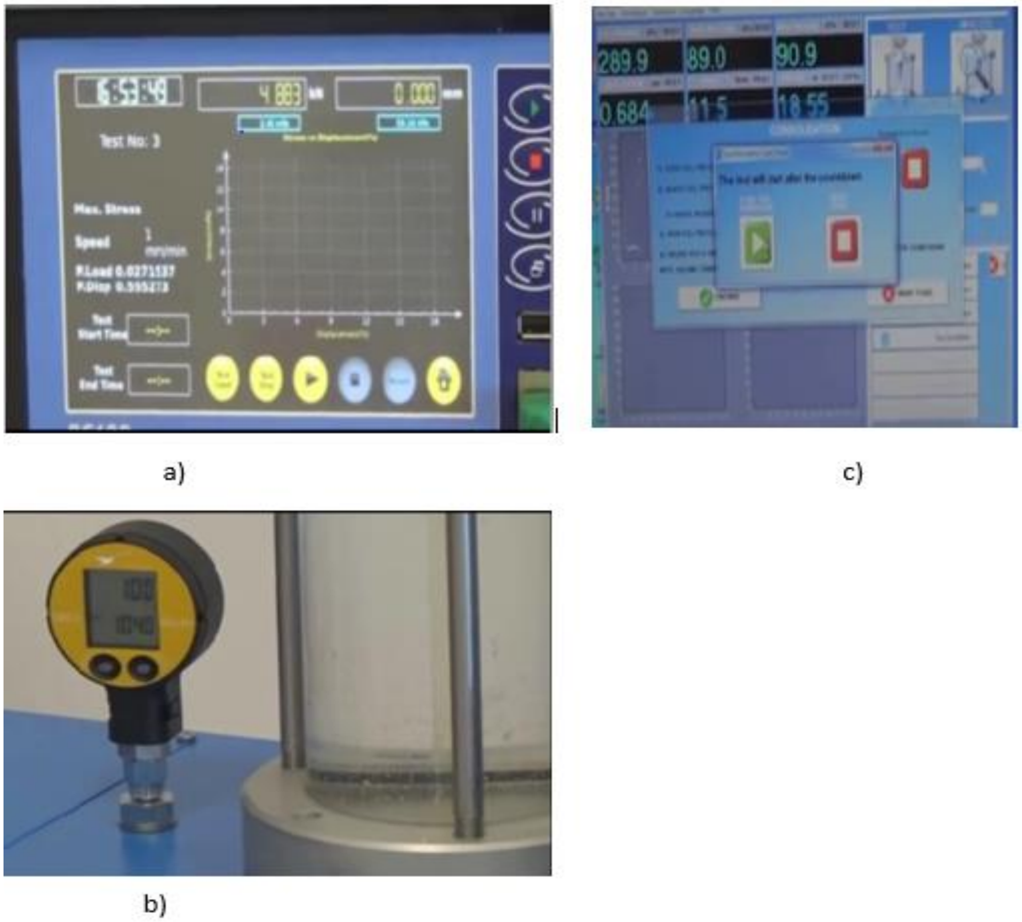

Figure 3.13: Image (a) Software assisted graphing program (b) back pressure application program and c) cell pressure device.

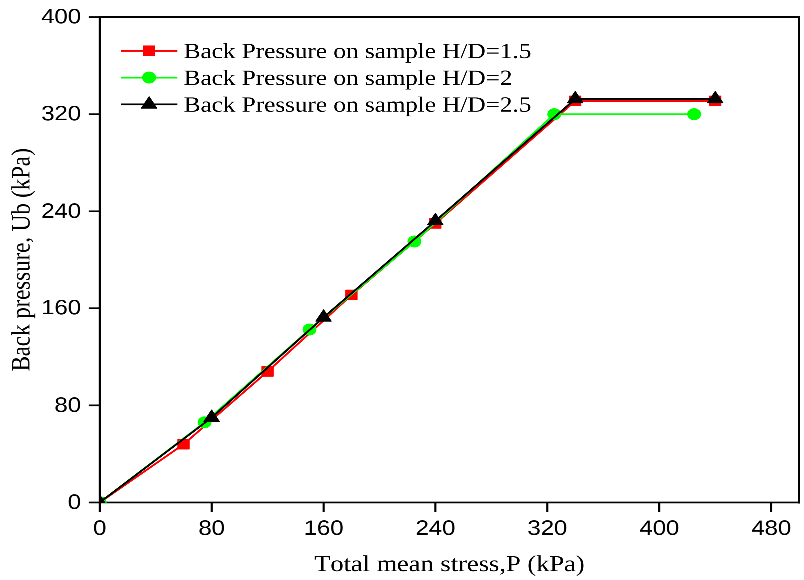

Figure 3.14: Graphical representation of back pressure versus total mean stress during saturation stage

3.7.3. Specimen shearing stage for UU-Tri-axial Test.

Once the sample satisfied the above condition shearing stage started using ASTM 2850 procedures. Deviator stress (σ_d) was applied in vertical direction only till the sample fails; Since it was the undrained condition, water does not permit to drain out and drainage valve is closed. The knob of the constant pressure unit is turned once the specimen is within the tri-axial cell, raising the cell pressure to a predetermined value. The specimen is then pushed to failure by raising the vertical stress by using a constant rate of axial strain of 1mm/min. In this UU triaxial test pore pressure, u will develop and increase but were not measured during shear test and therefore the results can only be interpreted in terms of total stress over a confinement pressure.

To conduct UU tri-axial shear Test: -The initial and subsequent length and diameter of the specimen was measured, the specimen on the bottom plate of the loading was put.

The upper plate to contact the specimen was adjusted. The load dial gauge and strain (compression) dial gauge were set at zero. See fig 3-14 below.

These tests are generally carried out on three specimens of the same sample subjected to different confining stresses. Since all specimens are fully saturated the shear strength are similar for all tests. Mohr circles are plotted using total stress for conditions with the largest principal stress differential (considered failure). The failure (Mohr) envelope was traced tangential to the Mohr circles to find the "undrained cohesion intercept" as in fig 3-15 below and the undrained "angle of shearing resistance," and the average undrained shear strength was calculated.

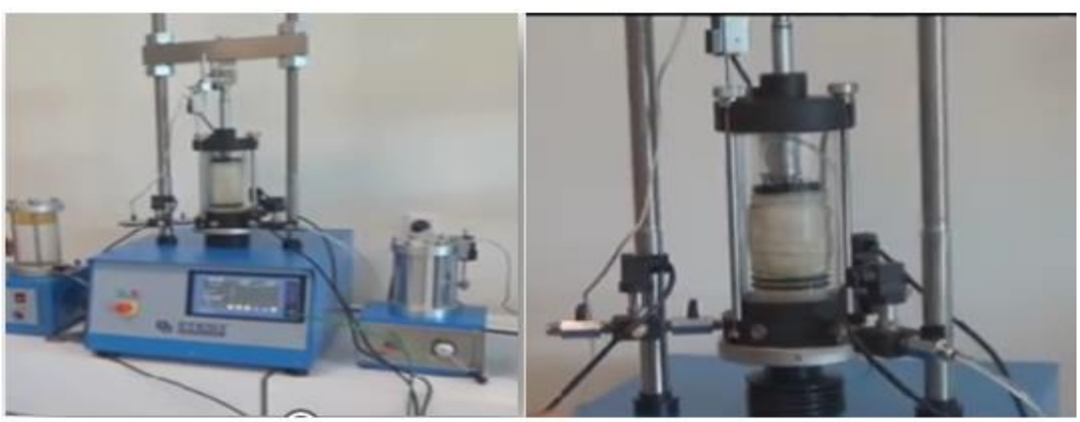

a) b)

Figure 3.15: Image (a) Sample is installed for shearing (b) Sample failure.

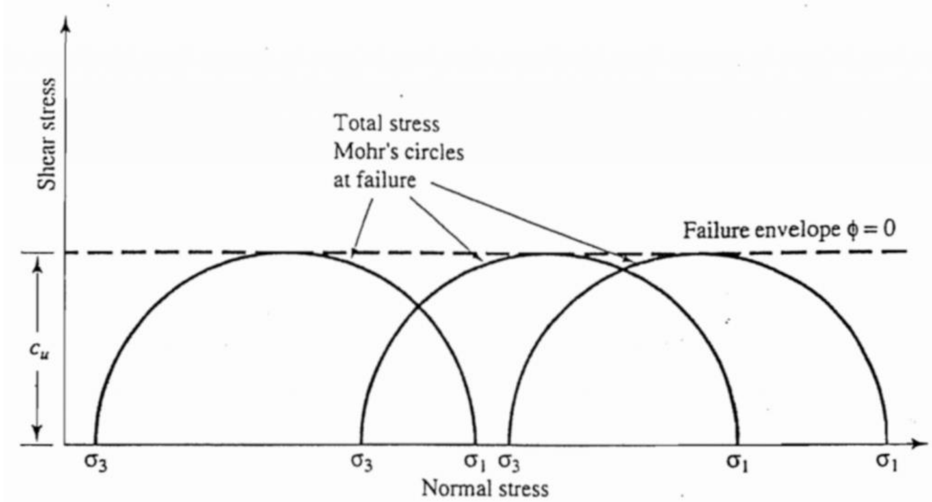

Figure 3.16: Example of Mohr circles and horizontal failure envelope from UU tri-axial test (Bobrowsky.P & Marker.B, 2018)

According to 2850-15, (2015) the definition of major and minor principal total stresses and unconsolidated-undrained compressive strength at failure are given as follows:

Calculate the axial strain for a given applied axial load, as follows:

$$\epsilon = \frac{\Delta H}{Ho} \qquad (30)$$

axial strain for the given axial load (expressed as a decimal),

ΔH = change in height of specimen during loading as read from deformation indicator, mm, and H0 = initial height of test specimen minus any change in length prior to loading, mm.

Calculate the average cross-sectional area for a given applied axial load as follows:

$$A = \frac{Ao}{(1-\epsilon)} \qquad (31)$$

where: A = average cross-sectional area, m2 and Ao = initial average cross-sectional area of the specimen, m

To Calculate the measured principal stress difference (deviator stress), for a given applied axial load as follows:

$$\sigma 1 - \sigma 3 = \frac{P}{A} \qquad (32)$$

where: σ1 – σ3 = measured principal stress difference (deviator stress), kN/m2 = kPa P = measured applied axial load (corrected for uplift and piston friction, if required as obtained and A = corresponding average cross-sectional area, m2.

Stress-Strain Curve—Prepare a graph showing the relationship between principal stress difference (deviator stress) and axial strain, plotting deviator stress as ordinate and axial strain (in percent) as abscissa. Select the unconsolidated-undrained compressive strength and axial strain at failure in accordance with the definitions given.

Correction for Rubber Membrane—The following equation shall be used to correct the principal stress difference (deviator stress) for the effect of the rubber membrane if the error in principal stress difference (deviator stress) due to the strength of the membrane exceeds 5 %: and was given by eqn (39) below.

$$\Delta\,(\sigma 1 - \sigma 3)m = \frac{4\mathrm{Em} * \mathrm{tm} * \epsilon 1}{\mathrm{D}} \tag{33}$$

where: Δ (σ1 − σ3) m = membrane correction to be subtracted from the measured principal stress difference, D = =4A/π diameter of specimen, m, Em = Young's modulus for the membrane material, kN/m2 = kPa, tm = thickness of the membrane, m, and ε1 = axial strain (decimal format).The Young's modulus of the rubber membrane (Em) may be determined by hanging a 15.0 mm (0.6 in.) circumferential strip of membrane over a thin rod, placing another rod through the bottom of the hanging membrane, and measuring the force per unit strain obtained by stretching the membrane. The modulus value may be computed using the following equation:

$$\mathrm{E}m = \left(\frac{\left(\frac{\mathrm{F}}{\mathrm{Am}}\right)}{\frac{\Delta \mathrm{l}}{\mathrm{Lo}}}\right) \tag{34}$$

where: Em = Young's modulus of the membrane material, kN/m2 = kPa, F = force applied to stretch the membrane, kg mass times 9.8087 m/s2 = N, L = unstretched length of the membrane, m, ΔL = change in length of the membrane due to applied force (F), m, Am = area of the membrane = 2tmWs, m2 , and Ws = width of circumferential strip of membrane, 15 mm (0.6 in.). A typical value of Em for latex membrane is 1400 kPa (203 lbf/in.2).

Calculate the major and minor principal total stresses and unconsolidated-undrained compressive strength at failure as follows:

$$= \sigma 1c - \sigma 3 \qquad (35)$$

σ_{1C} = major principal total stress corrected = deviator stress at failure minus the membrane correction plus chamber pressure, and σ_3 = minor principal total stress = chamber pressure.

Accordingly, the primary purpose of this test is to determine the stress-strain behavior and undrained shear strength of saturated red clay soil, which represented by the radius of Mohr circle is determined from Mohr circles constructed by chamber pressures (σ_3) of 60 kPa and 100 kPa. Undrained shear strength (Su) is necessary for the determination of the proper testing sample size, safety factor for slope stability analysis, bearing capacity of foundations, dams, etc. The undrained shear strength (Su) of clays is commonly determined from an undrained compression test, which is equal to half of undrained cohesion (c_u) when the soil's angle of internal friction (ϕ) is zero. As the most critical condition for any soil usually occurs immediately after construction, which represents undrained conditions, when the undrained shear strength is basically equal to the cohesion and expressed as:

$$\text{Su} = \frac{Cu}{2} = \sigma d/2 \qquad (36)$$

For different L/D ratios and cell pressures, the table below provides the results of UU tri-axial shear tests. Different trials of unconsolidated undrained tri-axial test for different H/D ratios are carried out at different cell pressures (σ_3) of 60 and 100 kPa. The results of the stress strain values obtained are tabulated in Table bellows. While conducting undrained tri-axial tests, accurate measurements of pore water pressure are required. A measurement of pore-pressure coefficient B could be made at the beginning of testing to assess the sensitivity of the water pressure gauges and to determine the saturation condition of the specimen. In tri-axial tests, the pore-pressure coefficient B is calculated by dividing an increment in pore water pressure by a corresponding increment in cell pressure.

CHAPTER FOUR

RESULT AND DISCUSSION

4.1. General

Laboratory experiments including natural moisture content, density-moisture relationships, consistency limit, free swell index, particle size distribution and specific gravity were conducted on soil collected from the study area to classify that the soil is red clay soil satisfying for supplementary studies. Thus, depending on the characterized soil, investigation of the effect of sample height (H/D) ratios of 1.5,2 & 2.5 and chamber pressure of 60 kPa and 100 kPa on stress-strain behavior and undrained shear stress parameters (cu and φu) of saturated red clay soil were determined. Finally, proper sampling size, safety factor for slope stability analysis and other foundation related issues of the in general is determined and saturated red clay soil. sample taken from 20+880 working station described earlier was done.

4.1.1. Natural moisture content of the red clay soil

The natural (in-situ) moisture content of the soil samples was determined from the undisturbed samples using ASTM D 4643-00, and Table presents the results. Natural (in-situ) moisture content is a key parameter to understand the characteristics and the performance of soil and its degree of compaction at the site. The results in Table 4-1 show that these soil samples can hold a significant level of moisture. As stated by Terzaghi *et al*., (1996) most of the typical values of the natural moisture content of clay soil is given below. The test results fall into the range in the the specified standard.

Table 4-1: Laboratory test results of the natural moisture content of the samples

Location	20+880			
Field sample	A		B	
Natural moisture content (%)	12.5	10.95	10.94	10.78
Average Natural moisture Content (%)	11.73		10.86	

4.1.2. Specific gravity of the red clay soil

The material's specific gravity was indicated in table 4-2 of the soil sample from the area is clay soil having specific gravity (Gs) of 2.801. The standard ASTM D 854, (2002) method is used to determine the soil's Gs for this study. Braja 6th edition P-30 reveals that clay specific gravity ranges 2.70-2.90 and hence the value is valid.

Table 4-2: Specific gravity of red clay soil

Location	Source of sampling	Specific gravity, G_s
20+880	3 m	2.801

4.1.3. Particle size distribution analysis of soil sample

Particle size analysis, which is carried out in accordance with D6913-04R2009, (2004) for coarse-grained soils and for ASTM 7928, (2017) fine-grained soils, is the quantitative assessment of the distribution of particle size in soils. According to table 4-2, 93.8% of the soil taken from station 20+880 passed through a sieve with a size of 0.075 mm, making it a fine-grained material.

Table 4-3: Summary of particle size analysis for clay soil

Sample	Source	Combination of particles size (%)			
		≥ 4.75 mm (Gravel)	0.075 mm 4.75mm (Sand)	0.075 mm-0.002 mm (Silt)	≤ 0.002 mm (Clay)
20+880	3 m	1.3	4.9	40.1	53.7

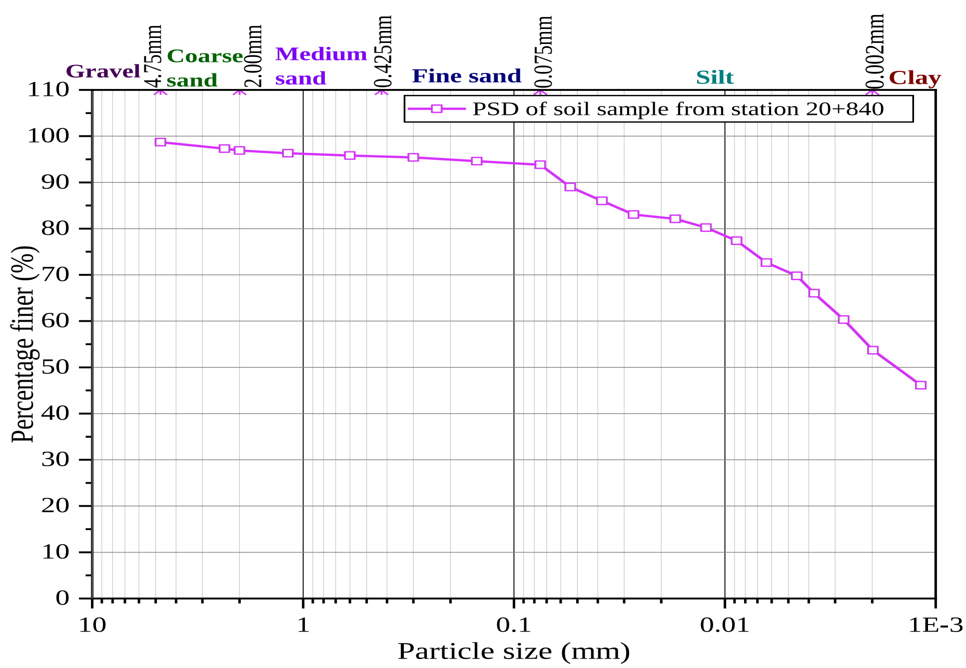

Figure 4-1: Particle size distribution curve of red clay soil

The soil sample has a liquid limit that is larger than 50% and is above the A-line on the USCS plasticity chart, which classifies it as an inorganic clay with a high plasticity group called CH. Moreover, the soil sample belongs to the A-7-5 group with a group index of 20 according to the plasticity chart for the AASHTO categorization system.

4.1.4. Atterberg limit of soil

The term "plasticity" refers to the soil's ability to be molded and describes how cohesive the soil is. Different organizations categorize soil flexibility in a variety of ways.

According to Wagner, (2013), if the soil's PI value is less than 20, it can be categorized as a cohesive clay soil with strong plasticity properties. The Plastic Index (PI), with a high value indicating a high degree of cohesion, is also employed as a measure of soil cohesiveness. The findings in Table 4-4 point to the soil samples' great plasticity, and the literature provides more support for this hypothesis. The liquid limits and plasticity index of the researched soils are both higher than the values advised by ERA, (2013), which specifies that for subgrade-appropriate materials, the liquid limit should be less than or equal to 60% and the plasticity index should be less than or equal to 30%. Fine-grained soils are not appropriate for use as subgrade material, according to AASHTO, (2006). Inferred from this is that these soils cannot serve as subgrades without upgrading. One of the crucial parameters for estimating consolidation in settlement estimation for the engineering foundation is the compression index (Cc). For the relationship between Cc and other soil qualities, numerous formulas were created by various academics. Most scholars, however, advocated Cc = 0.009 (LL: 2.0%); Terzaghi's technique, where Cc is the compression index, is the best for correlating compression index with Atterberg limits. According to Jain *et al*., (2015), the compression index (Cc) values of medium to soft clay soil range from 0.15 to 1.0. The correlation value for this study's compression index (Cc) is 0.372, indicating that the soils are moderately compressible.

Table 4-3: Atterberg limit test results of clay soil

Designation	Depth(m)	Atterberg limit results (%)			
		LL	PL	PI	LS
TP (20+880)	3	63.1	29.7	33.4	16

According to test results, the soil sample from TP (20+880) had linear shrinkage of 16%, liquid limit of 63.10%, plastic limit of 29.70%, and plasticity index of 33.40%. According to the USCS and AASHTO systems, respectively, soil is classed as CH and A-7-6 (20) according to the plastic limit and plasticity index results, which are displayed on figure 4-2.

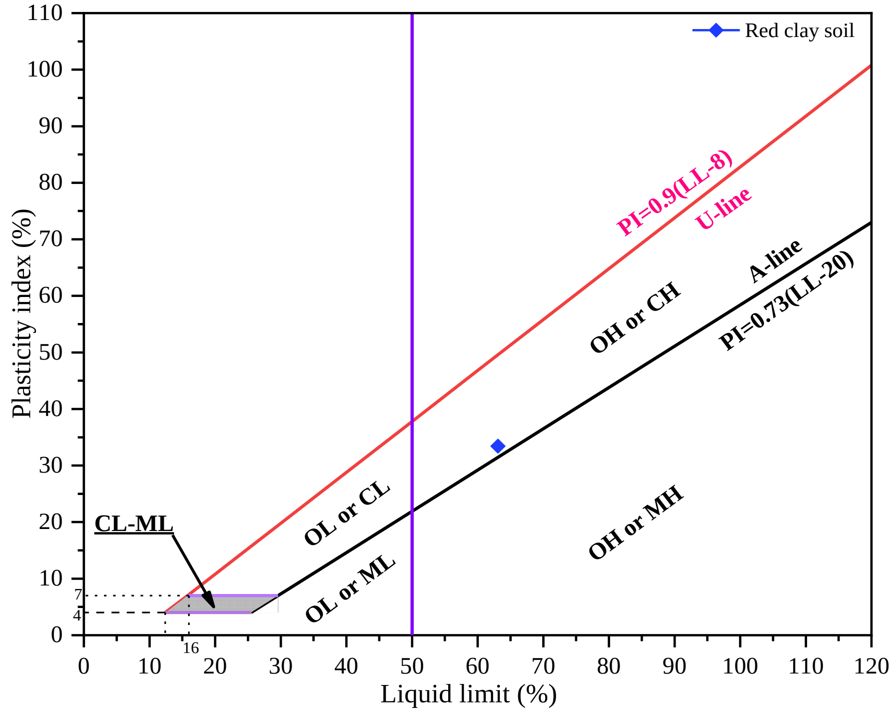

(a)

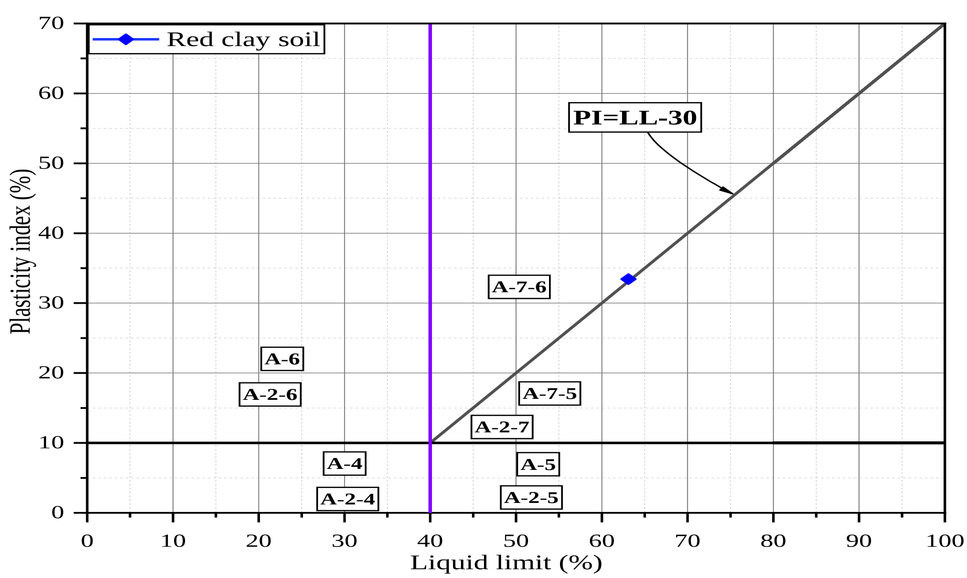

(b)

Figure 4-2: Plasticity chart for natural soil classification system (a) USCS and (b) AASHTO

4.1.5. Free swell index of red clay soil

Free swell is the increase in volume of a soil, without any external constraints, due to submergence in water and used to identify the potential of a soil to swell which might need further detailed investigation regarding swelling and swelling pressures under different field conditions. The test was performed under control of IS 2720 part 40, (2002) standard method.

Table 4-4: Free swell index of red clay soil

S/No.	Test Pit Depth	Reading after 24 hours		Free Swell Index (FSI) (%)	Free swell ratio (FSR)
		Kerosene	Distilled water		
1	3m	10	14.5	45.0	1.45

The soil samples from station 20+880 have free swell index of 45% which shows material from this test pit has high swelling potential.

4.1.6. Moisture-density relationship of red clay soil

This test helps to understand the relationship between the dry density and the moisture content of soil for some stated compaction energy. Up to a certain water content, the presence of water helps in the compaction process as a lubricant for grain packing. When the water content is increased beyond this, there is a negative impact on the soil dry density. The optimum moisture content (OMC) is the water content at which the maximum density is reached for specified compaction energy. This test was carried out according to standard test procedure. Compaction of soil is a procedure in which soil sustained under mechanical stress is densified by reducing the volume of void in the mass. Soil mass consists of solid particles and voids filled with water or/and air. When soil is subjected to stress, soil particles are redistributed within the soil mass and the void volume decreases, resulting in densification (ASTM D 698, 2000). The result of compaction test of clay soil was summarized in table 4.5 as shown below.

Table 4-5: Compaction test result of the clay soil specimen

Location	MDD(g/cm^3)	OMC (%)
TP (20+880)	1.37	27.3

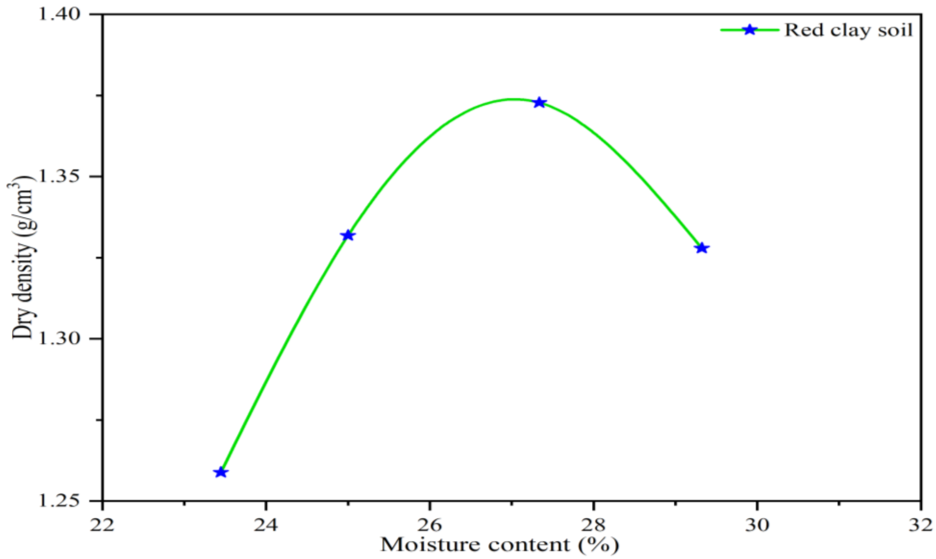

Figure 4-3: Compaction curves of red clay soil collected from TP on station 20+880

Results obtained reveal that red clay soil collected from test pit on station 20+880 have optimum moisture content of 27.3% and maximum dry density of 1.37g/cm^3 respectively.

Table 4-6: Summary of geotechnical properties of red clay soil

Properties of red clay soil	TP from station of (20+880)
Free swell index	45%
Free swell ratio	1.45
Liquid limit	63.10%
Plastic limit	29.70%
Plastic index	33.40%
Linear shrinkage	16%
Optimum moisture content	27.30%
Maximum dry density	1.37g/cm^3
Percent finer of No.4 sieve	98.70%
Percent finer of No.200 sieve	93.80%
C_u & C_C	2.69 & 0.372
Soil class based on USCS	CH
AASHTO system	A-7-6 (20)
Specific gravity, G_s	2.801
Color	Red

4.2. Mineralogical Composition Analysis of Soil Sample

4.2.1. XRD result analysis of soil sample.

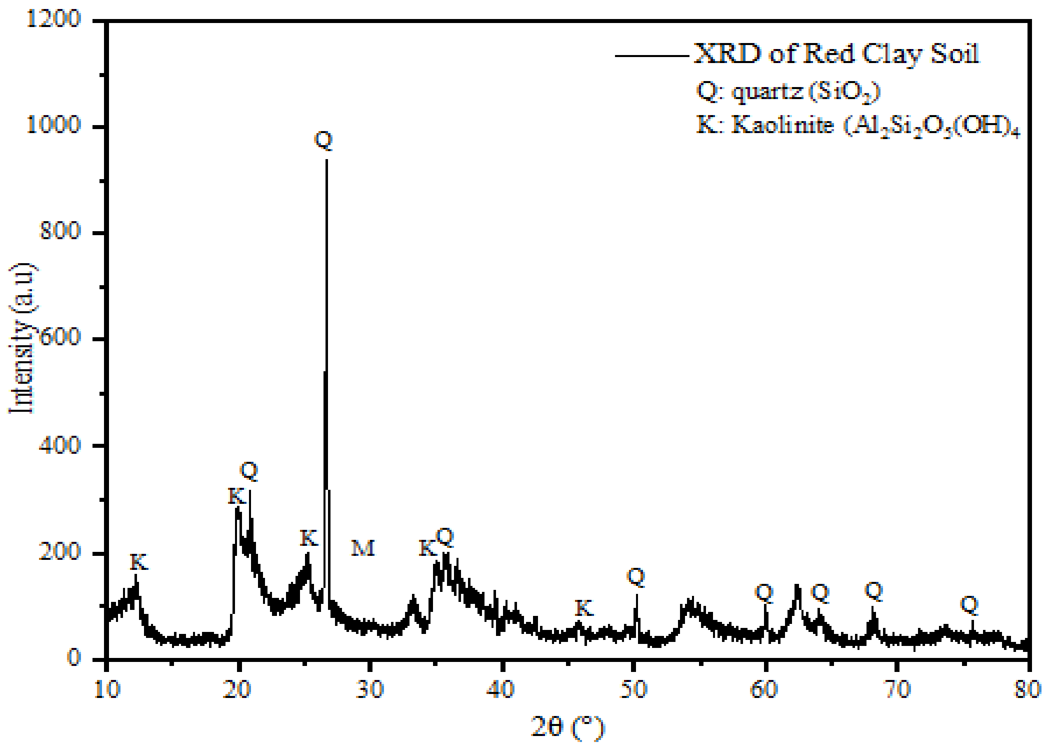

Figure 4-4: Image showing XRD pattern result of red clay soil.

The XRD pattern of red clay soil on Figure 4-4, shows that soil sample mainly composed of quartz, and kaolinite minerals. The characteristic peak of quartz occurred at 2θ=26.64996° or d=3.3422424Å is present as a sharp peak that indicates the pronounced crystallinity of the SiO_2 phase close to the values obtained from the JCPDS (046-1045) standard data.

This is a sign that the chosen soil sample is abundant in quartz and has illite and Kaolinite clay minerals mixed. Different sample preparation techniques will have a direct impact on the sample's structure, which will change how the sample responds to external loads mechanically (Shuo Zhang et al, 2022).

4.3. Unconsolidated-Undrained Triaxial Test Result of the Soil Sample

4.3.1. UU tri-axial specimen initial conditions

Before conducting the UU triaxial test of red clay soil initial conditions were set. Accordingly, the result of initial density, void ratios and degree of saturation for each sample was shown in table 4-7 below as an initial condition of the specimen before saturation stage.

Table 4-7: Summary of initial conditions of red clay soil

Aspect ratio (H/D)	**1.5**	**2**	**2.5**
Initial height, Ho (cm)	7.50	10.00	12.50
Initial Diameter, Do (cm)	5.00	5.00	5.00
Cross-Sectional area, Ao=π/4*(Do)2 (cm2)	19.64	19.64	19.64
Volume, Vo=Ao*Ho (cm3)	147.26	196.35	245.44
Wet Mass, Ms (g)	256.83	342.43	428.04
Water content, wo (%)	27.30	27.28	27.29
Total soil particle density, ρb=Ms/Vo (g/cm3)	1.74	1.74	1.74
Dry density, ρd=ρs/(1+wo/100) (g/cm3)	1.23	1.23	1.23
Void ratio, eo=(Gs*ρw/ρd)-1	1.27	1.27	1.27
Dagree of Saturation, So=wo*Gs/eo (%)	60.13	60.10	60.12

The initial conditions of the specimens were tabulated above that the remolded specimen at OMC and 90% of MDD were not fully saturated because the degree of saturation from shorter to longer is 60.13 %, 60.10 %, and 60.12 % respectively.

4.3.2. UU tri-axial saturation test results

The UU triaxial test of red clay soil saturation was conducted, and the result is shown in table 4-8 below. This result presents that the cell pressure, back pressure and pore water pressures employed to make the sample ready for the next specimen shearing stage. Based on the calculated Skemptems' B value tabulated below the complete saturation of the soil sample is confirmed.

Note: To saturate the soil specimen, the cell pressure was applied in several steps, as was analyzed in appendix G-1. The effective stress ($\sigma'v$) in this example, 52.32 kPa, acting on the soil sample in the field, however, is almost equivalent to the size of the cell pressure increment.

The soil sample is now assumed to be fully saturated as the B-value is validated to be (> 0.98), and saturation is achieved under back pressure employment (for example, increased +ve pore pressure).

Table 4-8: Summary of back pressure application for saturation specimen

Specimen Aspect ratio	Cell Pressure (σc)	Back Pressure Ub, (kpa)	Pore Pressure U, (kpa)	ΔU =U2-U1	Δσc =σc2-σc1	B=factor =ΔU/Δσc
H/D=1.5	240.00	170.00	229.00	59.00	60.00	0.98
	440.00	331.00	429.85	99.85	100.00	1.00
H/D=2	340.00	270.00	329.75	59.75	60.00	1.00
	425.00	320.00	416.50	98.50	100.00	0.99
H/D=2.5	315.00	332.50	313.45	59.45	60.00	0.99
	440.00	332.50	431.00	99.50	100.00	1.00

4.3.3. UU tri-axial shearing test results

The result of UU triaxial test conducted on red clay soil is shown in table 4-8 below. This result presents the undrained shear strength parameters at failure including the axial strain (ϵ_a), undrained shear strength (Su) and angle of internal friction (φ_u) at failure, obtained from the test. Based on the result analyzed, the corresponding stress-strain curves behavior, Mohr’s circle and failure patterns of the testing specimens were deduced as follows.

Table 4-9: Summary of specimen’s undrained shear parameters

Undrained Triaxial Compression test

Job reference: 1

Location: Gechi-Yanfa Road Project (20+880R)

Borehole no. 1

Soil description: Siff & red clay

Sample No. 1

Disturbed specimen — Location & orientation of test specimen

Method of preparation — Remolding compaction into various heights to diameter

Nominal dimensions		Date: 6/03/023
Diameter:	50 mm	
Heights:	75 mm, 100 mm, 125 mm	
Membrane thickness	0.2mm	
Rate of strain:	1.0 mm per minute	

Specimen ref no.	Bulk density (Mg/cm3)	Moisture content (%)	Dry density (Mg/cm3)	At failure: Cell pressure (kpa)	Compressive stress (kPa)	Angle of internal friction (degrs)	Strain (%)	Membrane Correction (kPa)	Shear strength (kPa)	Mode of failure
H/D=1.5	1.74	60.13	1.23	60.00	86.97	0.026	2.67	0.65	43.48	
	1.74	60.13	1.25	100	86.92		2.77	0.70	43.46	
H/D=2	1.74	60.12	1.25	60.00	84.89	0.030	2.80	0.85	42.45	
	1.74	60.12	1.24	100	84.85		3.00	0.75	42.43	

H/D=2.5	1.74	60.11	1.25	60.00	81.52	0.014	2.40	0.82	40.76	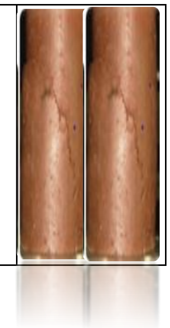
	1.74	60.11	1.24	100	81.53		2.56	0.83	40.77	

4.4. Effect of Sample Height on Stress-Strain Behavior and Undrained Shear Strength Parameters of Saturated Red Clay Soil

4.4.1. Effect of sample height on stress-strain behavior of saturated red clay soil

In this investigation, the soil sample was subjected to unconsolidated undrained Triaxial tests using varied H/D ratios of 1.5, 2 and 2.5. The sample was remolded using the normal proctor test procedure at MDD and OMC to run the test. Using sampler tubes with a 50 mm diameter, the soil sample is prepared. The sample extruder is then used to extract the soil sample from the sampler tubes. The extracted samples are then cut to the necessary lengths to produce the H/D ratios of 1.5, 2 and 2.5. UU triaxial tests were performed on specimens with 75mm, 100mm and 125mm height under two different cell pressures of 60 and 100 kPa. The specimens were sheared with a strain rate of 1mm/min and Stress-strain curve behavior were shown in fig 4-5 & 4-6 below.

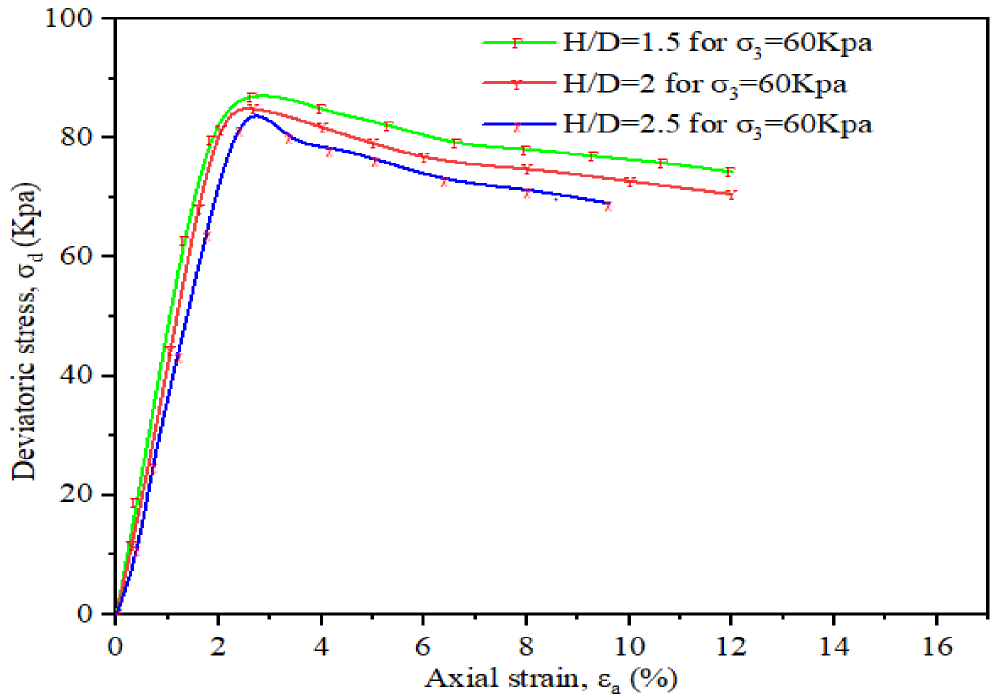

Figure 4-5: Axial stress versus axial strain (all three aspect ratios) for remolded and fully saturated red clay soil sample taken from a depth of 3m under cell pressure, σ3 = 60 kPa

As presented in the stress–strain plots of Fig. 4-5 above, a peak undrained shear strength, su is attained at $\varepsilon_a \approx 2.67$ % for samples with H/D=1.5, whereas samples with H/D=2 attained at the value of $\varepsilon_a \approx 2.65$ % and samples with H/D=2.5 attained $\varepsilon_a \approx 2.40$ % under confining pressure of σ3=60 kPa which shows that as specimen height (H/D) increases the stress-strain curve behavior of saturated red clay soil changes from gentler to steeper or smaller slope to larger slope.

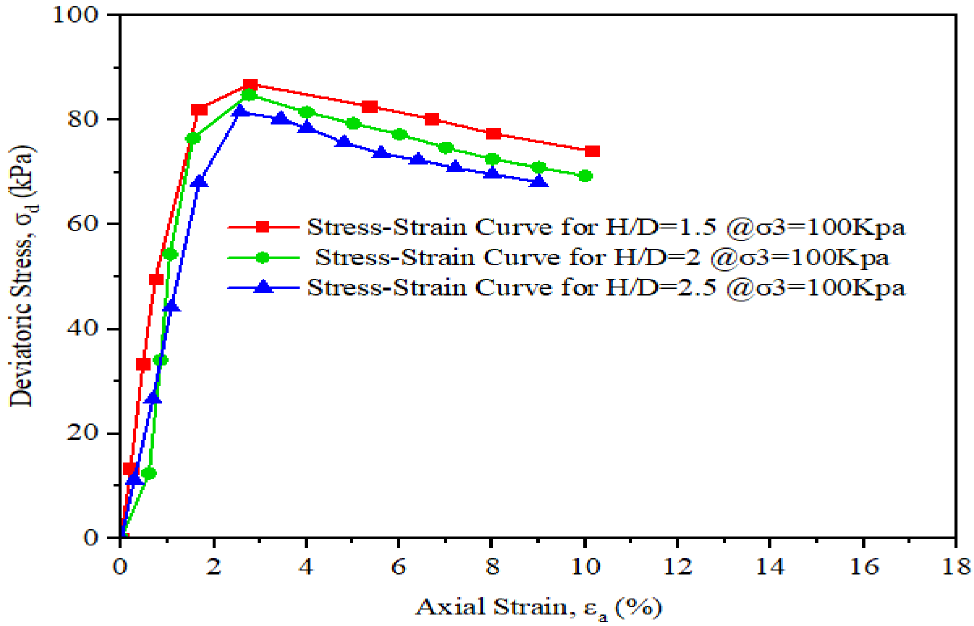

Figure 4-6: Axial stress versus axial strain (all three aspect ratios) for remolded and fully saturated red clay soil sample taken from a depth of 3m under cell pressure, σ3 = 100 kPa

As shown in the stress–strain curves of Fig. 4-6 above, a peak undrained shear strength (su) for samples with H/D=1.5 was attained at $\varepsilon_a \approx 2.77$ % whereas it was attained at $\varepsilon_a \approx 2.70$ % for specimen with H/D=2 and eventually it was attained at $\varepsilon_a \approx 2.56$ % for sample with H/D=2.5 under the application of confining pressure (σ3) =100 kPa. This also reveals that as specimen height (H/D) ratio increases the stress-strain curve behavior of saturated red clay soil changes from smaller slope to larger slope regardless of change of confining pressure. Likewise, the failure pattern exhibited by the specimens' changes from barelling failure to brittle failure as the aspect ratios of the specimen increases.

According to Omar & Sadrekarimi, (2015) , the steeper the specimen would indicate a higher stability and safety of a slope, while being less stable or even at failure based on a more representative φ' from the larger specimen. Testing of larger specimens is recommended and the specimen size effect should be carefully considered in landslides risk assessment.

In general, the failure pattern is clearer and more defined when sample size is shorter and mixed for medium length for instant for H/D=2 and was very brittle for specimen H/D=2.5.

4.4.2. Effect of saturated red clay soil sample height on undrained shear strength

In this work, tri-axial tests were carried out at various L/D ratios of 1.5, 2, and 2.5, to evaluate the characteristics of undrained shear strength. Based on the Mohr-Coulomb failure theory, the undrained shear strength (su) is obtained from the deviator stress expressed in equation (38) in chapter 3.

Further, it may be noted that if an identical soil sample is tested under different state of stress (application of increased cell pressure) and subjected to rapid loading without pore water pressure dissipation, the Mohr`s circle for each such soil sample has the same diameter but the circle shifts towards right side under increasing state of stress if pore water pressure is measured for each soil sample tested in the UU test, the principal effective stresses can be computed, which yield effective cohesion c'. Since effective stresses are independent of the cell pressure applied in the UU test.

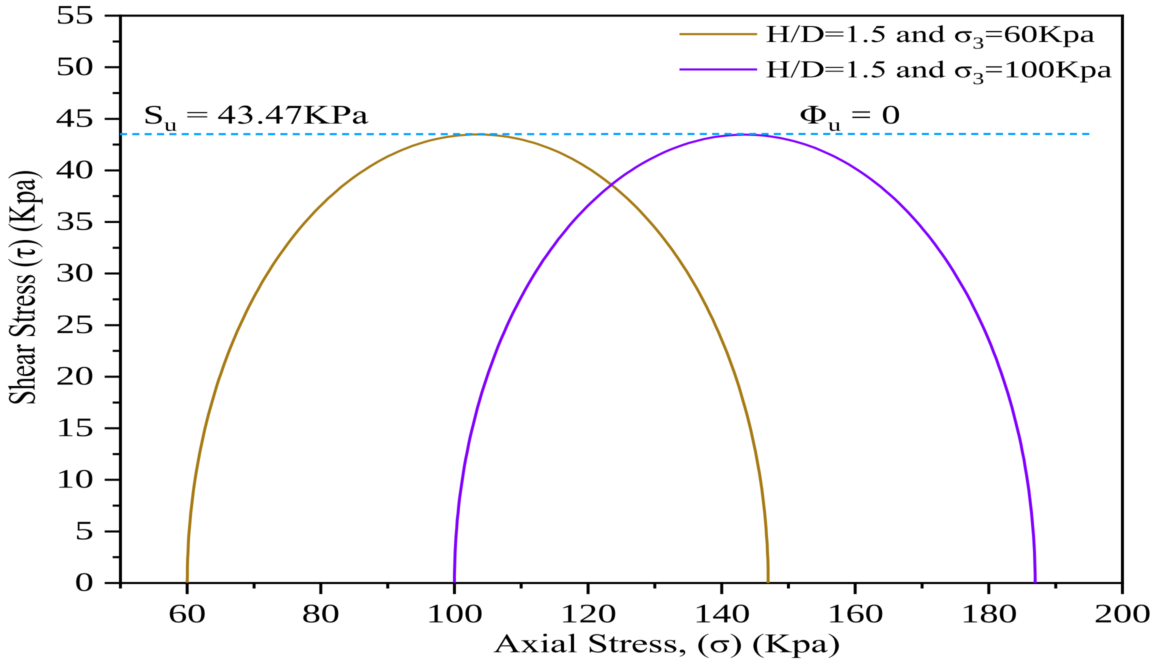

Figure 4-7: Mohr circle diagram for remolded and saturated red clay samples with different cell pressure, σ3 = 60 & 100 kPa and Height-to-diameter (H/D) =1.5 ratio at a depth of 3m.

Figure 4-7 represents the peak undrained shear strength (Su) 43.48 kPa & 43.46 kPa and undrained internal angle of friction ($\varphi_u \approx 0$) obtained, which is attained at maximum axial strain or failure strain of 2.67% & 2.77 % from saturated red clay soil specimen with H/D=1.5 subjected to different cell pressures of 60 kPa & 100 kPa respectively. The result indicates that undrained shear strength of saturated red clay is independent of cell pressure or confining pressure.

Figure 4-8 also represents the peak undrained shear strength (su) 42.45 kPa & 42.43 kPa and undrained internal angle of friction ($\varphi_u \approx 0$) obtained, which is attained at maximum axial strain or failure strain of 2.65% & 2.70 % from saturated red clay soil specimen with H/D=2 subjected to different cell pressures of 60 kPa & 100 kPa respectively. The result indicates that no significant discrepancy is seen on either axial strain or undrained shear strength of saturated red clay though it is independent of cell pressure or confining pressure too.

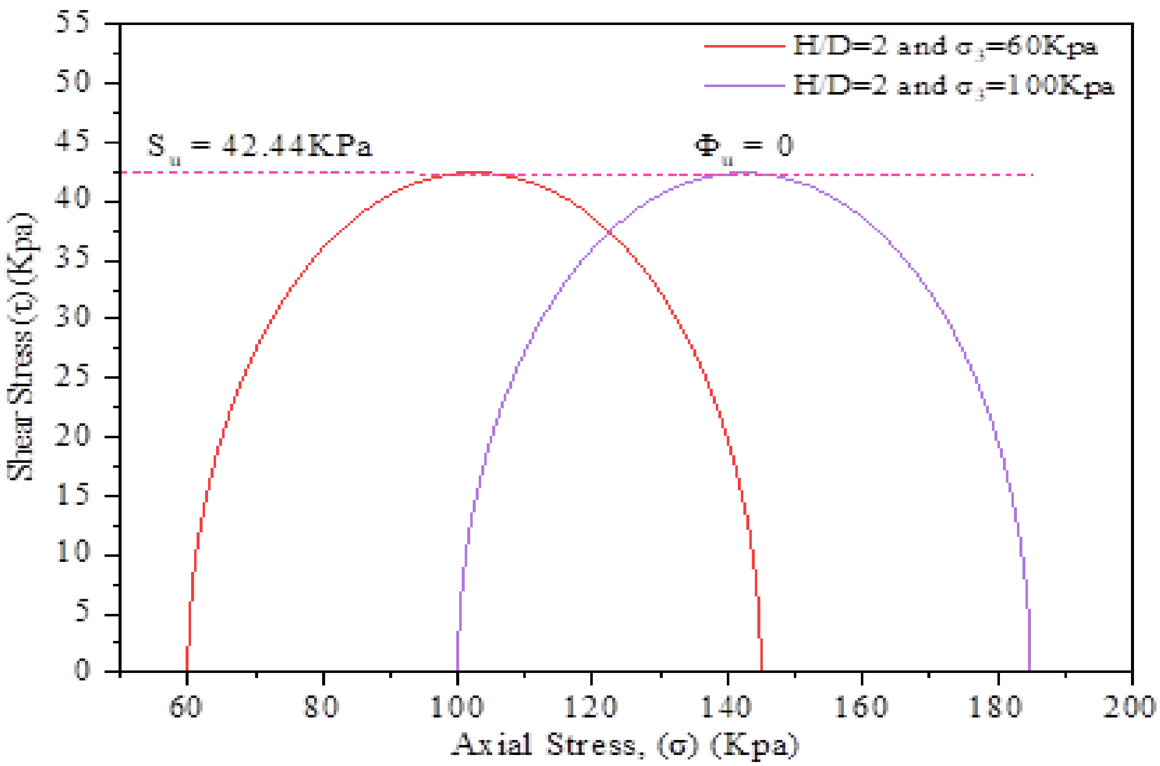

Figure 4-8: Mohr circle diagram for remolded and saturated red clay samples with different cell pressure, σ3 = 60 & 100 kPa and Height-to-diameter (H/D) =2 ratio at a depth of 3m.

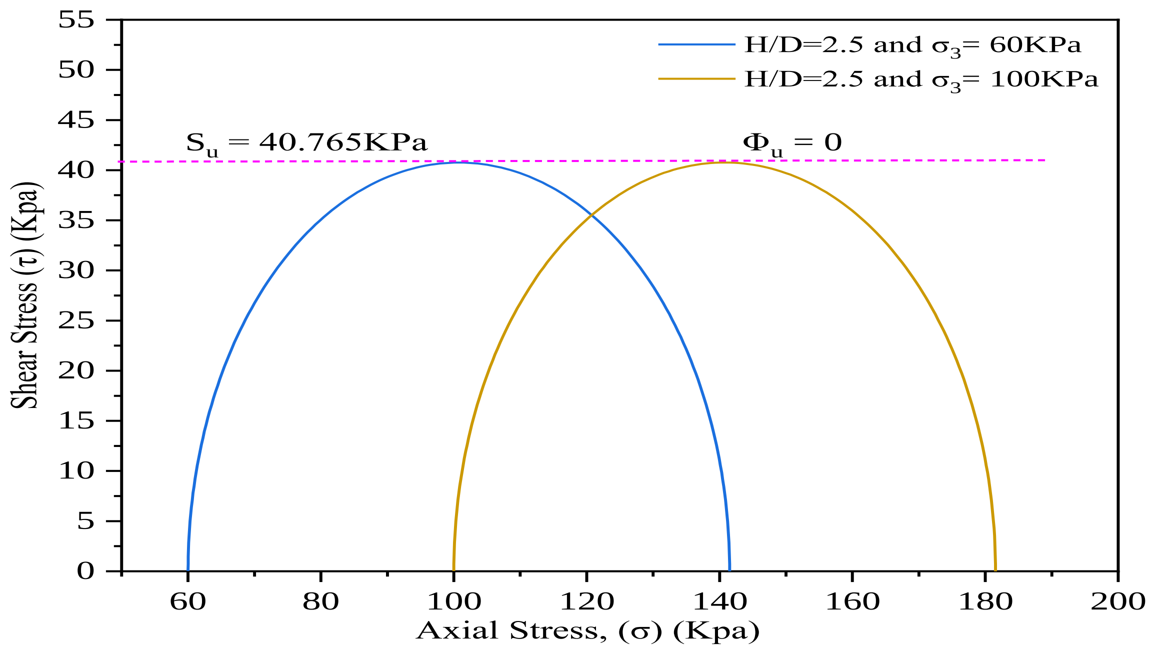

Figure 4-9: Mohr circle diagram for remolded and saturated red clay samples with different cell pressure, σ3 = 60 & 100 kPa and Height-to-diameter (H/D) =2.5 ratio at a depth of 3m

Figure 4-9 also represents the peak undrained shear strength (su) 40.76 kPa & 40.77 kPa and undrained internal angle of friction ($\varphi_u \approx 0$) obtained, which is attained at maximum axial strain or failure strain of 2.40% & 2.56 % from saturated red clay soil specimen with H/D=2.5 subjected to different cell pressures of 60 kPa & 100 kPa respectively. This result shows that there is a slight discrepancy of about 4.1% between specimen with H/D=2 and that of H/D=2.5 than specimen with H/D=1.5 and that of H/D=2 which is about 2.4% and is independent of cell pressure or confining pressure too.

The graph 4-10: shown below, represents the cell pressure effect on undrained shear stress which indicates that undrained shear strength, angle of internal friction is both independent of confining pressure in saturated red clay soil. Moreover, the two dotted lines indicate that slight variation is seen on undrained shear strength of the soil sample due to H/D ratios of the soil specimen.

Again, the lower undrained shear strengths of the 125 mm specimens partly the result from their slightly higher slenderness ratio whereas the effect of specimen size on the undrained shear strengths of the 75 mm and 100 mm specimens shows slight difference as explained above though they were sheared from the same saturation condition.

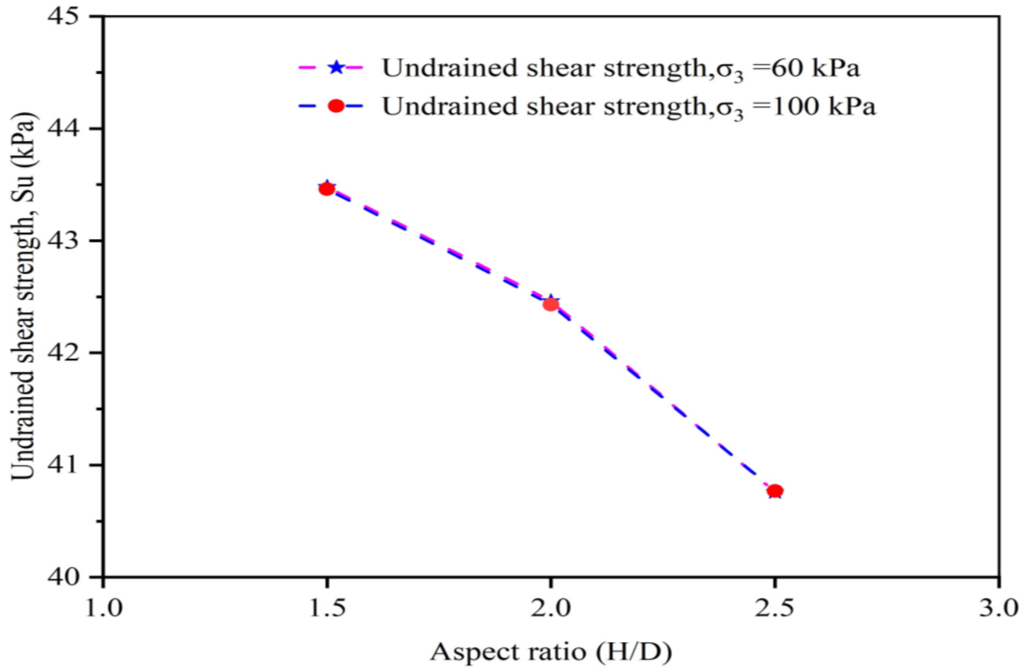

Figure 4-10: Graphs effect of soil specimen H/D ratio on undrained shear stress (Su)

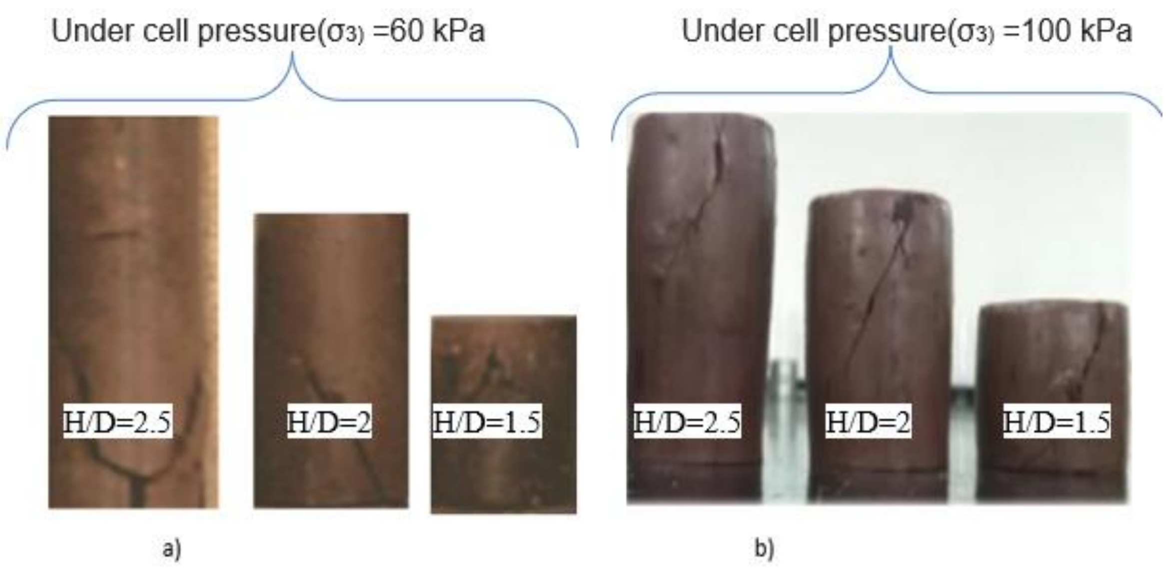

Figure 4-11: Specimen failure by UU tri-axial test under (a) chamber pressure (σ_3=60 kPa and (b) chamber pressure (σ_3=100 kPa

The failure pattern of the tested specimen as shown in fig 4-11 above changes from ductile or bulging or barelling failure to brittle or plastic failure as the aspect ratios of the specimen increases from H/D=1.5 to. H/D=2.5 and the failure pattern is defined when sample size is shorter.

CHAPTER FIVE

CONCLUSION AND RECOMMENDATION

5.1. Conclusion

This paper was targeted to investigate the effect of sample height (H/D) ratios on stress-strain behavior and undrained shear strength of saturated red clay soil under specified chamber pressures. Samples sizes with aspect ratios of 1.5, 2 & 2.5 and confining pressures of 60 kPa and 100 kPa were used to assess exclusive effect of sample size on total shear stress or undrained cohesion of soil. In conclusion, the following results were obtained.

- For saturated specimen's H/D=1.5, 2 and 2.5 stress-strain behavior or smaller (steeper) slope to larger or gentle slope as the soil specimen size increases from 1.5 to 2.5 aspect ratios regardless of the applied confining pressures respectively.
- For saturated specimen's H/D=1.5, 2 and 2.5, undrained shear strength (Su) decreased from 43.48 kPa at strain 2.67 % to 40.76 kPa at strain 2.40 % respectively under the application of 60 kPa cell pressure and Su decreased from 43.46 kPa at strain 2.77 % to 40.77 kPa at strain 2.56% respectively under the application of 100 kPa cell pressure. Moreover, the value of angle of internal friction or the slope of failure envelope in all cases is almost zero or horizontal. These results reveal that undrained shear strength of saturated red clay soil specimen is independent of cell pressure (and declined by 2-5% as (H/D) ratios of the specimen change from 1.5 to 2.5.
- The failure pattern shows that it changes from ductile to brittle failure or from bulging to barreling failure when specimen size (H/D) ratios increase from 1.5 to 2.5.

5.2. Recommendation

- ✓ For this study sample size /aspect ratio effect on undrained shear strength and stress-strain behavior of saturated red clay soil was limited to only undrained unconsolidated tri-axial test and it due to lack of comprehensive equipment including samplers and cost. Should be recommended for further study on other soil types and the rest tri-axial test methods (CU & CD) to determine the effects on total shear stress, effective stresses, and stress-strain behavior of undisturbed and disturbed soil samples.
- ✓ In this investigation the soil sample size for undrained shear strength test was limited to disturbed and height variation of specimen only and therefore further investigation on the impact

of diameter variation on strength property of clay soil using different tri-axial tests at various environmental conditions should be anticipated.

- ✓ It is assumed that a soil sample deforms uniformly during tri-axial testing. But one often faces a case when the sample in the tri-axial apparatus deforms on the contrary. The non-uniformity can be caused by the end restraining effect, the sample height influence factor, sample self-weight factor, and the insufficient drainage, etc.
- ✓ Shear strength parameters (c & ф) and deformation obtained can be studied for its relation between different sizes of the specimen. Size effect can be studied in analyzing stress-strain curve with respect to increasing confining pressure and its significance at higher confining pressures. Effect of specimen size on pre-peak, peak and post peak strength behavior with respect to strain can be researched.
- ✓ It is hoped that this information will be useful to potential users who are looking for new sources. The intension of this literature search is to uncover technical information and make them available for the potential users. It will help to make proper choice for specific problems/projects, and it will stimulate further development in this field.

REFERENCES

AASHTO:M 145-91. (2008). *Classification of Soil and Soil-Aggregate Mixtures For Highway Construction Purposes* (Vol. 91, Issue 2008).

Al-Khafaji Andersland, O. B., A. W. (1992). *Geotechnical Engineering and Soil Testing* (Issue January 1992).

Amšiejus, J., Dirgelienė, N., Norkus, A., & Žilionienė, D. (2009). Evaluation of soil shear strength parameters via triaxial testing by height versus diameter ratio of sample. *Baltic Journal of Road and Bridge Engineering*, *4*(2). https://doi.org/10.3846/1822-427X.2009.4.54-60

Andrade, F. A., Al-qureshi, H. A., & Hotza, D. (2011). Applied Clay Science Measuring the plasticity of clays : A review. *Applied Clay Science*, *51*(1–2), 1–7. https://doi.org/10.1016/j.clay.2010.10.028

ASTM 2850-15. (2015). Standard Test Method for Unconsolidated-Undrained Triaxial Compression Test on Cohesive Soils. *ASTM International*, *D2850 − 15*(2015), 1–6. https://doi.org/10.1520/D2850-15.2

ASTM D 2487. (2000). Standard Practice for Classification of Soils for Engineering Purposes (Unified Soil Classification System). *American Society for Testing and Materials International Standard*, *04*, 1–12.

ASTM D 698. (2000). Standard Test Methods for Laboratory Compaction Characteristics of Soil Using. *American Society of Testing Material Standard Guide*, *3*, 1–11.

Astm D6913-04R2009. (2004). Standard Test Methods for Particle-Size Distribution (Gradation) of Soils Using Sieve Analysis. *ASTM International, West Conshohocken, PA*, *04*(Reapproved 2009), 1–35. https://doi.org/10.1520/D6913-17.1.6

ASTM International. (2017). ASTM D7928-17 : Standard Test Method for Particle-Size Distribution (Gradation) of Fine-Grained Soils Using the Sedimentation (Hydrometer) Analysis. *ASTM International*, 1–25. https://doi.org/10.1520/D7928-17

Asuri, S., & Keshavamurthy, P. (2016). Expansive Soil Characterisation: an Appraisal. *IndiaNational Academy of Engineering*, *1*(1), 29–33. https://doi.org/10.1007/s41403-016-0001-9

Berhanu, B., Seleshi, Y., & Melesse, A. (2014). Nile River Basin: Ecohydrological challenges, climate change and hydropolitics. In *In: Melesse, A., Abtew, W., Setegn, S. (eds) Nile River Basin. Springer, Cham.* https://doi.org/10.1007/978-3-319-02720-3

BS1377-7 Cl 7. (1990.).

Chen, F. H. (1975). *Foundations On Expansive Soils. second ed.* Elsevier Scientific Publishing Company.Amesterdam, Netherland. https://doi.org/10.1016/s0376-7361(08)70127-4

Craig, R. F., & Knappett, J. A. (2012). *Craig's Soil Mechanics, 8th Edition* (8th editio). Spon Press: Taylor & Francis publisher.

Das, B. M., & Sobhan, K. (2014). Principles of Geotechnical engineering, Eight Edition. In *Global Engineering* (Vol. 5, Issue 1). Global Engineering.

Emmanuel, U. O., Ogbonnaya, I., & Uche, U. B. (2021). An investigation into the cause of road failure along Sagamu-Papalanto highway southwestern Nigeria. *Geoenvironmental Disasters*, *8*(1). https://doi.org/10.1186/s40677-020-00174-8

ERA, 2013. (2013). *Standard Technical Specifications and Method of Measurement for Road WORKS*.

Güneyli, H., & Rüşen, T. (2016). Effect of length-to-diameter ratio on the unconfined compressive strength of cohesive soil specimens. *Bulletin of Engineering Geology and the Environment*, *75*(2), 793–806. https://doi.org/10.1007/s10064-015-0835-5

Head I., 2014. (1994). Manual of soil laboratory testing. In *Soil Dynamics and Earthquake Engineering* (Vol. 13, Issue 2). https://doi.org/10.1016/0267-7261(94)90007-8

Herrmann, H., & Bucksch, H. (2014). Soil-Mechanical. In *Dictionary Geotechnical Engineering/Wörterbuch GeoTechnik*. https://doi.org/10.1007/978-3-642-41714-6_195264

IS:1498. (2007). Classification and identification of soils for general engineering purposes. *Indian Standards, Bureau of Indian Standards*, 1–28.

IS 2720 part 40. (2002). Methods of test for soils: Determination of free swell index of soils. In *Bureau of Indian Standard* (Vol. 3).

IS 2809. (1972). Glossary of terms and symbols relating to soil engineering. In *Bureau of Indian Standards* (Vol. 2, Issue Reaffirmed in 1992).

KH Head, 2011. (1994). Manual of soil laboratory testing. In *Soil Dynamics and Earthquake Engineering* (Vol. 13, Issue 2, p. 147). https://doi.org/10.1016/0267-7261(94)90007-8

Lukas, M. (2010). *A study on the effect of remolding on the mechanical behavior of Addis Ababa red clay soil*. *M.Sc. Thes*(April), 1–207. http://hdl.handle.net/123456789/4595

McCauley, A., Jones, C., & Jacobsen, J. (2005). Basic Soil Properties. *Soil and Water Management*, 1–12.

Merga, S. (2016). *Effect of Sample Height on Stress- Strain Behavior of Undrained Shear Strength of Addis Ababa Red Clay Soil Using UCS Test*.

Mir, B. A. (2013). *Compressibility and strength behavior of soft clays reinforced with sand compaction piles*. 421–431.

Mir, B. A. (2021). Manual of Geotechnical Laboratory Soil Testing. In *Manual of Geotechnical Laboratory Soil Testing*. https://doi.org/10.1201/9781003200260

Mitchell, J. K., & Soga, K. (2005). Chapter-3: Soil Mineralogy. In *Fundamentals of Soil Behavior* (3rd ed., pp. 35–82). John Wiley & Sons, Inc.

Muni Budhu. (2010). *Soil Mechanics and Foundations* (3rd ed., Vol. 3, Issue 2010). John Wiley & Sons, Inc.

Nelson, J. D., & Miller, D. J. (1975). *Expansive Soils: Problems and Practice in Foundation and Pavement Engineering*. John wiley & sons,inc.

Omar, T., & Sadrekarimi, A. (2015). Effect of triaxial specimen size on engineering design and analysis. *International Journal of Geo-Engineering*, *6*(1). https://doi.org/10.1186/s40703-015-0006-3

Ou, C.-Y. (2006). *Deep Excavation_ Theory and Practice - Chang-Yu Ou - Google Books*.

Prakash, K., & Sridharan, A. (2004). Free swell ratio and clay mineralogy of fine-grained soils. *Geotechnical Testing Journal*, *27*(2), 220–225. https://doi.org/10.1520/gtj10860

Rao, S. (2006). *Identification and classification of expansive soils.* (1st ed., Issue 2006, pp. 1–11). Engineering Geology. https://doi.org/10.1201/9780203968079.ch2

Seopal, M. S., & Kumar, P. A. (2023). *EasyChair Preprint Research Review Report on Effect of Moisture Content on Shear Strength of Soil*.

SM & FE Dr.Kr. Arora . (2003).

BS 1377-7 Cl-8, 1990. Soils for civil engineering purposes

Tibebu, H. (2008). *Parameters of Laterite soils in Southern Part of Ethiopia the case of Wolayita - Sodo*. *c*, 2004–2007.

Venkat Raman, K., Dayakar, P., & Sankaran, S. (2015). Effect of L/D Ratio of UCC Specimen on Shear Strength of Clay Soil. *Indian Journal of Science and Technology*, *8*(32). https://doi.org/10.17485/ijst/2015/v8i32/87783

Venkatramaiah, C. (2006). Geotechnical Engineering, 3Ed. In *New Age International Publishers* (Vol. 1999, Issue December).

Wesley, L. D. (n.d.). *Geotechnical Engineering in Residual Soils*.

Wiley, J. (2009). *SOIL MECHANICS FOR SEDIMENTARY SOIL MECHANICS FOR SEDIMENTARY AND RESIDUAL SOILS*.

Zarei, C., Soltani-Jigheh, H., & Liu, Y. (2023). Effects of Strain Rate and Specimen Size on the Behavior of Fine-Grained Soils. *Arabian Journal of Geosciences*, *16*(4). https://doi.org/10.1007/s12517-023-11344-x

APPENDICES

Appendix-A: Specific Gravity of Red Clay Soil

Table A-1: Specific gravity of red clay soil

S. No.	Specific gravity determination parameters	Pycnometer Id.	
		1	2
1	Weight of Pycnometer, M_p (gm)	41.95	33.44
2	Weight of (Pycnometer + water), $M_{a'}$ (gm)	144.42	133.6
3	Temperature of water at Ma' measured, T' (°C)	18.8	18.8
4	Density of water at T' (°C), $P_{w\ (T')}$	0.99845	0.99845
5	Weight of (Pycnometer + material + Water, M_b (gm)	150.78	139.9
6	Temperature of M_b measured, T (°C)	23.8	25
7	Density of water at T (°C), $P_{w\ (T)}$	0.99735	0.99705
8	Weight of (Pycnometer + water) at T °C, M_a (gm)	144.31	133.46
9	Weight of dry material,M_s (gm)	10.04	10
10	Specific gravity of material at T °C, G_T	2.807	2.801
11	Correction Factor	0.99914	0.99884
12	Specific gravity of material at 20 °C, G_{20}	2.805	2.798
13	Average G_s	2.801	

Appendix-B: Swelling Properties of Red Clay Soil

Table B-1: Free swell index and free swell ratio of soil sample

Sample	V_K (ml)	V_W (ml)	FSI (%)	Degree of swell	FSR	Swell potential
Red clay	10.5	19	81	Very high	1.81	Moderate

Appendix-C: Particle Size Distribution Result

Parameters used for test

Time (min) = t (min)	Adjusted percent finer (%) = P_a (%)
Actual hydrometer reading = R_a	Effective depth (Cm) = L (Cm)
Corrected hydrometer reading = R_c	Coefficient of temperature adjustment = K
Percent finer (%) = P (%)	Diameter of particle (mm) = D (mm)
Sieve number = SN	Percent retained (%) = P_R (%)
Sieve size(mm) = S_S (mm)	Cumulative percent retained (%) = CP_R (%)
Mass of soil retained (gm) = M_R(gm)	Percent passed (%) = P_P (%)

Table C-1: Grain size analysis result of soil sample

SN.	S_S (mm)	M_R (gm)	P_R (%)	CP_R (%)	P_P (%)
4	4.75	13	1.3	1.3	98.7
8	2.36	14	1.4	2.7	97.3
10	2	4	0.4	3.1	96.9
16	1.18	6	0.6	3.7	96.3
30	0.6	5	0.5	4.2	95.8
50	0.3	4	0.4	4.6	95.4
100	0.15	8	0.8	5.4	94.6
200	0.075	8	0.8	6.2	93.8
	Pan	937.42	93.74	100	0

Table C-2: Hydrometer analysis result of soil sample

t(min)	R_a	R_c	P	P_a	L (Cm)	$\sqrt{L/T}$	K	D (mm)
0.5	46	44.35	89.55	89.00	8.8	4.2	0.0129	0.054
1	46	44.35	89.55	86.00	8.8	2.97	0.0129	0.038
2	45.5	43.85	88.54	83.05	8.85	2.1	0.0129	0.027
5	45	43.35	87.53	82.11	8.9	1.33	0.0129	0.017
10	44	42.35	85.51	80.21	9.1	0.95	0.0129	0.012
20	42.5	40.85	82.49	77.37	9.3	0.68	0.0129	0.009
40	40	38.35	77.44	72.64	9.7	0.49	0.0129	0.006
80	38.5	36.85	74.41	69.80	10	0.35	0.0129	0.005
120	36.5	34.85	70.37	66.01	10.3	0.29	0.0129	0.004
240	33.5	31.85	64.31	60.33	10.8	0.21	0.0129	0.003
480	30	28.35	57.25	53.70	11.4	0.15	0.0129	0.002
1440	26	24.35	49.17	46.12	12	0.09	0.0129	0.001

Appendix-D: Atterberg Limit Test Results

Parameters and formulas used for LL and PL calculation

Mass of water = (Mass of can +Wet soil) - mass of can

Mass of dry soil = (Mass of can +Wet soil) - mass of can

Moisture content (%) = Mass of water *100/ Mass of dry soil

Liquid limit = Water content at number of blows is equal to 25.

Plastic limit =Average water content of plastic limit test trials

Table D-1: Liquid limit and plastic limit of red clay soil

Can ID	Liquid limit			Plastic Limit	
	1	2	3	4	5
Mass (wet soil + can) (gm)	60.42	61.34	60.78	40.34	40.65
Mass (dry soil + can) (gm)	52.13	52.56	51.6	39.92	39.79
Mass of can (gm)	38.38	38.71	37.68	38.5	36.9
Mass of dry soil (gm)	13.75	13.85	13.92	1.42	2.89
Mass of water (gm)	8.29	8.78	9.18	0.42	0.86
Water content (%)	60.29	63.39	65.95	29.58	29.76
Number of blows (counts)	33.00	24.00	18.00	29.67	
Liquid limit (%)	63.05				

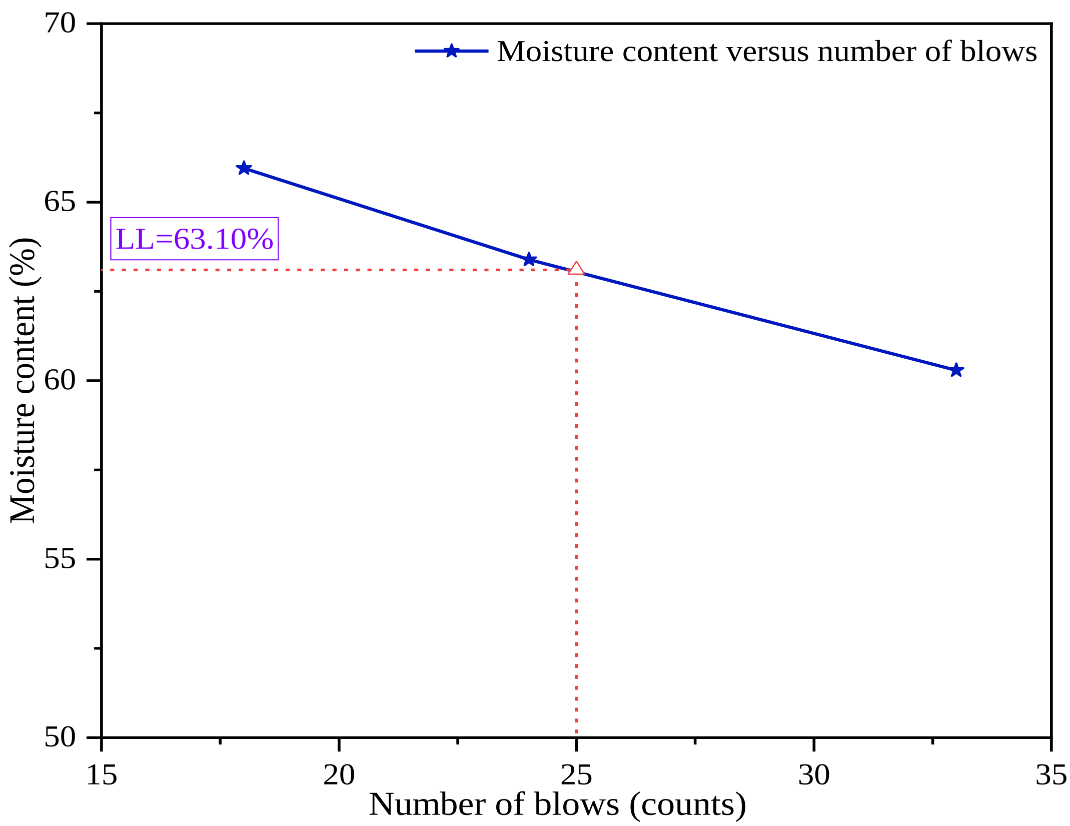

Figure D-1: Moisture content versus number of blows graph for red clay soil

Parameters and formulas used for LS calculation.

Average length of oven dry soil=L_D

Linear shrinkage (%) =$(L_O-L_D)/(L_O))$ *100%

Table D-2: Linear shrinkage of red clay soil

Source	Test pit
Length of wet sample (cm)	14
Average length of oven dry soil (cm)	11.8
Linear shrinkage (%)	15.71

Appendix-E: Compaction Test Results

Table E-1: Compaction test results of red clay soil

DENSITY	Trial number	1	2	3	4
	Mass of mold (gm)	5329	5329	5329	5329
	Mass of (mold + soil) (gm)	8611	8845	9021	8956
	Mass of soil (gm)	3282	3516	3692	3627
	Volume of mold (cm^3)	2112	2112	2112	2112
	Bulk density (gm/cm^3)	1.55	1.66	1.75	1.72
MOISTURE CONTENT	Can identity	A	B	C	D
	Weight of can (gm)	57	74	46	48
	Weight of (wet soil + can) (gm)	236	214	223	220
	Weight of (dry soil + can) (gm)	202	186	185	181
	Weight of water (gm)	34	28	38	39
	Weight of dry soil (gm)	145	112	139	133
	Average moisture content (%)	23.45	25	27.34	29.32
Dry density of soil (gm/cm^3)		1.259	1.339	1.373	1.328
ZAV	Specific gravity of soil, G_s	2.801	2.801	2.801	2.801
	Density of water (gm/cm^3)	1	1	1	1
	ZAV dry density	1.69	1.65	1.59	1.54

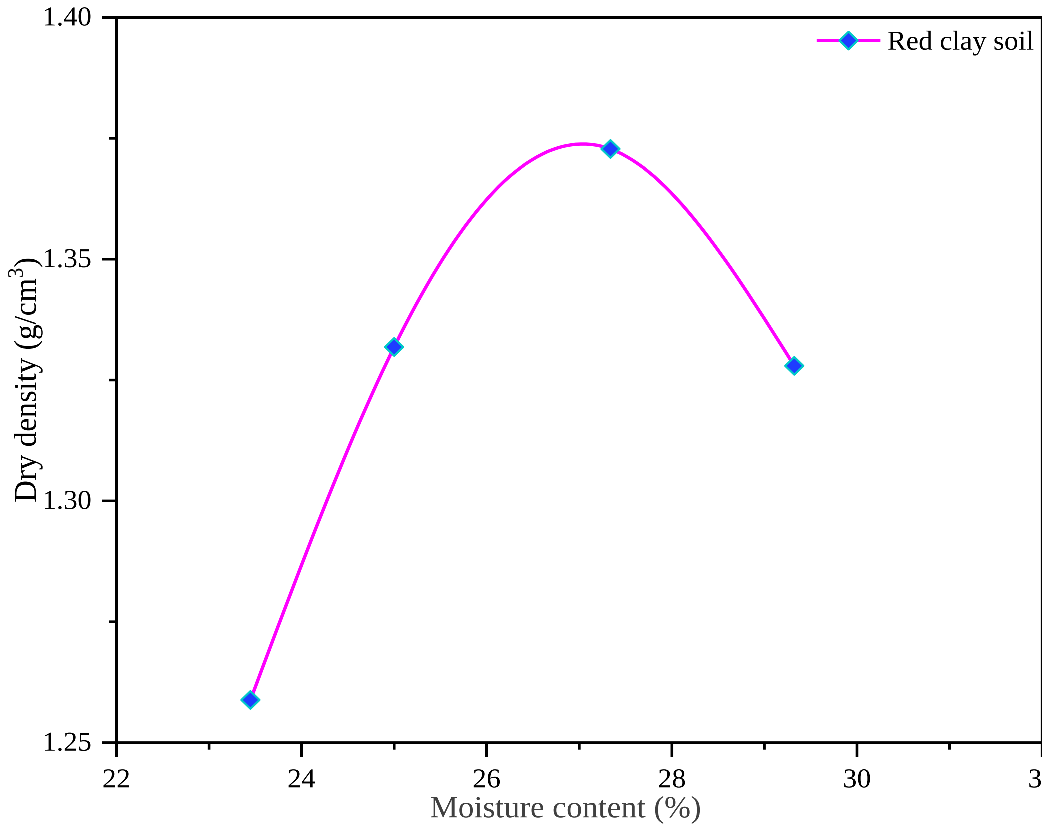

Figure E-1: Compaction curve of red clay soil

Appendix-F: Consolidation Test Results

Parameters and formulas used for consolidation test

Height of solid soil mass = $H_s = \frac{4V_s}{\pi D^2}$

Total volume of specimen = $V = \frac{\pi D^2}{4} * H$

Initial wet density = $\rho_{wet} = \frac{M_s}{V}$

Initial void ratio = $e_0 = \frac{V_v}{V_s}$

Length of drainage path= H_{dr}

Change in void ratio=$\Delta e = \frac{\Delta H * (1+e_0)}{H}$

Void ratio=$e = e_0 - \Delta e$

Deformation at 50% consolidation= d_{50}

Initial dry density of specimen = $\rho_{dry} = \frac{\rho_{wet}}{1+w_{initial}}$

Volume of solid in soil specimen = $V_s = \frac{M_s}{G_s * \rho_w}$

Volume of voids in soil specimen = $V_v = V - V_s$

Moisture content = $w = \frac{w_w}{w_s} * 100\%$

Depth of specimen at 50% consolidation=H_{50}

Deformation at 100% consolidation=$\Delta H = d_{100}$

Elapsed time to reach 50% consolidation=t_{50}

Coefficient of consolidation=$C_v = \frac{0.197 * {H_{dr}}^2}{t_{50}}$

Table F-1: Moisture content result of samples

	Parameters	Red clay soil
Initial moisture content	weight of container, w_c(gm)	30.11
	weight of (container + wet soil), w_{cw}(gm)	67.05
	weight of (container + dry soil), w_{cd}(gm)	59.13
	weight of water, w_w (gm)	7.92
	weight of soil, w_s (gm)	29.02
	Moisture content, w (%)	27.29
Final moisture content	weight of container, w_c(gm)	29.29
	weight of (container + wet soil), w_{cw}(gm)	122.1
	weight of (container + dry soil), w_{cd}(gm)	96.08
	weight of water, w_w (gm)	26.02
	weight of soil, w_s (gm)	66.79
	Moisture content, w (%)	38.96

Table F-2: Specimen data and properties result

Parameters	Soil
Weight of specimen ring + soil, M_{rs}(gm)	175.14
Weight of specimen ring, M_r(gm)	76.57
Weight of specimen, M_s(gm)	98.57
Diameter of specimen, D (cm)	6
Initial height of specimen, H (cm)	2
Total volume of specimen, V(cm^3)	56.52
Initial wet density, ρ_{wet} (gm/cm^3)	1.74
Initial moisture content, $w_{initial}$, %	27.30
Initial Dry density of specimen, ρ_{dry} (gm/cm^3)	1.37
Specific gravity, G_s	2.801
Density of water, ρ_w (gm/cm^3)	1
Volume of solid in soil specimen, V_s (cm^3)	23.85
Height of solid soil mass, H_s (cm)	0.84
Volume of voids in soil specimen, V_v (cm^3)	32.67
Initial void ratio, e_0	1.370

Final moisture content, w_{final}, %	38.96

Table F-3: Recorded specimen data of red clay soil

time (min)	Red clay soil					
	50KPa	100KPa	200KPa	400KPa	800KPa	1600KPa
	Deformation (mm)					
0	2.25	2.649	2.7026	2.7633	2.8894	3.2104
0.1	2.382	2.666	2.7341	2.796	2.958	3.305
0.25	2.396	2.668	2.7358	2.802	2.968	3.324
0.5	2.407	2.671	2.7373	2.809	2.976	3.342
1	2.422	2.674	2.7388	2.816	2.988	3.362
2	2.44	2.677	2.7412	2.826	3	3.389
4	2.461	2.68	2.743	2.836	3.02	3.422
8	2.491	2.683	2.7453	2.847	3.04	3.456
15	2.512	2.686	2.7472	2.855	3.06	3.483
30	2.541	2.689	2.7492	2.863	3.09	3.512
60	2.562	2.692	2.7519	2.871	3.12	3.534
120	2.584	2.695	2.7543	2.88	3.14	3.554
240	2.608	2.698	2.7576	2.885	3.16	3.569
480	2.622	2.701	2.7602	2.8878	3.18	3.578
1440	2.649	2.7026	2.7633	2.8894	3.2104	3.5854

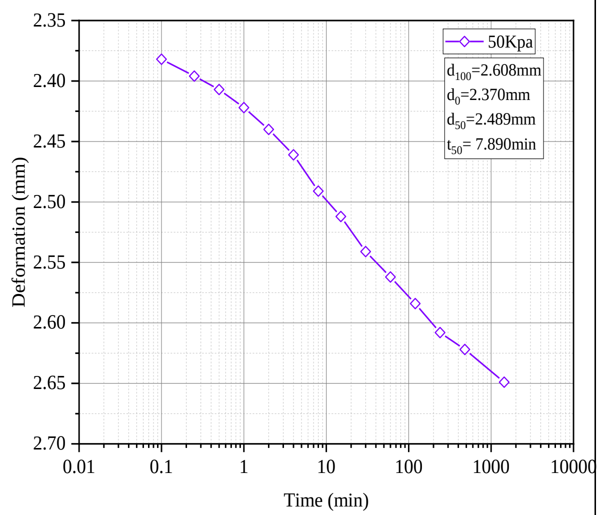

Figure H-1: Deformation versus log time curve of red clay soil for P = 50KPa

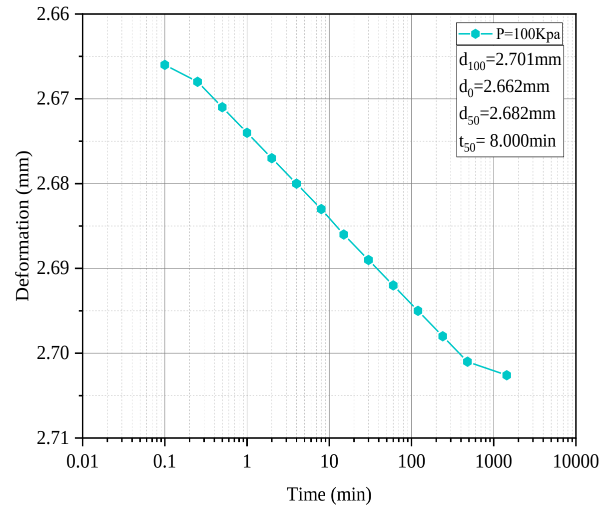

Figure H-2: Deformation versus log time curve of red clay soil for P = 100KPa

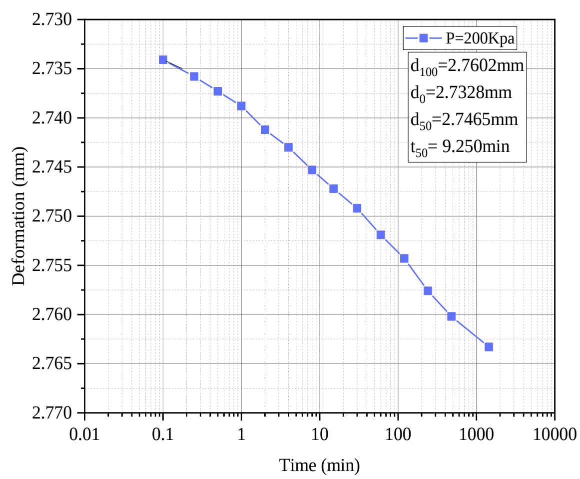

Figure H-3: Deformation versus log time curve of red soil for P = 200KPa

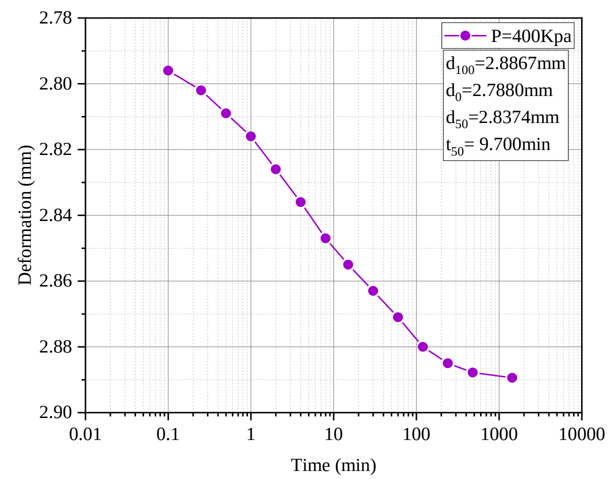

Figure H-4: Deformation versus log time curve of red soil for P = 400KPa

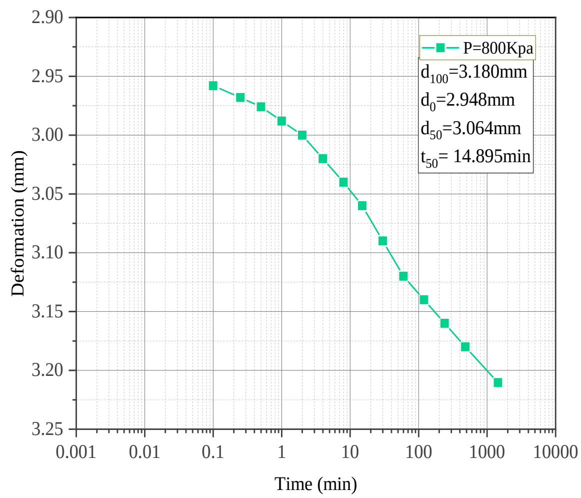

Figure H-5: Deformation versus log time curve of red clay soil for P = 800KPa

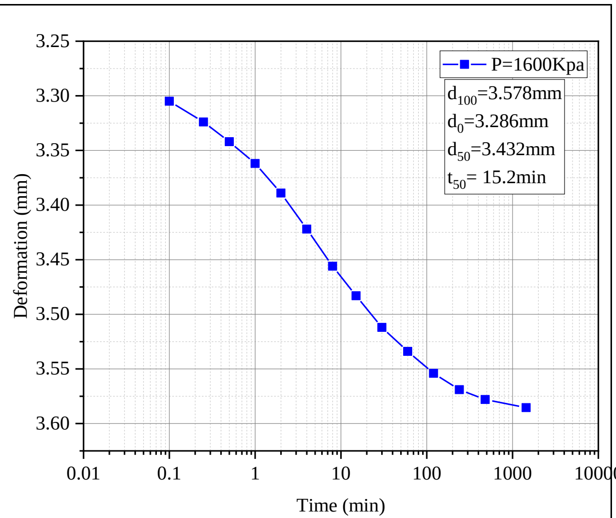

Figure H-6: Deformation versus log time curve of red clay soil for P = 1600KPa

Table F-4: Consolidation test result of natural soil

Conditions	Pressure (Kpa)	$d_{100}=\Delta H$(cm)	H(cm)	e_0	Δe	E	m_v
Loading Case	50	0.2608	2	1.37	0.3091	1.061	0.093
	100	0.2701	2	1.37	0.3201	1.050	0.030
	200	0.27602	2	1.37	0.3271	1.043	0.032
	400	0.28867	2	1.37	0.3421	1.028	0.037
	800	0.318	2	1.37	0.3769	0.993	0.024
	1600	0.3578	2	1.37	0.4240	0.949	-
Unloading case	50	0.3275	2	1.37	0.3881	0.982	
	100	0.3387	2	1.37	0.4014	0.969	
	200	0.34213	2	1.37	0.4055	0.965	
	400	0.34561	2	1.37	0.4096	0.961	
	800	0.35112	2	1.37	0.4161	0.954	
	1600	0.3559	2	1.37	0.4218	0.949	

Coefficient of consolidation, C_v Calculation

Pressure (KPa)	H(cm)	d_{50}(cm)	H_{50}	H_{dr}	t_{50}(min)	C_v(m^2/year)
50	2	0.2489	1.7511	0.87555	7.89	0.01914
100	2	0.2682	1.7318	0.8659	8	0.01846

200	2	0.27465	1.72535	0.862675	9.25	0.01585
400	2	0.28374	1.71626	0.85813	9.7	0.01496
800	2	0.3064	1.6936	0.8468	14.895	0.00948
1600	2	0.3432	1.6568	0.8284	15.2	0.00889

Observation Data Sheet and Analysis for "UU" Triaxial shear Test

Table 4-10: Summary of back pressure application for saturation specimen

	H/D=1.5		H/D=2		H/D=2.5	
Cell Pressure (σc) (kPa)	60	100	60	100	60	100
Plot strain vresu Stress curve	Plotted		Plotted		Plotted	
Correct post-shear x-section area, Asc=(Ac/1-εa%)*1/10000 (m2)	0.21	0.21	0.21	0.21	0.21	0.21
Saturated length, Lsat=Lo-Δl (cm)	7.30	7.29	9.72	9.70	12.20	12.18
Major principal stress, σ1 (kpa)	146.97	186.92	144.89	184.85	141.52	181.53
Minor principal stress, σ3 (kpa)	60.00	100.00	60.00	100.00	60.00	100.00
Stress ratio, σ1/σ3	2.45	1.87	2.41	1.85	2.36	1.82
Mean stress, P=(σ1+2σ3)/3 (kpa)	88.99	128.97	88.30	128.28	87.17	127.18
Eff. mean stress, p′ = p-u (kPa) (if pore water pressure is measured in UU test)	29.99	29.12	28.55	29.78	27.72	27.68
Mean stress ratio, M = q/p=d)c/p	1.48	1.29	1.47	1.28	1.45	1.27
Compute ϕ’ (Degrees) =sin-1 (3 M/(6 + M))	0.010	0.009	0.010	0.01	0.01	0.01
Compute ko = 1 - sin ϕ′ (NC Soils: Jakay, 1944)	0.41	0.47	0.41	0.47	0.42	0.48
Undrained strength, su = cu = qu/p=d)c/2	43.48	43.46	42.45	42.43	40.76	40.77
Strength ratio, sr =su/σo	0.39	0.29	0.38	0.28	0.36	0.27

Compute A-factor, A = Δu/(Δσ1-Δσ3)=Δu/Δσd (if pore water pressure is measured in UU test)	0.68	0.69	0.70	1.18	1.21	1.22

Appendix-G: Tri-axial Test Results

Table G-1: Application of Back-pressure for specimen saturation under σ_c=60 kPa

Aspect ratio	Cell Pressure (σc)	Back Pressure Ub, (kpa)	Pore Pressure U, (kpa)	ΔU=U2-U1	Δσc=σc2-σc1	B=factor=ΔU/Δσc
H/D=1.5	30.00	20.00	19.00	19.00	30.00	-
	60.00	-	40.00	21.00	30.00	0.70
	60.00	50.00	48.00	8.00	-	-
	90.00	-	72.00	24.00	30.00	0.80
	90.00	80.00	78.00	6.00	-	-
	120.00	-	104.00	26.00	30.00	0.87
	120.00	110.00	110.00	6.00	-	-
	180.00	-	168.00	58.00	60.00	0.97
	180.00	170.00	170.00	2.00	-	-
	240.00	-	229.00	59.00	60.00	0.98
H/D=2	80.00	-	55.00	55.00	80.00	0.69
	80.00	72.00	70.00	-	-	-
	120.00	-	105.00	35.00	40.00	0.88

	120.00	112.00	114.00	-	-	-
	160.00	-	150.00	36.00	40.00	0.90
	160.00	150.00	150.00	-	-	-
	220.00	-	207.00	57.00	60.00	0.95
	220.00	210.00	210.00	3.00	-	-
	280.00	-	268.00	58.00	60.00	0.97
	280.00	270.00	270.00	2.00	-	-
	340.00	0	329.75	59.75	60.00	1.00
H/D=2.5	90.00	-	62.00	62.00	90.00	0.69
	90.00	79.85	78.00	16.00	-	-
	135.00	-	116.50	38.50	45.00	0.86
	135.00	122.00	116.50	-	-	-
	195.00	-	172.50	56.00	60.00	0.93
	195.00	184.00	194.75	22.25	-	-
	255.00	-	252.55	57.80	60.00	0.96
	255.00	254.00	254.00	1.45	-	-
	315.00	-	313.45	59.45	60.00	0.99

Table G-2: Application of Back-pressure for specimen saturation under σ_c=100 kPa

Aspect ratio	Cell Pressure (σc)	Back Pressure Ub, (kpa)	Pore Pressure U, (kpa)	ΔU=U2-U1	Δσc=σc2-σc1	B=factor=ΔU/Δσc
H/D=1.5	120.00	-	85.00	85.00	120.00	0.71
	120.00	108.00	106.00	21.00	-	-
	180.00	-	158.45	52.45	60.00	0.87
	180.00	171.00	171.00	12.55	-	-
	240.00	-	226.20	55.20	60.00	0.92
	240.00	230.00	230.00	3.80	-	-
	340.00	-	326.80	96.80	100.00	0.97
	340.00	331.00	330.00	3.20	-	-
	440.00	-	429.85	99.85	100.00	1.00
H/D=2	150.00	-	120.00	120.00	150.00	0.80
	150.00	142.50	142.50	22.50	-	-
	225.00	-	210.00	67.50	75.00	0.90
	225.00	215.00	214.00	4.00	-	-
	325.00	-	311.00	97.00	100.00	0.97
	325.00	320.00	318.00	7.00	-	-
	425.00	-	416.50	98.50	100.00	0.99
H/D=2.5	160.00	-	124.35	124.35	160.00	0.78

	160.00	152.55	151.75	27.40	-	-
	240.00	-	222.35	70.60	80.00	0.88
	240.00	232.00	230.00	7.65	-	-
	340.00	-	324.00	94.00	100.00	0.94
	340.00	332.50	331.50	7.50	-	-
	440.00	-	431.00	99.50	100.00	1.00

Test data for the stress-strain plot for "UU" triaxial Shear Tes

Stress-strain Characteristic of "UU" triaxial Test; Sample No. one

Strain Rate =1mm/min Designated Confining Stress or Cell Pressure=**σ_c=σ_3=0.6kg/cm2=60kpa**;

PR. Lc (kg/divn) =8.772N/divns; D_o=5 cm; A_o=19.635 cm^2

L_o=7.5cm; V_o=19.635 cm^2*7.5 cm=147.262 cm^3

Site: **Gechi Yanfa Road Project from station 20+880 at the Center**

Sample Type: **Disturbed red clay soil** BH **1** Depth (m) **3**

Table G-1: Triaxial test result on red clay soil specimen with Ho=7.5 cm under cell pressure (σ3=60kpa)

ΔL	ϵ_a=ΔL/L_o	1-ϵ_a	A_c=A_o/(1-ϵ_a)	Proving Dial reading	Applied axial load(P) (N)	σ_d=P/A_c (Mpa)	σ_d (Deviatoric stress (kpa)	Major principal stress (σ1) (kpa)	(σ1-σ3)/2	(σ1+σ3)/2
0.00	0.00	1.00	1963.50	0.00	0.00	0.00	0.00	60.00	0.00	60.00
0.30	0.40	1.00	1971.39	4.25	37.28	0.02	18.91	78.91	9.46	69.46
1.00	1.33	0.99	1990.03	14.25	125.00	0.06	62.81	122.81	31.41	91.41
1.40	1.87	0.98	2000.85	18.20	159.65	0.08	79.79	139.79	39.90	99.90
2.00	2.67	0.97	2017.29	20.00	175.44	0.09	86.97	146.97	43.48	103.48

3.00	4.00	0.96	2045.31	19.80	173.69	0.08	84.92	144.92	42.46	102.46
4.00	5.33	0.95	2074.12	19.40	170.18	0.08	82.05	142.05	41.02	101.02
5.00	6.67	0.93	2103.75	19.00	166.67	0.08	79.22	139.22	39.61	99.61
6.00	8.00	0.92	2134.24	19.00	166.67	0.08	78.09	138.09	39.05	99.05
7.00	9.33	0.91	2165.63	19.00	166.67	0.08	76.96	136.96	38.48	98.48
8.00	10.67	0.89	2197.95	19.00	166.67	0.08	75.83	135.83	37.91	97.91
9.00	12.00	0.88	2231.25	18.90	165.79	0.07	74.30	134.30	37.15	97.15
10.00	13.33	0.87	2265.58	18.75	164.48	0.07	72.60	132.60	36.30	96.30
11.25	15.00	0.85	2310.00	18.60	163.16	0.07	70.63	130.63	35.32	95.32

Test data for the stress-strain plot for "UU" triaxial Shear Test

Stress-strain Characteristic of "UU" triaxial Test; Sample No. Two

Strain Rate =1mm/min; Designated Confining Stress or Cell Pressure=**σ_c=σ_3=0.6kg/cm2=60kpa**

PR. Lc (kg/divn) =8.772N/divns; D_o=5cm; A_o=19.635 cm^2

L_o=10cm; V_o=19.635cm^2*10 cm=196.35cm^3

Site: **Gechi Yanfa Road Project from station 20+880 at the Center**

Sample Type: **Disturbed red clay soil** BH **1** Depth (m) **3**

Table G-2: Triaxial test result on red clay soil specimen with Ho=10 cm under cell pressure (σ3=60kpa)

ΔL	ϵ_a=ΔL/L_o	1-ϵ_a	A_c=A_o/(1-ϵ_a)	Proving Dial reading	Applied axial load(P)(N)	σ_d=P/A_c (Mpa)	σ_d (Deviatoric stress (kpa)	Major principal stress (σ1) (kpa)	(σ1-σ3)/2	(σ1+σ3)/2
-	0.00	1.00	1,963.50	-	-	-	-	60.00	-	60.00
0.30	0.30	1.00	1,969.41	2.60	22.81	0.01	11.58	71.58	5.79	65.79
1.05	1.05	0.99	1,984.34	10.00	87.72	0.04	44.21	104.21	22.10	82.10
1.60	1.60	0.98	1,995.43	15.50	135.97	0.07	68.14	128.14	34.07	94.07

2.05	2.05	0.98	2,004.59	18.60	163.16	0.08	81.39	141.39	40.70	100.70
2.80	2.65	0.97	2,020.06	19.55	171.49	0.08	84.89	144.89	42.45	102.45
4.00	4.00	0.96	2,045.31	19.08	167.40	0.08	81.84	141.84	40.92	100.92
5.00	5.00	0.95	2,066.84	18.65	163.60	0.08	79.15	139.15	39.58	99.58
6.00	6.00	0.94	2,088.83	18.30	160.53	0.08	76.85	136.85	38.43	98.43
8.00	8.00	0.92	2,134.24	18.20	159.65	0.07	74.80	134.80	37.40	97.40
10.00	10.00	0.90	2,181.67	18.10	158.77	0.07	72.78	132.78	36.39	96.39
12.00	12.00	0.88	2,231.25	17.95	157.46	0.07	70.57	130.57	35.28	95.28
14.00	14.00	0.86	2,283.14	17.75	155.70	0.07	68.20	128.20	34.10	94.10
15.00	15.00	0.85	2,310.00	17.60	154.39	0.07	66.83	126.83	33.42	93.42

Stress-strain Characteristic of "UU" triaxial Test; Sample No. Three

Strain Rate =1mm/min; Designated Confining Stress or Cell Pressure=**σ_c=σ_3=0.6kg/cm2=60kpa**

PR. Lc (kg/divn) =8.772N/divns; D_o=5cm; A_o=19.635 cm^2

L_o=12.5cm; V_o=19.635cm^2*12.5 cm=245.44cm^3

Site: **Gechi Yanfa Road Project from station 20+880 at the Center**

Sample Type: **Disturbed red clay soil** BH **1** Depth **3m**

ΔL	ϵ_a=ΔL/L_o	1-ϵ_a	A_c=A_o/(1-ϵ_a)	Proving Dial reading	Applied axial load(P) (N)	σ_d=P/A_c (Mpa)	σ_d (Deviatoric stress (kpa)	Major principal stress (σ1) (kpa)	(σ1-σ3)/2	(σ1+σ3)/2
-	-	1.00	1,963.50	-	-	-	-	60.00	-	60.00

0.50	0.4	1.00	1,971.39	2.50	21.93	0.01	11.12	71.12	5.56	65.56
0.90	0.7	0.99	1,977.74	5.65	49.55	0.03	25.05	85.05	12.53	72.53
1.50	1.2	0.99	1,987.35	9.90	86.82	0.04	43.69	103.69	21.84	81.84
2.20	1.8	0.98	1,998.68	14.62	128.22	0.06	64.15	124.15	32.08	92.08
3.00	2.4	0.98	2,011.78	18.70	164.00	0.08	81.52	141.52	40.76	100.76
4.20	3.4	0.97	2,031.77	18.50	162.25	0.08	79.85	139.85	39.93	99.93
5.20	4.2	0.96	2,048.73	18.30	160.49	0.08	78.34	138.34	39.17	99.17
6.30	5.0	0.95	2,067.71	17.80	156.11	0.08	75.50	135.50	37.75	97.75
8.00	6.4	0.94	2,097.76	17.52	153.65	0.07	73.25	133.25	36.62	96.62
10.00	8.0	0.92	2,134.24	17.35	152.16	0.07	71.29	131.29	35.65	95.65
12.00	9.6	0.90	2,172.01	17.10	149.97	0.07	69.05	129.05	34.52	94.52

Test data for the stress-strain plot for "UU" triaxial Shear Test

Stress-strain Characteristic of "UU" triaxial Test; Sample No. Four

Strain Rate =1mm/min; Designated Confining Stress or Cell Pressure=**σ_c=σ_3=1kg/cm2=100kpa**

PR. Lc (kg/divn) =8.772N/divns; D_o=5cm; A_o=19.635 cm^2

L_o=7.5cm; V_o=19.635cm^2*7.5 cm=147.262cm^3

Site: **Gechi Yanfa Road Project from station 20+880 at the Center**

SampleType: **Disturbed red clay soil** BH **1** Depth **3m**

ΔL	ϵ_a=Δ L/L_o	1-ϵ_a	A_c=A_o/(1-ϵ_a)	Proving Dial reading	Applied axial load(P) (N)	σ_d=P/A_c (Mpa)	σ_d (Deviatoric stress (kpa)	Major principal stress (σ1) (kpa)	(σ1-σ3)/2	(σ1+σ3)/2

-	0.00	1.00	1,963.50	-	-	-	-	100.00	-	100.00
0.15	0.20	1.00	1,967.43	3.00	26.32	0.01	13.38	113.38	6.69	106.69
0.35	0.47	1.00	1,972.71	7.50	65.79	0.03	33.35	133.35	16.68	116.68
0.55	0.73	0.99	1,978.01	11.20	98.25	0.05	49.67	149.67	24.83	124.83
1.25	1.67	0.98	1,996.78	18.70	164.04	0.08	82.15	182.15	41.08	141.08
2.90	2.77	0.96	2,042.48	20.24	177.55	0.09	86.93	186.93	43.46	143.46
4.00	5.33	0.95	2,074.12	19.55	171.49	0.08	82.68	182.68	41.34	141.34
5.00	6.67	0.93	2,103.75	19.25	168.86	0.08	80.27	180.27	40.13	140.13
6.00	8.00	0.92	2,134.24	18.85	165.35	0.08	77.48	177.48	38.74	138.74
7.60	10.13	0.90	2,184.90	18.45	161.84	0.07	74.07	174.07	37.04	137.04
9.40	12.53	0.87	2,244.86	18.24	160.00	0.07	71.27	171.27	35.64	135.64
10.80	14.40	0.86	2,293.81	18.12	158.95	0.07	69.29	169.29	34.65	134.65
12.20	16.27	0.84	2,344.94	17.95	157.46	0.07	67.15	167.15	33.57	133.57

Stress-strain Characteristic of "UU" triaxial Test; Sample No. Five

Strain Rate =1mm/min; Designated Confining Stress or Cell Pressure=**σ_c=σ_3=1kg/cm2=100kpa**

PR. Lc (kg/divn) =8.772N/divns; D_o=5cm; A_o=19.635 cm^2

L_o=10 cm; V_o=19.635 cm^2*10 cm=196.35 cm^3

Site: **Gechi Yanfa Road Project from station 20+880 at the Center**

Sample Type: **Disturbed red clay soil** BH **1** Depth **3m**

Table G-5: Triaxial test result on red clay soil specimen with H_o=10 cm under cell pressure (σ_3=100kpa)

ΔL	$\epsilon_a=\Delta L/L_o$	$1-\epsilon_a$	$A_c=A_o/(1-\epsilon_a)$	Proving Dial reading	Applied axial load (P)(N)	$\sigma_d=P/A_c$ (Mpa)	σ_d (Deviatoric stress (kpa)	Major principal stress ($\sigma 1$) (kpa)	($\sigma 1-\sigma 3$)/2	($\sigma 1+\sigma 3$)/2
-	0.00	1.00	1,963.50	-	-	-	-	100.00	-	100.00
0.60	0.60	0.99	1,975.35	6.60	57.90	0.03	29.31	129.31	14.65	114.65
0.85	0.85	0.99	1,980.33	9.70	85.09	0.04	42.97	142.97	21.48	121.48
1.05	1.05	0.99	1,984.34	12.30	107.90	0.05	54.37	154.37	27.19	127.19
1.55	1.55	0.98	1,994.41	17.40	152.63	0.08	76.53	176.53	38.27	138.27
2.70	2.70	0.98	2,007.67	19.42	170.35	0.08	84.85	184.85	42.43	142.43
4.00	4.00	0.96	2,045.31	19.00	166.67	0.08	81.49	181.49	40.74	140.74
5.00	5.00	0.95	2,066.84	18.70	164.04	0.08	79.37	179.37	39.68	139.68
6.00	6.00	0.94	2,088.83	18.40	161.40	0.08	77.27	177.27	38.64	138.64
7.00	7.00	0.93	2,111.29	17.98	157.72	0.07	74.70	174.70	37.35	137.35
8.00	8.00	0.92	2,134.24	17.65	154.83	0.07	72.54	172.54	36.27	136.27
9.00	9.00	0.91	2,157.69	17.45	153.07	0.07	70.94	170.94	35.47	135.47
10.00	10.00	0.90	2,181.67	17.25	151.32	0.07	69.36	169.36	34.68	134.68

Stress-strain Characteristic of "UU" triaxial Test; Sample No. Six

Strain Rate =1mm/min; Designated Confining Stress or Cell Pressure=**$\sigma_c=\sigma_3$=1kg/cm^2=100kpa**

PR. Lc (kg/divn) =8.772N/divns; D_o=5cm; A_o=19.635 cm^2

L_o=12.5 cm; V_o=19.635 cm^2*12.5 cm=245.44 cm^3

Site: **Gechi Yanfa Road Project from station 20+880 at the Center**

Sampl eType:	**Disturbed red clay soil**	BH	**1**	Depth	**3m**

Table G-6: Triaxial test result on red clay soil specimen with H_o=12.5 cm under cell pressure (σ_3=100kpa)

ΔL	ϵ_a=ΔL/ L_o (%)	1-ϵ_a	A_c=A_o/ (1-ϵ_a) (cm)	Proving Dial reading	Applied axial load(P) (N)	σ_d=P/ A_c (Mpa)	σ_d (Deviatoric stress (kpa)	Major principal stress (σ1) (kpa)	(σ1-σ3)/2	(σ1+σ3)/2
-	0.00	1.00	1,963.50	-	-	-	-	100.00	-	100.00
0.35	0.28	1.00	1,969.01	2.50	21.93	0.01	11.14	111.14	5.57	105.57
0.85	0.68	0.99	1,976.94	6.00	52.63	0.03	26.62	126.62	13.31	113.31
1.35	1.08	0.99	1,984.94	10.00	87.72	0.04	44.19	144.19	22.10	122.10
2.10	1.68	0.98	1,997.05	15.50	135.97	0.07	68.08	168.08	34.04	134.04
3.20	2.56	0.97	2,015.09	18.73	164.30	0.08	81.53	181.53	40.77	140.77
4.30	3.44	0.97	2,033.45	18.60	163.16	0.08	80.24	180.24	40.12	140.12
5.00	4.00	0.96	2,045.31	18.30	160.53	0.08	78.49	178.49	39.24	139.24
6.00	4.80	0.95	2,062.50	17.80	156.14	0.08	75.71	175.71	37.85	137.85
7.00	5.60	0.94	2,079.98	17.45	153.07	0.07	73.59	173.59	36.80	136.80
8.00	6.40	0.94	2,097.76	17.30	151.76	0.07	72.34	172.34	36.17	136.17
9.00	7.20	0.93	2,115.84	17.10	150.00	0.07	70.89	170.89	35.45	135.45

10.00	8.00	0.92	2,134.24	16.95	148.69	0.07	69.67	169.67	34.83	134.83
11.25	9.00	0.91	2,157.69	16.75	146.93	0.07	68.10	168.10	34.05	134.05

Table G-7: Triaxial test result on red clay soil specimen with H/D=1.5 cm under cell pressure (σ_3=60kpa)

H/D=1.5

	Axial stress		σ1	146.97	
	Cell pressure		σ3	60.00	
	R		(σ1-σ3)/2	43.48	
	σ_{avg}		(σ3+σ3)/2	103	
	τ_{xy}			0	
Angle,θ	$\sigma_n=\sigma_{avg}+R\cos\theta$	$\tau_n=R\sin\theta$	Angle,θ	σn=σavg+RCosθ	τn=RSinθ
0	146.968	0.000	46	133.695	31.275
1	146.961	0.759	47	133.145	31.798
2	146.941	1.517	48	132.586	32.310
3	146.908	2.275	49	132.017	32.813
4	146.862	3.033	50	131.440	33.306
5	146.803	3.789	51	130.855	33.789
6	146.730	4.544	52	130.261	34.261
7	146.644	5.298	53	0129.659	34.723
8	146.545	6.051	54	129.049	35.175
9	146.433	6.801	55	128.432	35.615
10	146.308	7.550	56	127.807	36.045
11	146.169	8.296	57	127.174	36.464
12	146.018	9.039	58	126.534	36.872
13	145.854	9.780	59	125.887	37.269
14	145.677	10.518	60	125.233	37.654
15	145.487	11.252	61	124.573	38.028
16	145.284	11.984	62	123.906	38.390
17	145.069	12.711	63	123.233	38.740

18	144.841	13.435	64	122.554	39.079
19	144.600	14.154	65	121.870	39.406
20	144.347	14.870	66	121.179	39.721
21	144.081	15.580	67	120.483	40.023
22	143.803	16.286	68	119.782	40.314
23	143.512	16.988	69	119.076	40.592
24	143.210	17.683	70	118.366	40.858
25	142.895	18.374	71	117.651	41.112
26	142.569	19.059	72	116.931	41.353
27	142.230	19.738	73	116.207	41.581
28	141.880	20.411	74	115.480	41.797
29	141.518	21.078	75	114.749	42.000
30	141.144	21.738	76	114.014	42.190
31	140.759	22.392	77	113.276	42.367
32	140.363	23.039	78	112.536	42.531
33	139.955	23.679	79	111.792	42.683
34	139.537	24.312	80	111.046	42.821
35	139.107	24.937	81	110.298	42.947
36	138.666	25.555	82	109.547	43.059
37	138.215	26.165	83	108.795	43.158
38	137.753	26.767	84	108.041	43.245
39	137.281	27.361	85	107.286	43.317
40	136.798	27.947	86	106.530	43.377
41	136.306	28.524	87	105.772	43.424
42	135.803	29.092	88	105.014	43.457
43	135.290	29.652	89	104.256	43.477
44	134.768	30.202	90	103.497	43.484
45	134.236	30.743	91	102.738	43.478
92	101.980	43.458	136	72.218	30.221
93	101.222	43.425	137	71.695	29.670
94	100.464	43.379	138	71.182	29.111

95	99.708	43.320	139	70.679	28.543
96	98.952	43.247	140	70.186	27.966
97	98.198	43.162	141	69.703	27.381
98	97.446	43.063	142	69.231	26.787
99	96.696	42.951	143	68.768	26.186
100	95.947	42.826	144	68.317	25.576
101	95.201	42.688	145	67.876	24.958
102	94.457	42.537	146	67.446	24.333
103	93.717	42.373	147	67.027	23.701
104	92.979	42.196	148	66.619	23.061
105	92.244	42.006	149	66.222	22.414
106	91.513	41.804	150	65.836	21.761
107	90.785	41.588	151	65.463	21.100
108	90.061	41.361	152	65.100	20.434
109	89.342	41.120	153	64.749	19.761
110	88.626	40.867	154	64.411	19.082
111	87.916	40.601	155	64.083	18.397
112	87.209	40.324	156	63.768	17.707
113	86.508	40.034	157	63.466	17.011
114	85.812	39.731	158	63.175	16.310
115	85.122	39.417	159	62.896	15.605
116	84.437	39.090	160	62.630	14.894
117	83.758	38.752	161	62.377	14.179
118	83.084	38.402	162	62.135	13.459
119	82.417	38.040	163	61.907	12.736
120	81.757	37.667	164	61.691	12.008
121	81.103	37.282	165	61.488	11.277
122	80.456	36.886	166	61.297	10.543
123	79.816	36.478	167	61.120	9.805
124	79.183	36.060	168	60.955	9.064
125	78.557	35.630	169	60.804	8.321
126	77.939	35.190	170	60.665	7.575

127	77.329	34.739	171	60.539	6.827
128	76.727	34.277	172	60.427	6.076
129	76.133	33.805	173	60.327	5.324
130	75.547	33.323	174	60.241	4.570
131	74.970	32.830	175	60.168	3.815
132	74.402	32.328	176	60.108	3.058
133	73.842	31.815	177	60.061	2.301
134	73.291	31.293	178	60.027	1.543
135	72.750	30.761	179	60.007	0.785
			180	60.000	0.026

Table G-8: Triaxial test result on red clay soil specimen with H/D=2 cm under cell pressure (σ_3=60kpa)

H/D=2					
	Axial stress			σ1	144.89
	Cell pressure			σ3	60.00
	R			(σ1-σ3)/2	42.45
	σavg			(σ3+σ3)/2	102.45
	τxy				0
Angle,θ	$\sigma_n=\sigma_{avg}$+RCosθ	τn=RSinθ	Angle,θ	σn=σavg+RCosθ	τn=RSinθ
0	144.895	0.000	46	131.938	30.530
1	144.888	0.741	47	131.401	31.040
2	144.869	1.481	48	130.855	31.540
3	144.837	2.221	49	130.301	32.031
4	144.791	2.960	50	129.737	32.512
5	144.733	3.699	51	129.166	32.983
6	144.662	4.436	52	128.586	33.445
7	144.578	5.172	53	127.999	33.896
8	144.482	5.906	54	127.403	34.336
9	144.372	6.639	55	126.800	34.766

10	144.250	7.370	56	126.190	35.186
11	144.115	8.098	57	125.573	35.595
12	143.968	8.824	58	124.948	35.993
13	143.807	9.547	59	124.316	36.380
14	143.634	10.267	60	123.678	36.756
15	143.449	10.984	61	123.034	37.121
16	143.251	11.698	62	122.383	37.475
17	143.041	12.408	63	121.726	37.817
18	142.818	13.115	64	121.063	38.148
19	142.583	13.817	65	120.395	38.467
20	142.336	14.515	66	119.721	38.774
21	142.076	15.209	67	119.041	39.069
22	141.805	15.898	68	118.357	39.353
23	141.522	16.583	69	117.668	39.625
24	141.226	17.262	70	116.974	39.884
25	140.919	17.936	71	116.276	40.132
26	140.600	18.604	72	115.574	40.367
27	140.270	19.267	73	114.868	40.590
28	139.928	19.924	74	114.157	40.800
29	139.575	20.575	75	113.444	40.998
30	139.210	21.220	76	112.727	41.184
31	138.834	21.858	77	112.006	41.357
32	138.447	22.490	78	111.283	41.518
33	138.049	23.115	79	110.558	41.665
34	137.640	23.732	80	109.829	41.801
35	137.221	24.343	81	109.099	41.923
36	136.791	24.946	82	108.366	42.033
37	136.350	25.541	83	107.632	42.130
38	135.900	26.129	84	106.896	42.214
39	135.439	26.709	85	106.159	42.285
40	134.968	27.280	86	105.420	42.343
41	134.487	27.844	87	104.681	42.389

42	133.996	28.398	88	103.941	42.421
43	133.496	28.945	89	103.201	42.441
44	132.986	29.482	90	102.460	42.447
45	132.467	30.010	91	101.719	42.441
92	100.979	42.422	138	70.916	28.417
93	100.239	42.390	139	70.425	27.863
94	99.499	42.345	140	69.943	27.300
95	98.761	42.287	141	69.472	26.728
96	98.024	42.216	142	69.011	26.149
97	97.288	42.133	143	68.559	25.561
98	96.553	42.036	144	68.119	24.966
99	95.821	41.927	145	67.688	24.363
100	95.090	41.805	146	67.268	23.753
101	94.362	41.670	147	66.859	23.136
102	93.636	41.523	148	66.461	22.511
103	92.913	41.363	149	66.074	21.880
104	92.193	41.190	150	65.697	21.242
105	91.475	41.005	151	65.332	20.597
106	90.762	40.807	152	64.979	19.947
107	90.051	40.597	153	64.636	19.290
108	89.345	40.375	154	64.305	18.627
109	88.642	40.140	155	63.986	17.959
110	87.944	39.893	156	63.679	17.285
111	87.250	39.634	157	63.383	16.606
112	86.561	39.362	158	63.099	15.922
113	85.876	39.079	159	62.827	15.233
114	85.197	38.784	160	62.568	14.539
115	84.523	38.477	161	62.320	13.841
116	83.854	38.159	162	62.085	13.138
117	83.191	37.828	163	61.861	12.432
118	82.534	37.487	164	61.651	11.722

119	81.883	37.133	165	61.452	11.008
120	81.238	36.769	166	61.266	10.291
121	80.600	36.393	167	61.093	9.571
122	79.968	36.006	168	60.932	8.848
123	79.343	35.609	169	60.784	8.123
124	78.725	35.200	170	60.649	7.394
125	78.115	34.781	171	60.526	6.664
126	77.512	34.351	172	60.416	5.931
127	76.916	33.911	173	60.319	5.197
128	76.328	33.460	174	60.235	4.461
129	75.748	32.999	175	60.164	3.724
130	75.177	32.528	176	60.105	2.986
131	74.613	32.047	177	60.059	2.246
132	74.058	31.557	178	60.027	1.506
133	73.512	31.057	179	60.007	0.766
134	72.974	30.547	180	60.000	0.025
135	72.446	30.028			
136	71.926	29.500			
137	71.416	28.963			

Table G-9: Triaxial test result on red clay soil specimen with H/D=2.5 cm under cell pressure (σ_3=60kpa)

H/D=2.5					
	Axial stress			σ1	141.52
	Cell pressure			σ3	60.00
	R			(σ1-σ3)/2	40.76
	σavg			(σ3+σ3)/2	100.76
	τxy				0.00
Angle,θ	σn=σavg+RCosθ	τn=RSinθ	Angle,θ	σn=σavg+RCosθ	τn=RSinθ
0	141.519	0.000	46	129.078	29.316

1	141.513	0.711	47	128.562	29.805
2	141.494	1.422	48	128.038	30.286
3	141.463	2.133	49	127.505	30.757
4	141.420	2.843	50	126.965	31.219
5	141.364	3.552	51	126.416	31.672
6	141.296	4.260	52	125.859	32.115
7	141.216	4.966	53	125.295	32.548
8	141.123	5.672	54	124.723	32.971
9	141.018	6.375	55	124.144	33.384
10	140.900	7.077	56	123.558	33.787
11	140.771	7.776	57	122.965	34.180
12	140.629	8.473	58	122.366	34.562
13	140.475	9.167	59	121.759	34.934
14	140.309	9.859	60	121.146	35.295
15	140.131	10.547	61	120.527	35.645
16	139.941	11.233	62	119.902	35.985
17	139.739	11.915	63	119.272	36.313
18	139.525	12.593	64	118.635	36.631
19	139.299	13.268	65	117.993	36.937
20	139.062	13.938	66	117.346	37.232
21	138.813	14.604	67	116.694	37.516
22	138.552	15.266	68	116.037	37.788
23	138.280	15.923	69	115.375	38.049
24	137.997	16.575	70	114.709	38.298
25	137.702	17.223	71	114.039	38.536
26	137.396	17.865	72	113.364	38.762
27	137.078	18.501	73	112.686	38.976
28	136.750	19.132	74	112.004	39.178
29	136.411	19.757	75	111.319	39.368
30	136.060	20.376	76	110.630	39.546
31	135.700	20.989	77	109.939	39.713
32	135.328	21.596	78	109.244	39.867

33	134.946	22.196	79	108.547	40.009
34	134.553	22.789	80	107.848	40.139
35	134.151	23.375	81	107.147	40.256
36	133.738	23.954	82	106.443	40.361
37	133.315	24.526	83	105.738	40.454
38	132.882	25.090	84	105.031	40.535
39	132.439	25.647	85	104.323	40.604
40	131.987	26.196	86	103.614	40.660
41	131.525	26.737	87	102.904	40.703
42	131.054	27.269	88	102.194	40.734
43	130.573	27.794	89	101.483	40.753
44	130.084	28.310	90	100.772	40.760
45	129.585	28.817	91	100.060	40.754
92	99.349	40.735	137	70.962	27.811
93	98.639	40.704	138	70.482	27.287
94	97.929	40.661	139	70.010	26.755
95	97.220	40.606	140	69.548	26.214
96	96.512	40.538	141	69.095	25.666
97	95.805	40.457	142	68.652	25.109
98	95.100	40.365	143	68.219	24.545
99	94.397	40.260	144	67.796	23.974
100	93.695	40.143	145	67.382	23.395
101	92.996	40.013	146	66.979	22.809
102	92.299	39.872	147	66.586	22.216
103	91.604	39.718	148	66.204	21.616
104	90.913	39.552	149	65.832	21.010
105	90.224	39.374	150	65.471	20.397
106	89.538	39.185	151	65.120	19.778
107	88.856	38.983	152	64.781	19.153
108	88.178	38.769	153	64.452	18.523
109	87.503	38.544	154	64.134	17.886
110	86.833	38.307	155	63.828	17.245

111	86.167	38.058	156	63.532	16.598
112	85.505	37.797	157	63.248	15.945
113	84.848	37.525	158	62.976	15.288
114	84.195	37.242	159	62.715	14.627
115	83.548	36.947	160	62.465	13.961
116	82.906	36.641	161	62.228	13.290
117	82.269	36.324	162	62.002	12.616
118	81.638	35.996	163	61.787	11.938
119	81.013	35.657	164	61.585	11.256
120	80.394	35.307	165	61.395	10.571
121	79.781	34.946	166	61.216	9.882
122	79.174	34.575	167	61.050	9.191
123	78.574	34.193	168	60.895	8.496
124	77.981	33.801	169	60.753	7.800
125	77.395	33.398	170	60.623	7.100
126	76.815	32.985	171	60.505	6.399
127	76.243	32.562	172	60.400	5.695
128	75.679	32.130	173	60.307	4.990
129	75.122	31.687	174	60.226	4.284
130	74.573	31.235	175	60.157	3.576
131	74.032	30.773	176	60.101	2.867
132	73.499	30.302	177	60.057	2.157
133	72.975	29.822	178	60.026	1.446
134	72.459	29.333	179	60.007	0.735
135	71.951	28.834	180	60.000	0.024
136	71.452	28.327			

Table G-10: Triaxial test result on red clay soil specimen with H/D=1.5 cm under cell pressure (σ_3=100kpa)

H/D=1.5		
Axial stress	σ_1	186.93

	Cell pressure			σ_3	100.00
	R			$(\sigma_1-\sigma_3)/2$	43.46
	σavg			$(\sigma_1+\sigma_3)/2$	143.46
	τxy				0
Angle,θ	σn=σavg+RCosθ	τn=RSinθ	Angle,θ	σn=σavg+RCosθ	τn=RSinθ
0	186.93	0.00	46	173.66	31.26
1	186.92	0.76	47	173.11	31.78
2	186.90	1.52	48	172.55	32.29
3	186.87	2.27	49	171.98	32.80
4	186.82	3.03	50	171.41	33.29
5	186.76	3.79	51	170.82	33.77
6	186.69	4.54	52	170.23	34.24
7	186.60	5.30	53	169.63	34.71
8	186.50	6.05	54	169.02	35.16
9	186.39	6.80	55	168.40	35.60
10	186.27	7.55	56	167.77	36.03
11	186.13	8.29	57	167.14	36.45
12	185.98	9.03	58	166.50	36.85
13	185.81	9.78	59	165.86	37.25
14	185.64	10.51	60	165.20	37.64
15	185.45	11.25	61	164.54	38.01
16	185.24	11.98	62	163.88	38.37
17	185.03	12.71	63	163.20	38.72
18	184.80	13.43	64	162.52	39.06
19	184.56	14.15	65	161.84	39.39
20	184.31	14.86	66	161.15	39.70
21	184.04	15.57	67	160.45	40.00
22	183.76	16.28	68	159.75	40.29
23	183.47	16.98	69	159.05	40.57
24	183.17	17.67	70	158.34	40.84

25	182.86	18.37	71	157.62	41.09
26	182.53	19.05	72	156.90	41.33
27	182.19	19.73	73	156.18	41.56
28	181.84	20.40	74	155.45	41.78
29	181.48	21.07	75	154.72	41.98
30	181.11	21.73	76	153.99	42.17
31	180.72	22.38	77	153.25	42.35
32	180.32	23.03	78	152.51	42.51
33	179.92	23.67	79	151.77	42.66
34	179.50	24.30	80	151.02	42.80
35	179.07	24.93	81	150.27	42.93
36	178.63	25.54	82	149.52	43.04
37	178.18	26.15	83	148.77	43.14
38	177.72	26.75	84	148.02	43.22
39	177.24	27.35	85	147.26	43.30
40	176.76	27.93	86	146.51	43.36
41	176.27	28.51	87	145.75	43.40
42	175.77	29.08	88	144.99	43.44
43	175.25	29.64	89	144.23	43.46
44	174.73	30.19	90	143.48	43.46
45	174.20	30.73	91	142.72	43.46
92	141.96	43.44	137	111.69	29.66
93	141.20	43.40	138	111.18	29.10
94	140.44	43.36	139	110.67	28.53
95	139.69	43.30	140	110.18	27.95
96	138.93	43.23	141	109.70	27.37
97	138.18	43.14	142	109.23	26.77
98	137.43	43.04	143	108.76	26.17
99	136.68	42.93	144	108.31	25.56
100	135.93	42.81	145	107.87	24.95
101	135.18	42.67	146	107.44	24.32
102	134.44	42.52	147	107.02	23.69

103	133.70	42.35	148	106.62	23.05
104	132.96	42.18	149	106.22	22.40
105	132.23	41.99	150	105.83	21.75
106	131.50	41.78	151	105.46	21.09
107	130.77	41.57	152	105.10	20.42
108	130.05	41.34	153	104.75	19.75
109	129.33	41.10	154	104.41	19.07
110	128.61	40.85	155	104.08	18.39
111	127.90	40.58	156	103.77	17.70
112	127.20	40.30	157	103.46	17.00
113	126.50	40.01	158	103.17	16.30
114	125.80	39.71	159	102.89	15.60
115	125.11	39.40	160	102.63	14.89
116	124.43	39.07	161	102.38	14.17
117	123.75	38.73	162	102.13	13.45
118	123.07	38.38	163	101.91	12.73
119	122.41	38.02	164	101.69	12.00
120	121.75	37.65	165	101.49	11.27
121	121.09	37.26	166	101.30	10.54
122	120.45	36.87	167	101.12	9.80
123	119.81	36.46	168	100.95	9.06
124	119.17	36.04	169	100.80	8.32
125	118.55	35.61	170	100.66	7.57
126	117.93	35.17	171	100.54	6.82
127	117.32	34.72	172	100.43	6.07
128	116.72	34.26	173	100.33	5.32
129	116.13	33.79	174	100.24	4.57
130	115.54	33.31	175	100.17	3.81
131	114.96	32.81	176	100.11	3.06
132	114.39	32.31	177	100.06	2.30
133	113.84	31.80	178	100.03	1.54
134	113.28	31.28	179	100.01	0.78

135	112.74	30.75	180	100.00	0.03
136	112.21	30.21			

Table G-11: Triaxial test result on red clay soil specimen with H/D=2 cm under cell pressure (σ_3=100kpa)

H/D=2					
	Axial stress			σ_1	184.85
	Cell pressure			σ_3	100.00
	R			$(\sigma_1-\sigma_3)/2$	42.43
	σavg			$(\sigma_1+\sigma_3)/2$	142.43
	τxy				0
Angle,θ	σ_n=σavg+RCosθ	τ_n=RSinθ	Angle,θ	σn=σ_{avg}+RCosθ	τ_n=RSinθ
0	184.85	0.00	45	172.43	29.99
1	184.84	0.74	46	171.90	30.51
2	184.82	1.48	47	171.36	31.02
3	184.79	2.22	48	170.82	31.52
4	184.75	2.96	49	170.26	32.01
5	184.69	3.70	50	169.70	32.50
6	184.62	4.43	51	169.13	32.97
7	184.53	5.17	52	168.55	33.43
8	184.44	5.90	53	167.96	33.88
9	184.33	6.64	54	167.37	34.32
10	184.21	7.37	55	166.77	34.75
11	184.07	8.09	56	166.16	35.17
12	183.92	8.82	57	165.54	35.58
13	183.76	9.54	58	164.91	35.97
14	183.59	10.26	59	164.28	36.36
15	183.41	10.98	60	163.65	36.74
16	183.21	11.69	61	163.00	37.10

17	183.00	12.40	62	162.35	37.46
18	182.78	13.11	63	161.69	37.80
19	182.54	13.81	64	161.03	38.13
20	182.29	14.51	65	160.36	38.45
21	182.03	15.20	66	159.69	38.75
22	181.76	15.89	67	159.01	39.05
23	181.48	16.57	68	158.33	39.33
24	181.18	17.25	69	157.64	39.60
25	180.88	17.93	70	156.94	39.86
26	180.56	18.59	71	156.25	40.11
27	180.23	19.26	72	155.55	40.35
28	179.89	19.91	73	154.84	40.57
29	179.53	20.56	74	154.13	40.78
30	179.17	21.21	75	153.42	40.98
31	178.79	21.85	76	152.70	41.16
32	178.41	22.48	77	151.98	41.34
33	178.01	23.10	78	151.26	41.50
34	177.60	23.72	79	150.53	41.64
35	177.18	24.33	80	149.80	41.78
36	176.75	24.93	81	149.07	41.90
37	176.31	25.53	82	148.34	42.01
38	175.86	26.12	83	147.61	42.11
39	175.40	26.69	84	146.87	42.19
40	174.93	27.27	85	146.13	42.26
41	174.45	27.83	86	145.40	42.32
42	173.96	28.38	87	144.66	42.37
43	173.46	28.93	88	143.92	42.40
44	172.95	29.47	89	143.18	42.42
90	142.44	42.43	136	111.92	29.48
91	141.70	42.42	137	111.41	28.95
92	140.96	42.40	138	110.91	28.40
93	140.22	42.37	139	110.42	27.85

94	139.48	42.32	140	109.94	27.29
95	138.74	42.27	141	109.47	26.71
96	138.00	42.19	142	109.01	26.14
97	137.27	42.11	143	108.55	25.55
98	136.53	42.01	144	108.11	24.95
99	135.80	41.91	145	107.68	24.35
100	135.07	41.78	146	107.26	23.74
101	134.34	41.65	147	106.86	23.12
102	133.62	41.50	148	106.46	22.50
103	132.90	41.34	149	106.07	21.87
104	132.18	41.17	150	105.69	21.23
105	131.46	40.98	151	105.33	20.59
106	130.75	40.79	152	104.98	19.94
107	130.04	40.58	153	104.63	19.28
108	129.33	40.35	154	104.30	18.62
109	128.63	40.12	155	103.98	17.95
110	127.93	39.87	156	103.68	17.28
111	127.24	39.61	157	103.38	16.60
112	126.55	39.34	158	103.10	15.91
113	125.86	39.06	159	102.83	15.22
114	125.18	38.76	160	102.57	14.53
115	124.51	38.46	161	102.32	13.83
116	123.84	38.14	162	102.08	13.13
117	123.18	37.81	163	101.86	12.43
118	122.52	37.47	164	101.65	11.72
119	121.87	37.11	165	101.45	11.00
120	121.23	36.75	166	101.27	10.29
121	120.59	36.37	167	101.09	9.57
122	119.96	35.99	168	100.93	8.84
123	119.33	35.59	169	100.78	8.12
124	118.72	35.18	170	100.65	7.39
125	118.11	34.76	171	100.53	6.66

126	117.50	34.33	172	100.42	5.93
127	116.91	33.89	173	100.32	5.19
128	116.32	33.44	174	100.23	4.46
129	115.74	32.98	175	100.16	3.72
130	115.17	32.51	176	100.11	2.98
131	114.61	32.03	177	100.06	2.25
132	114.05	31.54	178	100.03	1.51
133	113.50	31.04	179	100.01	0.77
134	112.97	30.53	180	100.00	0.03
135	112.44	30.01			

Table G-12: Triaxial test result on red clay soil specimen with H/D=2.5 cm under cell pressure (σ_3=100kpa)

H/D=2.5					
	Axial stress			σ_1	181.53
	Cell pressure			σ_3	100.00
	R			$(\sigma_1-\sigma_3)/2$	40.77
	σ_{avg}			$(\sigma_1+\sigma_3)/2$	140.77
	τxy				0.00
Angle,θ	$\sigma_n=\sigma_{avg}+R\cos\theta$	$\tau_n=R\sin\theta$	Angle,θ	$\sigma_n=\sigma_{avg}+R\cos\theta$	$\tau_n=R\sin\theta$
0	181.53	0.00	45	169.60	28.82
1	181.53	0.71	46	169.09	29.32
2	181.51	1.42	47	168.58	29.81
3	181.48	2.13	48	168.05	30.29
4	181.44	2.84	49	167.52	30.76
5	181.38	3.55	50	166.98	31.23
6	181.31	4.26	51	166.43	31.68
7	181.23	4.97	52	165.87	32.12
8	181.14	5.67	53	165.31	32.55
9	181.03	6.38	54	164.74	32.98

10	180.92	7.08	55	164.16	33.39
11	180.79	7.78	56	163.57	33.79
12	180.64	8.47	57	162.98	34.19
13	180.49	9.17	58	162.38	34.57
14	180.32	9.86	59	161.77	34.94
15	180.15	10.55	60	161.16	35.30
16	179.96	11.23	61	160.54	35.65
17	179.75	11.92	62	159.91	35.99
18	179.54	12.60	63	159.28	36.32
19	179.31	13.27	64	158.65	36.64
20	179.08	13.94	65	158.00	36.94
21	178.83	14.61	66	157.36	37.24
22	178.57	15.27	67	156.70	37.52
23	178.30	15.93	68	156.05	37.80
24	178.01	16.58	69	155.39	38.06
25	177.72	17.23	70	154.72	38.31
26	177.41	17.87	71	154.05	38.54
27	177.09	18.50	72	153.37	38.77
28	176.76	19.14	73	152.70	38.98
29	176.43	19.76	74	152.01	39.19
30	176.07	20.38	75	151.33	39.38
31	175.71	20.99	76	150.64	39.55
32	175.34	21.60	77	149.95	39.72
33	174.96	22.20	78	149.25	39.87
34	174.57	22.79	79	148.56	40.02
35	174.16	23.38	80	147.86	40.15
36	173.75	23.96	81	147.16	40.26
37	173.33	24.53	82	146.45	40.37
38	172.90	25.09	83	145.75	40.46
39	172.45	25.65	84	145.04	40.54
40	172.00	26.20	85	144.33	40.61
41	171.54	26.74	86	143.62	40.67

42	171.07	27.27	87	142.91	40.71
43	170.59	27.80	88	142.20	40.74
44	170.10	28.32	89	141.49	40.76
90	140.78	40.77	136	111.45	28.33
91	140.07	40.76	137	110.96	27.82
92	139.36	40.74	138	110.48	27.29
93	138.65	40.71	139	110.01	26.76
94	137.94	40.67	140	109.55	26.22
95	137.23	40.61	141	109.10	25.67
96	136.52	40.55	142	108.65	25.11
97	135.81	40.47	143	108.22	24.55
98	135.11	40.37	144	107.80	23.98
99	134.40	40.27	145	107.38	23.40
100	133.70	40.15	146	106.98	22.81
101	133.00	40.02	147	106.59	22.22
102	132.30	39.88	148	106.21	21.62
103	131.61	39.73	149	105.83	21.01
104	130.92	39.56	150	105.47	20.40
105	130.23	39.38	151	105.12	19.78
106	129.54	39.19	152	104.78	19.16
107	128.86	38.99	153	104.45	18.53
108	128.18	38.78	154	104.13	17.89
109	127.51	38.55	155	103.83	17.25
110	126.84	38.31	156	103.53	16.60
111	126.17	38.06	157	103.25	15.95
112	125.51	37.80	158	102.98	15.29
113	124.85	37.53	159	102.72	14.63
114	124.20	37.25	160	102.47	13.96
115	123.55	36.95	161	102.23	13.29
116	122.91	36.65	162	102.00	12.62
117	122.27	36.33	163	101.79	11.94
118	121.64	36.00	164	101.59	11.26

119	121.02	35.66	165	101.39	10.57
120	120.40	35.31	166	101.22	9.88
121	119.78	34.95	167	101.05	9.19
122	119.18	34.58	168	100.90	8.50
123	118.58	34.20	169	100.75	7.80
124	117.98	33.81	170	100.62	7.10
125	117.40	33.40	171	100.51	6.40
126	116.82	32.99	172	100.40	5.70
127	116.25	32.57	173	100.31	4.99
128	115.68	32.14	174	100.23	4.28
129	115.13	31.69	175	100.16	3.58
130	114.58	31.24	176	100.10	2.87
131	114.03	30.78	177	100.06	2.16
132	113.50	30.31	178	100.03	1.45
133	112.98	29.83	179	100.01	0.74
134	112.46	29.34	180	100.00	0.02
135	111.95	28.84			